Chemically Defined and Tailorable Synthetic Materials for Human Cell Manufacturing

By

John Dolgner Krutty

A dissertation submitted in partial fulfillment of

the requirements for the degree of

Doctor of Philosophy

(Biomedical Engineering)

At the

UNIVERSITY OF WISCONSIN-MADISON

2019

Date of final Oral Examination: December 20th, 2019

This dissertation is approved by the following members of the Final Oral Committee:

William L Murphy, Professor, Biomedical Engineering

Padma Gopalan, Professor, Materials Science and Engineering

Sean P Palecek, Professor, Chemical and Biological Engineering

David M. Lynn, Professor, Chemical and Biological Engineering

Ian M Bird, Professor, Obstetrics & Gynecology

ABSTRACT

Human cell-based therapeutics have the potential to treat a wide and ever-expanding array of diseases and disabilities, with an increasing number of potential therapeutics being evaluated by the FDA each year. In order for these therapeutics to be viable, cell production and potency must be able to keep pace with the increasing demand. Chemically defined biomaterials have the potential to address some of the challenges endemic to the cell production and manufacturing landscape by enabling control over the cell-material interaction, cell adhesion, and local concentration of soluble signals. In this thesis, we describe a synthetic, chemically defined, tailorable polymer coating that can be applied to existing cell culture materials. The first part of this thesis describes a novel strategy for the application of a synthetic copolymer, poly(poly(ethylene glycol) methyl ether methacrylate-*ran*-vinyl dimethyl azlactone-*ran*-glycidyl methacrylate) (P(PEGMEMA-*r*-VDM-*r*-GMA); abbreviated PVG), to the surface of existing biomaterials for the expansion of human mesenchymal stromal cells (hMSC, also referred to as mesenchymal stem cells). Specifically, part one details a method for sequential anchoring of the PVG copolymer to polystyrene (PS), glass, and other polymer surfaces. This method was then used to apply the copolymer coating to microcarriers - solid spheres of 100-400 μm that provide a surface for cell culture when kept in suspension - creating a chemically defined surface for hMSC expansion in serum-containing media. Cells cultured on these surfaces retained their ability to differentiate down multiple lineages. We then use these PVG coated surface for hMSC culture in media with no animal components (xeno-free media). hMSC attached to and expanded on PVG-coated microcarriers in xeno-free media at a much higher rate than the standard PS microcarriers. Additionally, hMSC could be separated from the PVG microcarriers using non-enzymatic passaging methods, representing an improvement over standard of the field. In the second part of

this work, we describe the use of chemically defined surfaces to present growth factor receptor-binding peptides to adherent cells. We demonstrate control over the relative spacing of multiple growth factor receptor-binding peptides at the nanometer scale, resulting in altered signal transduction and microparticle uptake in human umbilical vein endothelial cells (HUVEC). We then demonstrate the potential for this technology in a cell manufacturing application by creating growth factor receptor-binding magnetic beads that can be used to sort cells based on their growth factor receptor expression. In summary, we have developed a tailorable, chemically defined polymer coating and demonstrated its utility across multiple disciplines within the cell manufacturing field. These studies demonstrate the potential for synthetic materials to improve the process by which we develop human cells for therapeutic applications. The implications of this work would enable tighter control over the manufacturing process at a reduced cost, which could then be passed onto patients, increasing the availability of revolutionary cell-based therapeutics.

For my parents – Thank you for all you have given me

and

For Dally – You are a constant source of inspiration

ACKNOWLEDGEMENTS

First and foremost, I would like to acknowledge my advisors, William Murphy and Padma Gopalan, both of whom were patient, thoughtful stewards of my PhD work and my development as a researcher. I would not have accomplished what I have to this point without their guidance. In addition to being intelligent, creative, and hardworking scientists, they are caring and kind people whose impact on my research, thought process, and personal growth cannot be overstated. I would also like to thank the members of my committee: Professors David Lynn, Sean Palecek, and Ian M Bird for contributing their time and effort to this work. I would like to acknowledge the Holton family, whose fellowship provided me with funding for my first year at UW-Madison and allowed me to find a lab where I could continue my studies.

I could not have finished any of the work that is described here without the work of some undergraduate researchers that have helped me along the way. I am especially grateful to Stephen Schwartz and Kevin Koesser, who as undergraduates were eager to learn, quick to master new techniques and dedicated to the work. They contributed more than was asked of them and I am sure they will find success in whatever they pursue.

Throughout my time in graduate school, I have been fortunate to have two full labs of coworkers. The current and former members of the Gopalan and Murphy labs are some of the brightest people I have ever known and have made me smile every day in the lab. Thank you to the members of the Murphy lab - Buffy Aisenbrey, Hamisha Ardalani, Kate Barteau, Dave Belair, Beko Binder Connie Chamberlain, Anna Clements, Bill Daly, Gianluca Fontana, Tori Harms, Gaurav Kaushik, Nhi Le, Jae-Sung Lee, Leona Liu, Hannah Martin, Ulrika Müller, Eric Nguyen, Matt Parlato, Liz Torr, Angie Xie, and Junsu Yun – and the Gopalan Lab –

Balamurugan Ayyakkalai, Ri Chen, Jon Choi, Jonathan Dwyer, Peishen Huang, Yongho Joo, Catherine Kanimozhi, Haridas Kar, Jaehyoung Ko, and Jian Sun. Andrew Khalil was full of knowledge and even more full of nonsensical arguments and jokes. As I was told by another coworker, there was much less giggling from our corner of the lab after he graduated. Samantha Schmitt laid the groundwork for my research through her own thesis work and taught me many of the techniques used in this work. Wei Wei started his PhD program at the same time as me, and I have watched him grow into a thoughtful, skeptical scientist whose work is often outstanding. I am thankful to have had these people during my graduate career. I was able to find funding and a lab to join in Wisconsin through the selfless effort of Danielle Bourgeois, despite the fact that we were little more than strangers. I will always be grateful for the work she put in to help me find my place, which was probably much more important to me than she knows.

I have made many friends in Madison, far too many to list here. Thank you all for providing me with an outlet to clear my head; your joy and kindness has helped me immensely. Brandon Joachim was an important force in bringing me to Madison and introduced me to many of who would become my lifelong friends, and I am very thankful for his influence and his friendship. My friends from college, who became like family when I was far from home, have been a constant source of laughter and encouragement. Thank you to Max Krapff, Nick Dalheim, Kristian Ford, Cole Stutz, Drew Donica, Matt Niemitalo, Nick Pugh, Nick Lovett, Emily Zander, and Alex Long for not allowing me to take myself too seriously.

Finally, and most importantly, I would like to thank my family. I believe that I am the first of either side of my family to complete a PhD - I recognize that I have been put in this position to succeed through the effort of my grandparents and parents and want to thank them for their hard work. My parents, Dean and Marion Krutty, have been wonderful examples and

sacrificed plenty to allow me to become the person I am today. My siblings Paul, Lynne, and Nancy, and in-laws Daphne, Trevor, Leah and Kyle are intelligent and hilarious and have provided me with much-needed comfort over the years. Thank you all for making it clear that no degree will ever protect me from being ridiculed when I deserve it. Most of all, my wife Rachael has been more loving and supportive than I could have imagined. I am extremely lucky to have her in my life.

TABLE OF CONTENTS

LIST OF FIGURES

CHAPTER 1. INTRODUCTION

1.1 BACKGROUND AND SIGNIFICANCE

Cell-based therapeutics, including human cells or biologic cell products, have the potential to create revolutionary treatments for a wide and ever-expanding array of diseases and conditions. To date, multiple cell-based therapeutics have received approval for use in humans from the FDA, with thousands of additional applications that have been or are currently being evaluated. One cell type, the mesenchymal stromal cell (hMSC), often referred to as the mesenchymal stem cell, has been a target for a large number of therapeutic applications due to its differentiation potential[1-5] and immunosuppressive capabilities[6, 7], with over 900 ongoing or completed clinical trials focusing on hMSC as of 2019 (clinicaltrials.gov). With a typical treatment requiring up to 1M cells per kg of body mass, the demand for scalable, cost effective manufacturing of reproducible, high potency hMSC is clearly underscored[8]. In addition to therapeutic applications, a wider variety of human cells have become a component of disease models for high-throughput drug efficacy and toxicity screening. These cells remain a crucial part of research into the mechanisms of human biological functions and diseases. Current methods and materials for culturing human cells have difficulty scaling at cost and largely rely on animal components that introduce heterogeneity and the potential for immune response to eventual cell-derived therapeutics.

Human cells cultured *in vitro* respond to signals of multiple types, ranging from a multitude of soluble factors as well as solids and the stiffness of the cell culture substrate. Adherent cell culture relies on the presence of proteins on a solid surface, in the form of a whole protein surface treatment (e.g. Matrigel®, vitronectin) or the nonspecific adsorption of serum-derived proteins onto surfaces like glass or tissue culture polystyrene (TCPS). Each of these materials that promote

adhesion may derive from a wide array of sources which can be broadly categorized as having synthetic or natural origins, each with its own advantages and disadvantages. Natural materials are capable of recapitulating complex mixtures of signals present in the cell microenvironment but suffer from high batch-to-batch variability, high cost, and a poorly characterized culture system[9]. Recombinant proteins have greater consistency between batches and are well characterized but are expensive and aren't readily applicable to large surfaces for scaled up cell culture. Synthetic, customizable polymer materials have the potential to create chemically defined, cell-adherent surfaces at a large scale. Furthermore, synthetic materials can be tailored to provide specific biological cues and be used across a wide range of manufacturing and bioprocessing applications.

This thesis describes a synthetic copolymer (PVG) and a novel mechanism for its application to existing, three-dimensional cell culture materials. It is a chemically defined biomaterial surface capable of providing control over adhesion in large scale cell culture systems as well as tightly controlling growth factor signaling, either through sequestration of soluble GFs or through directly binding the growth factor receptors from the material surface. We show that microcarriers, solid beads with a diameter ranging from 100-400 μm that are used to culture cells in suspension, resist cell adhesion when coated with the PVG copolymer, until adhesion is restored specifically through an Asp-Arg-Gly (RGD) containing peptide that binds to integrin receptors on the cell surface. This copolymer coating provides significant advantages over common polystyrene microcarriers, including the ability to culture in xeno-free media and passage cells without the use of enzymes. We then use the chemically defined copolymer coating to induce growth factor signaling directly from the surface in the absence of expensive, soluble, recombinant growth factors, and demonstrate the utility of this function in a cell-sorting application.

1.2 SUMMARY OF THE WORK

In Chapter 2 of this thesis, we provide a background and overview of the use of synthetic materials in stem cell culture. The modification of low-cost polymer substrates with synthetic or naturally derived coatings are specifically addressed. We go on to discuss the advantages and potential drawbacks to chemically defined polymer coatings, including methods by which they may become chemically modified by the components of the cell culture environment or the cells themselves.

Chapter 3 introduces the polymer coating PVG and describes a novel mechanism for the application of synthetic polymers to three-dimensional cell culture materials. We characterize the material and confirm its presence and effect on glass and polystyrene surfaces and ensure that it retains the ability to react with biologically relevant peptides. The coating's utility in cell culture applications is then demonstrated through its use in microcarrier culture. We show that PVG coated microcarriers with no functionalization resist the adhesion of hMSC in serum-containing media. We are then able to restore adhesion through the use of an integrin-specific RGD peptide, which enables cells to expand in number on the microcarriers. These cells retained their ability to differentiate down adipogenic and osteogenic lineages, demonstrating a retention of hMSC phenotype. Chapter 4 expands upon this work by conducting the cell culture in readily scalable bioreactors and in media that does not contain animal derived products such as serum (xeno-free media). We show that while hMSC do not adhere to polystyrene microcarriers under these conditions, they do adhere to PVG coated, RGD functionalized microcarriers. Additionally, the PVG coated microcarriers enable efficient passaging of hMSC on microcarriers using Ethylenediaminetetraacetic acid (EDTA), a non-enzymatic chelating agent that disrupts integrin binding activity to lift cells from the surface.

Finally, in Chapter 5, the synthetic polymer coating is used to directly bind to growth factor receptors on the cell surface. Specifically, we use the PVG coating to control the presentation and spacing of growth factor binding peptides for multiple different growth factor receptors. The spacing of these molecules is controlled on a nanometer scale using synthetic, heterobifunctional chemical crosslinkers of a known length. We then demonstrate the ability of these peptides to engage with vascular endothelial growth factor receptor 2 (VEGFR2) and neuropilin-1 (Nrp1), two growth factor receptors, on the cell surface and impact cell behavior. The utility of this growth factor receptor binding material is expanded upon through its use in cell processing applications. By applying the PVG coating and VEGFR-binding peptides to magnetic microspheres, we successfully isolated a population of VEGFR2+ cells from a heterogeneous population.

1.3 REFERENCES

[1] M. F. Pittenger, A. M. Mackay, S. C. Beck, R. K. Jaiswal, R. Douglas, J. D. Mosca, M. A. Moorman, D. W. Simonetti, S. Craig, D. R. Marshak. *Science* 1999;284:143-7.

[2] X. Shen, B. Pan, H. Zhou, L. Liu, T. Lv, J. Zhu, X. Huang, J. Tian. Journal of Biomedical *Science* **2017**;24:29.

[3] A. Singh, A. Singh, D. Sen. *Stem Cell Research & Therapy* **2016**;7:82.

[4] G. V. Silva, S. Litovsky, J. A. R. Assad, A. L. S. Sousa, B. J. Martin, D. Vela, S. C. Coulter, J. Lin, J. Ober, W. K. Vaughn, R. V. C. Branco, E. M. Oliveira, R. He, Y.-J. Geng, J. T. Willerson, E. C. Perin. *Circulation* **2005**;111:150-6.

[5] A. Augello, C. De Bari. *Human Gene Therapy* **2010**;21:1226-38.

[6] G. Ren, L. Zhang, X. Zhao, G. Xu, Y. Zhang, A. I. Roberts, R. C. Zhao, Y. Shi. *Cell Stem Cell*;2:141-50.

[7] Y. Shi, Y. Wang, Q. Li, K. Liu, J. Hou, C. Shao, Y. Wang. *Nature Reviews Nephrology* **2018**;14:493-507.

[8] C. Mennan, J. Garcia, S. Roberts, C. Hulme, K. Wright. *Stem Cell Research & Therapy* **2019**;10:99.

[9] G. D. Prestwich. *Journal of Cellular Biochemistry* **2007**;101:1370-83.

CHAPTER 2. SURFACE FUNCTIONALIZATION AND DYNAMICS OF POLYMERIC CELL CULTURE SUBSTRATES

Elements of this chapter have been published as:

John D. Krutty, Samantha K Schmitt, Padma Gopalan, and William L. Murphy (2016). Surface functionalization and dynamics of polymeric cell culture substrates. *Current Opinions in Biotechnology*.

2.2 ABSTRACT

The promise of growing tissues to replace or improve the function of failing ones, a practice often referred to as regenerative medicine, has been driven in recent years by the development of stem cells and cell lines. Stem cells are typically cultured outside the body to increase cell number or differentiate the cells into mature cell types. In order to maximize the regenerative potential of these cells, there is a need to understand cell-material interactions that direct cell behavior and cell-material dynamics. Most synthetic surfaces used for growth and differentiation of cells in the lab are impractical and cost prohibitive in clinical labs. This review focuses on the modification of low-cost polymer substrates that are already widely used for cell culture so that they may be used to control and understand cell-material interactions. In addition, we discuss the ability of cells to exert dynamic control over the microenvironment leading to a more complex, less controlled surface.

2.3 INTRODUCTION

The therapeutic potential of stem cells is leading to their increased use in clinical trials for treatment of wounds, disease, and as scientific models for drug discovery and toxicology. A major barrier to the reproducibility of cell-based treatments and models is the limited control over cell behavior. *In vitro*, cells interact with soluble signals, such as growth factors, and the extracellular matrix (ECM), which is tissue-specific and consists of insoluble proteins and glycosaminoglycans. Evidence in the last decade suggests that the properties of the insoluble microenvironment can guide cell behaviors such as adhesion, proliferation, morphology and differentiation [1-4]. The combination of these soluble and insoluble signals regulates cell behavior [5, 6]. While insoluble matrix components can be derived from animal sources, clinical application of stem cells will benefit from chemically defined and animal-product-free culture materials to reduce potential immunogenicity and batch-to-batch variability [7]. In particular, stem cells can internalize components of animal-derived culture materials, which have been shown to cause anaphylactic reactions and the production of anti-serum antibodies in clinical treatments [8, 9]. Understanding and selectively presenting parts of the *in vivo* extracellular matrix in a cell culture setting can potentially improve the success of stem cell therapies and help answer fundamental scientific questions.

The overwhelming majority of cell culture is performed on 2D polymer surfaces (e.g. tissue culture polystyrene), which can non-specifically adsorb serum-borne proteins and thereby provide adhesion sites for cells [10]. These plastic cell culture materials are low cost, scalable (e.g. T flasks, stacked cultures), and have low batch-to-batch variation.

However, plastic cell culture materials typically cannot be used to control cell-material interactions. While a series of chemistries have been developed to coat plastic, glass, and metal substrates, achieving control over the cell-surface interactions and maintaining long-term substrate stability in cell culture conditions remains a challenge [11-14]. This concise review presents a subset of recent advances and challenges in the modification of polymer substrates to control cell behavior (**Figure 2.10.1**). We address surface functionalization of cell culture systems, emerging chemically defined surfaces amenable to biological functionalization, and the ongoing challenge of understanding and controlling time-dependent cell-surface interactions.

Figure 2.10.1. Cell culture systems can reproduce aspects of the cell microenvironment. A) Cells cultured on untreated TCPS adhere to adsorbed serum proteins and interact with soluble signals B) Complex biological functionalization adds insoluble cues derived from the extracellular matrix. C) Chemically defined, functionalizable materials (red) enable tailored presentation of bioactive ligands

2.4 BIOLOGICAL FUNCTIONALIZATION

Most mammalian cells are adherent, meaning they must attach to a surface to survive. In order to achieve this adhesion, traditional cell culture relies on the adsorption of serum proteins from the media to the solid surface. Protein adsorption occurs within seconds through non-covalent interactions between the protein and the material [10]. This

use of adsorbed proteins to achieve cell-surface adhesion has the advantage of simplicity; however, it is not without drawbacks. Proteins that are adsorbed to a surface can denature, and may change in α-helix content, β-sheet content, and structural rigidity [15, 16]. In addition, studies on the kinetics of protein adsorption in a two-component system are rare, dependent on many parameters (including diffusion, components, competitive adsorption, pH, temperature, and others) and are ineffective at accurately predicting adsorption in multi-component systems [17-19]. Thus, it is difficult to predict the concentration and conformation of adsorbed proteins in a cell culture environment.

Coatings that form the cell-material interface can also be composed of individually purified glycoproteins (e.g. fibronectin) or heterogeneous mixtures of proteins (*e.g.* Matrigel). The orientation of these adsorbed proteins is not easily controlled [20]. The availability of integrin-binding Arg-Gly-Asp (RGD) cell adhesion motifs in Fibronectin coatings, for example, is dependent on the surface chemistry of the material to which fibronectin has adsorbed. This, in turn, may influence cell adhesion and behavior [21-23]. A study by Ba et al. covalently anchored fibronectin via reactions through thiols or primary amines on amine-functionalized polystyrene in an attempt to restrict the orientation of fibronectin on the surface. These reactions increased the retention of fibronectin to the surface, resulting in higher amounts of immobilized fibronectin and a resistance to deformation, but did not increase the availability of binding sites [24]. Klotzsch et al. used single-molecule imaging of fibronectin to track the relative distance between four available cysteines labeled with Cy3B and tracked using photobleaching and total internal reflectance spectroscopy. The average distance between the four sites increased from 33 nm to 43 nm upon fibronectin adsorption to glass in denaturing conditions, indicating a

conformational change in the molecule. In the same study, the intra-label distance ranged from 24nm to over 51nm upon denaturing when fibronectin was adsorbed to glass that had been rendered more or less hydrophobic through plasma cleaning, pyrolysis, and chemical silanization [25]. Recently, Lin et al. demonstrated that the adsorption force between fibronectin and the underlying material can affect the morphology of cells grown on the surface [26]. Taken together, studies to date demonstrate that while protein coatings can enable cells to interact with a material, they do not allow for a high level of control over the orientation, density and availability of cell adhesion epitopes.

2.5 SYNTHETIC BIOLOGICAL FUNCTIONALIZATION OF POLYMER SUBSTRATES

To better control the concentration and identity of biologically active sequences on the cell culture surface, the polymer substrate can be modified with a non-fouling layer and short peptide sequences derived from ECM proteins – like collagen, fibronectin, and laminin – or growth factor mimicking peptides [2, 3, 27-30]. A variety of synthetic approaches have been developed with a goal of generating cell culture substrates that: (a) require low concentrations of peptides to reduce cost and complexity; (b) are functionalized via peptide coupling chemistry which is efficient in aqueous media; (c) are scalable over large surface areas or complex geometries with uniform coverage; and (d) are stable during long-term (days-weeks) culture of cells. Modification of polymer substrates presents some additional, unique challenges when compared to modification of glass or metal substrates. Polymeric materials often must be modified in aqueous or ethanolic solutions, and in some cases

crosslinked at low temperature or using UV irradiation in order to prevent damage to the polymer.

Many polymer substrates lack the reactive groups required for direct covalent functionalization with peptides. These substrates require additional functionalization steps, such as a plasma treatment, silanization or other chemical treatment, or coating with a reactive layer. Treatment of TCPS with allylamine, for example, adds primary amines to the substrate, which can then covalently couple to PEG-N-hydrocysuccinimide (NHS) containing copolymers to form a crosslinked coating [31]. Qian et al. used chemical vapor deposition to coat TCPS with an initiator molecule which initiated growth of poly[2-(methacryloyloxy)ethyl dimethyl-(3-sulfopropyl)ammonium hydroxide] (PMEDSAH) brushes via atom transfer radical polymerization (ATRP) for embryonic stem cell culture [32]. This study compared the ATRP coatings to PMEDSAH polymerized by UV-ozone initiated free radical polymerization, first demonstrated in Nandivada et al. [33]. Lavanant et al. used a simple photobromination reaction to modify polyethylene and thereby polymerize polyethylene glycol methacrylate brushes in a water/ethanol mixture.[34] The resulting brushes were robust in a one month water stability test and facilitated cell adhesion through RGD peptides.

Coating a substrate with an insoluble layer may also provide an appealing method to introduce functional groups for subsequent non-fouling brush growth or peptide immobilization [35, 36]. An illustrative example of this is polydopamine which can coat many surface types and have been used for both zwitterionic polymer brush growth and peptide attachment [37, 38]. In another coating approach, Schmitt et.al recently reported the synthesis of a PEG-based random copolymer in solution that was then spin-coated onto an untreated

TCPS substrate [28-30]. The polymer coating contained azlactone functional groups for peptide attachment in aqueous solution at room temperature and low concentration (1mM in aqueous solution) with no activation step. The resultant thin film permitted peptide surface density quantification (12.6 pmol/cm^2) by X-ray photoelectron spectroscopy and RGD-mediated cell attachment.

2.6 TIME-DEPENDENT SURFACE REMODELING

In vivo, cells and the ECM are typically in a state of dynamic remodeling. *In vitro*, scientists have made significant progress in understanding and manipulating the initial characteristics of the cell culture substrate, prior to cell culture. However, despite the progress that has been made in generating and characterizing chemically defined surfaces for cell culture, there is still only a limited understanding of the dynamics of cell-surface interactions over time. In particular, while surfaces can be designed to present a single epitope (e.g. a cell adhesion peptide) for binding of cell surface receptors, it is not clear how long the cell has access to that epitope. Do cell adhesion epitopes rapidly become unavailable due to peptide-material bond scission, peptide instability, protein adsorption, cell-mediated ECM protein secretion, or other mechanisms (**Figure 2.10.2**)? This is an intriguing, poorly addressed question in cell culture applications. In the following paragraphs we introduce these dynamic mechanisms at the cell-material interface, and discuss the limited insights gained to date regarding the putative dynamics of cell-substrate interactions.

Common peptide-polymer bonds include amide, carbamate, alkyl sulfide, thioester, triazole, ester, thioether, and disulfide bonds, which may be vulnerable to hydrolysis,

displacement, or protease-mediated degradation [39]. Carbamate [40], thioester [41], and ester [42] bonds are generally susceptible to hydrolytic degradation at physiological pH, while amide bonds are more stable [28, 29]. Studies on the effect of polymer-peptide bond stability in cell culture systems are limited, although degradation of thioester, amide, and carbamate linkers has been observed on PEG thin films using cell-based assays [28, 29].

In addition to cleavage of peptide epitopes from the culture surface, the peptide itself can be subject to degradation or damage in the culture environment via oxidation, deamidation, reduction and hydrolysis [43]. Methionine (Met), cysteine (Cys), histidine (His), tryptophan (Trp) and tyrosine (Tyr) are all subject to oxidation in the presence of oxygen radicals or alkaline pH [43, 44]. Oxidation of these amino acids can also be triggered by visible light in the presence of oxygen, resulting in a decreased biological activity of the peptide, or, in the case of whole proteins, changes to the secondary and tertiary structure [45]. Met and Cys are susceptible to oxidation at their sulfur atoms, while His, Trp and Tyr undergo oxidation of their aromatic rings [44]. In the case of cysteine, this can lead to unwanted disulfide bonds [46]. Glutamine and asparagine residues are susceptible to deamidation, resulting in isomerization or racemization of the residue [47, 48]. Fragmentation of peptides via amide hydrolysis is possible, usually occurring at Asp-Gly and Asp-Pro sequences, but amide hydrolysis is not likely to occur near physiological pH (pH 7-8) [49]. Taken together, studies performed to date, and reviewed in more detail elsewhere [50], indicate that changes to the primary structure of peptides or whole proteins are likely to occur during cell culture on functionalized biomaterials. These changes can result in altered biological activity over time, which may result in unintended changes in the cell microenvironment. However, if changes in peptide and protein stability can be understood

and harnessed they may provide adaptable mechanisms for intentional, transient presentation of cell-interactive epitopes.

Cell-mediated remodeling of synthetic surfaces is another source of dynamic variation. Many cell types have been shown to synthesize ECM molecules *in vitro*, including collagen, elastin, laminin, fibronectin, aggrecan, decorin, glycosaminoglycans, and calcium deposits. [51-57] These cell-secreted matrices can then be decellularized and used to direct stem cell differentiation [58-60], which provides evidence that cells interact with cell-secreted ECM molecules. Even in environments designed to be "non-fouling" or "low-fouling", protein adsorption is commonly observed [61, 62], and degradation of the initially non-fouling surfaces can reduce their ability to resist protein adsorption [63]. Cells can also dynamically modify their surrounding ECM by enzymatic degradation in concert with ECM molecule secretion. Cell-secreted or cell-associated matrix-metalloproteases (MMP) can mediate cell-mediated remodeling of the microenvironment *in vitro.* [64-68] However, the dynamic interplay of ECM protein secretion, protein adsorption, and cell-mediated ECM degradation is poorly understood. For example, quantitative understanding of how long a cell can engage with the initial substrate before cell-secreted ECM molecules or metalloprotease activity significantly alter the initial surface is lacking.

Figure 2. Over time, the cell-material interface can be dynamically altered through (A) removal of a cell-adhesive ligand from the surface, (B) degradation/denaturation of the ligand, and (C) fouling over time due to secreted or adsorbed molecules.

2.7 CONCLUDING REMARKS

Recent studies have made significant progress toward controlling the initial cell-surface interface, and understanding the effect that this may have on cell behavior. While the initial conditions of these types of substrates are thoroughly examined, they may be susceptible to increasingly complex modifications after hours to days of cell culture. The quantitative characterization of cell secreted ECM molecules, protein adsorption through surface degradation, and degradation of functional peptides on cell culture materials is likely to be a highly significant area of study that is as of yet largely unexplored. In order to maintain control and biological relevance *in vitro*, there is a need to create cell culture surfaces that are designed for real-time characterization of polymer stability, peptide stability, ECM molecule secretion, protein adsorption, and cell-mediated ECM degradation/remodeling. Ultimately, a clearer understanding of cell-substrate dynamics may lead to innovative approaches to dynamically adapt to cell behavior in a controlled and predictable manner.

2.8 ACKNOWLEDGEMENTS

This research was funded by the National Science Foundation (NSF DMR 1306482), the National Institutes of Health (R01HL093282), and the Environmental Protection Agency (STAR grant no. 83573701).

2.9 REFERENCES

1. Maheshwari, G., et al., *Cell adhesion and motility depend on nanoscale RGD clustering.* Journal of Cell Science, 2000. **113**(10): p. 1677-1686.
2. Lin, E., et al., *Peptide microarray patterning for controlling and monitoring cell growth.* Acta Biomaterialia.
3. Li, L., et al., *Spatial control of cell fate using synthetic surfaces to potentiate TGF-β signaling.* Proceedings of the National Academy of Sciences, 2011. **108**(29): p. 11745-11750.
4. Lutolf, M.P. and J.A. Hubbell, *Synthetic biomaterials as instructive extracellular microenvironments for morphogenesis in tissue engineering.* Nat Biotech, 2005. **23**(1): p. 47-55.
5. Cheng, C.W., L.D. Solorio, and E. Alsberg, *Decellularized tissue and cell-derived extracellular matrices as scaffolds for orthopaedic tissue engineering.* Biotechnology Advances, 2014. **32**(2): p. 462-484.
6. Lutolf, M.P. and H.M. Blau, *Artificial Stem Cell Niches.* Advanced materials (Deerfield Beach, Fla.), 2009. **21**(32-33): p. 3255-3268.
7. Zheng, X., et al., *Proteomic Analysis for the Assessment of Different Lots of Fetal Bovine Serum as a Raw Material for Cell Culture. Part IV. Application of Proteomics to the Manufacture of Biological Drugs.* Biotechnology Progress, 2006. **22**(5): p. 1294-1300.
8. Mackensen, A., et al., *Presence of IgE antibodies to bovine serum albumin in a patient developing anaphylaxis after vaccination with human peptide-pulsed dendritic cells.* Cancer Immunol Immunother, 2000. **49**(3): p. 152-6.

9. Spees, J.L., et al., *Internalized Antigens Must Be Removed to Prepare Hypoimmunogenic Mesenchymal Stem Cells for Cell and Gene Therapy[ast].* Mol Ther, 2004. **9**(5): p. 747-756.

10. Mrksich, M., *A surface chemistry approach to studying cell adhesion.* Chemical Society Reviews, 2000. **29**(4): p. 267-273.

11. Saha, K., et al., *Surface Creasing Instability of Soft Polyacrylamide Cell Culture Substrates.* Biophysical Journal, 2010. **99**(12): p. L94-L96.

12. Tugulu, S. and H.-A. Klok, *Stability and Nonfouling Properties of Poly(poly(ethylene glycol) methacrylate) Brushes under Cell Culture Conditions.* Biomacromolecules, 2008. **9**(3): p. 906-912.

13. Sha, J., et al., *Sequential Nucleophilic Substitutions Permit Orthogonal Click Functionalization of Multicomponent PEG Brushes.* Biomacromolecules, 2013. **14**(9): p. 3294-3303.

14. Hudalla, G.A. and W.L. Murphy, *Chemically well-defined self-assembled monolayers for cell culture: toward mimicking the natural ECM.* Soft Matter, 2011. **7**(20): p. 9561-9571.

15. Sethuraman, A., et al., *Protein unfolding at interfaces: Slow dynamics of α-helix to β-sheet transition.* Proteins: Structure, Function, and Bioinformatics, 2004. **56**(4): p. 669-678.

16. Renner, L., et al., *Fibronectin Displacement at Polymer Surfaces.* Langmuir, 2005. **21**(10): p. 4571-4577.

17. Cano, T., N. Offringa, and R.C. Willson, *The effectiveness of three multi-component binding models in describing the binary competitive equilibrium*

adsorption of two cytochrome b5 mutants. Journal of Chromatography A, 2007. **1144**(2): p. 197-202.

18. Sun, Y. and K. Yang, *Analysis of mass transport models based on Maxwell–Stefan theory and Fick's law for protein uptake to porous anion exchanger.* Separation and Purification Technology, 2008. **60**(2): p. 180-189.
19. Yang, K., *Dynamic binary protein adsorption in ion-exchange media depicted with a parallel diffusion model derived from Maxwell–Stefan theory.* Chemical Engineering Science, 2016. **139**: p. 163-172.
20. Daly, S.M., T.M. Przybycien, and R.D. Tilton, *Coverage-Dependent Orientation of Lysozyme Adsorbed on Silica.* Langmuir, 2003. **19**(9): p. 3848-3857.
21. Iuliano, D.J., S.S. Saavedra, and G.A. Truskey, *Effect of the conformation and orientation of adsorbed fibronectin on endothelial cell spreading and the strength of adhesion.* Journal of Biomedical Materials Research, 1993. **27**(8): p. 1103-1113.
22. Lewandowska, K., et al., *Cell-Type-Specific adhesion mechanisms mediated by fibronectin adsorbed to chemically derivatized substrata.* Journal of Biomedical Materials Research, 1992. **26**(10): p. 1343-1363.
23. Keselowsky, B.G., D.M. Collard, and A.J. García, *Surface chemistry modulates fibronectin conformation and directs integrin binding and specificity to control cell adhesion.* Journal of Biomedical Materials Research Part A, 2003. **66A**(2): p. 247-259.
24. Ba, O.M., et al., *Protein covalent immobilization via its scarce thiol versus abundant amine groups: Effect on orientation, cell binding domain exposure and*

conformational lability. Colloids and Surfaces B: Biointerfaces, 2015. **134**: p. 73-80.

25. Klotzsch, E., et al., *Conformational distribution of surface-adsorbed fibronectin molecules explored by single molecule localization microscopy.* Biomaterials Science, 2014. **2**(6): p. 883-892.

26. Lin, M., et al., *Adsorption Force of Fibronectin on Various Surface Chemistries and Its Vital Role in Osteoblast Adhesion.* Biomacromolecules, 2015. **16**(3): p. 973-984.

27. Koepsel, J.T., et al., *Combinatorial screening of chemically defined human mesenchymal stem cell culture substrates.* Journal of materials chemistry, 2012. **22**(37): p. 19474-19481.

28. Schmitt, S.K., W.L. Murphy, and P. Gopalan, *Crosslinked PEG mats for peptide immobilization and stem cell adhesion.* Journal of Materials Chemistry B, 2013. **1**(9): p. 1349-1360.

29. Schmitt, S.K., et al., *Polyethylene Glycol Coatings on Plastic Substrates for Chemically Defined Stem Cell Culture.* Advanced Healthcare Materials, 2015: p. n/a-n/a.

30. Schmitt, S.K., et al., *Peptide Conjugation to a Polymer Coating via Native Chemical Ligation of Azlactones for Cell Culture.* Biomacromolecules, 2016.

31. Ameringer, T., et al., *Polymer coatings that display specific biological signals while preventing nonspecific interactions.* Journal of Biomedical Materials Research Part A, 2012. **100**(2): p. 370-379.

32. Qian, X., et al., *Enhancement of the propagation of human embryonic stem cells by modifications in the gel architecture of PMEDSAH polymer coatings.* Biomaterials, 2014. **35**(36): p. 9581-9590.

33. Nandivada, H., et al., *Fabrication of synthetic polymer coatings and their use in feeder-free culture of human embryonic stem cells.* Nat. Protocols, 2011. **6**(7): p. 1037-1043.

34. Lavanant, L., et al., *A Facile Strategy for the Modification of Polyethylene Substrates with Non-Fouling, Bioactive Poly (poly (ethylene glycol) methacrylate) Brushes.* Macromolecular bioscience, 2010. **10**(1): p. 101-108.

35. Telford, A.M., C. Neto, and L. Meagher, *Robust grafting of PEG-methacrylate brushes from polymeric coatings.* Polymer, 2013. **54**(21): p. 5490-5498.

36. Sweat, D.P., et al., *A Single-Component Inimer Containing Cross-Linkable Ultrathin Polymer Coating for Dense Polymer Brush Growth.* Langmuir, 2013. **29**(11): p. 3805-3812.

37. Kuang, J. and P.B. Messersmith, *Universal Surface-Initiated Polymerization of Antifouling Zwitterionic Brushes Using a Mussel-Mimetic Peptide Initiator.* Langmuir, 2012. **28**(18): p. 7258-7266.

38. Yang, K., et al., *Polydopamine-mediated surface modification of scaffold materials for human neural stem cell engineering.* Biomaterials, 2012. **33**(29): p. 6952-6964.

39. Canalle, L.A., D.W.P.M. Lowik, and J.C.M. van Hest, *Polypeptide-polymer bioconjugates.* Chemical Society Reviews, 2010. **39**(1): p. 329-353.

40. Dworak, A., et al., *Degradable polymeric nanoparticles by aggregation of thermoresponsive polymers and "click" chemistry.* Nanoscale, 2015. **7**(40): p. 16823-16833.

41. Thapa, P., et al., *Native Chemical Ligation: A Boon to Peptide Chemistry.* Molecules, 2014. **19**(9): p. 14461.

42. Charton, M., *Steric effects. I. Esterification and acid-catalyzed hydrolysis of esters.* Journal of the American Chemical Society, 1975. **97**(6): p. 1552-1556.

43. Manning, M.C., K. Patel, and R.T. Borchardt, *Stability of Protein Pharmaceuticals.* Pharmaceutical Research. **6**(11): p. 903-918.

44. Li, S., C. Schöneich, and R.T. Borchardt, *Chemical instability of protein pharmaceuticals: Mechanisms of oxidation and strategies for stabilization.* Biotechnology and Bioengineering, 1995. **48**(5): p. 490-500.

45. Kerwin, B.A. and R.L. Remmele, *Protect from light: Photodegradation and protein biologics.* Journal of Pharmaceutical Sciences, 2007. **96**(6): p. 1468-1479.

46. Astafieva, I.V., G.A. Eberlein, and Y. John Wang, *Absolute on-line molecular mass analysis of basic fibroblast growth factor and its multimers by reversed-phase liquid chromatography with multi-angle laser light scattering detection.* Journal of Chromatography A, 1996. **740**(2): p. 215-229.

47. Shahrokh, Z., et al., *Major Degradation Products of Basic Fibroblast Growth Factor: Detection of Succinimide and Iso-aspartate in Place of Aspartate15.* Pharmaceutical Research. **11**(7): p. 936-944.

48. Geiger, T. and S. Clarke, *Deamidation, isomerization, and racemization at asparaginyl and aspartyl residues in peptides. Succinimide-linked reactions that*

contribute to protein degradation. Journal of Biological Chemistry, 1987. **262**(2): p. 785-794.

49. Schrier, J.A., et al., *Degradation Pathways for Recombinant Human Macrophage Colony-Stimulating Factor in Aqueous Solution.* Pharmaceutical Research. **10**(7): p. 933-944.

50. Jaipa Patel, R.K., Rashbehari Tunga, Nadine M. Ritter, and Binita S. Tunga, *Stability Considerations for Biopharmaceuticals, Part 1: Overview of Protein and Peptide Degradation Pathways.* BioProcess International, 2011.

51. Bosnakovski, D.M., Morimichi; Kim, Gonhung; Takagi, Satoshi; Okumura, Masahiro; Fujinaga, Toru, *Chondrogenic differentiation of bovine bone marrow mesenchymal stem cells (MSCs) in different hydrogels: Influence of collagen type II extracellular matrix on MSC chondrogenesis.* Biotechnology and Bioengineering, 2006. **93**(6): p. 1152-1163.

52. Amable, P., et al., *Protein synthesis and secretion in human mesenchymal cells derived from bone marrow, adipose tissue and Wharton's jelly.* Stem Cell Research & Therapy, 2014. **5**(2): p. 53.

53. Bahramsoltani, M., et al., *Angiogenesis and Collagen Type IV Expression in Different Endothelial Cell Culture Systems.* Anatomia, Histologia, Embryologia, 2014. **43**(2): p. 103-115.

54. van der Smissen, A., et al., *Artificial extracellular matrices support cell growth and matrix synthesis of human dermal fibroblasts in macroporous 3D scaffolds.* Journal of Tissue Engineering and Regenerative Medicine, 2015: p. n/a-n/a.

55. Mann, B.K., et al., *Modification of surfaces with cell adhesion peptides alters extracellular matrix deposition.* Biomaterials, 1999. **20**(23–24): p. 2281-2286.

56. Wu, Y., et al., *Ascorbic acid promotes extracellular matrix deposition while preserving valve interstitial cell quiescence within 3D hydrogel scaffolds.* Journal of Tissue Engineering and Regenerative Medicine, 2015: p. n/a-n/a.

57. Elhadj, S., S.A. Mousa, and K. Forsten-Williams, *Chronic pulsatile shear stress impacts synthesis of proteoglycans by endothelial cells: Effect on platelet aggregation and coagulation.* Journal of Cellular Biochemistry, 2002. **86**(2): p. 239-250.

58. Decaris, M.L. and J.K. Leach, *Design of Experiments Approach to Engineer Cell-Secreted Matrices for Directing Osteogenic Differentiation.* Annals of Biomedical Engineering, 2010. **39**(4): p. 1174-1185.

59. Pham, Q.P., et al., *The influence of an in vitro generated bone-like extracellular matrix on osteoblastic gene expression of marrow stromal cells.* Biomaterials, 2008. **29**(18): p. 2729-2739.

60. Datta, N., et al., *Effect of bone extracellular matrix synthesized in vitro on the osteoblastic differentiation of marrow stromal cells.* Biomaterials, 2005. **26**(9): p. 971-977.

61. Ryu, J.Y., et al., *New Antifouling Platform Characterized by Single-Molecule Imaging.* ACS Applied Materials & Interfaces, 2014. **6**(5): p. 3553-3558.

62. Zhang, F., et al., *Modification of gold surface by grafting of poly(ethylene glycol) for reduction in protein adsorption and platelet adhesion.* Journal of Biomaterials Science, Polymer Edition, 2001. **12**(5): p. 515-531.

63. Herold, D.A., K. Keil, and D.E. Bruns, *Oxidation of polyethylene glycols by alcohol dehydrogenase.* Biochemical Pharmacology, 1989. **38**(1): p. 73-76.

64. Kloxin, A.M., et al., *Photodegradable Hydrogels for Dynamic Tuning of Physical and Chemical Properties.* Science, 2009. **324**(5923): p. 59-63.

65. Lutolf, M.P., P.M. Gilbert, and H.M. Blau, *Designing materials to direct stem-cell fate.* Nature, 2009. **462**(7272): p. 433-441.

66. Qiu, Y., et al., *PEG-based hydrogels with tunable degradation characteristics to control delivery of marrow stromal cells for tendon overuse injuries.* Acta Biomaterialia, 2011. **7**(3): p. 959-966.

67. Wilson, M.J., et al., *Hydrogels with well-defined peptide-hydrogel spacing and concentration: impact on epithelial cell behavior.* Soft Matter, 2012. **8**(2): p. 390-398.

68. Eyrich, D., et al., *Long-term stable fibrin gels for cartilage engineering.* Biomaterials, 2007. **28**(1): p. 55-65.

2.10 FIGURES

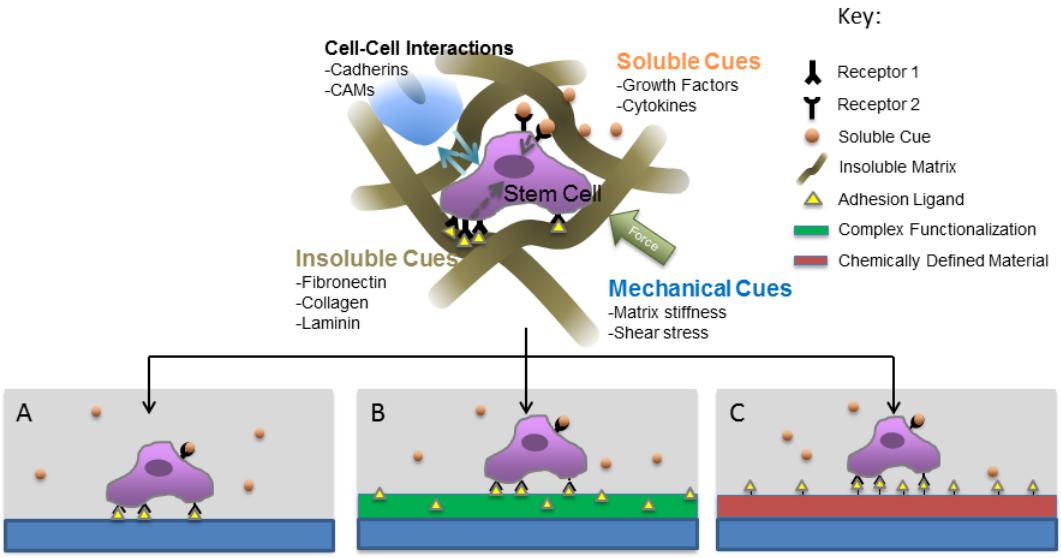

Figure 1. Cell culture systems can reproduce aspects of the cell microenvironment. A) Cells cultured on untreated TCPS adhere to adsorbed serum proteins and interact with soluble signals B) Complex biological functionalization adds insoluble cues derived from the extracellular matrix. C) Chemically defined, functionalizable materials (red) enable tailored presentation of bioactive ligands

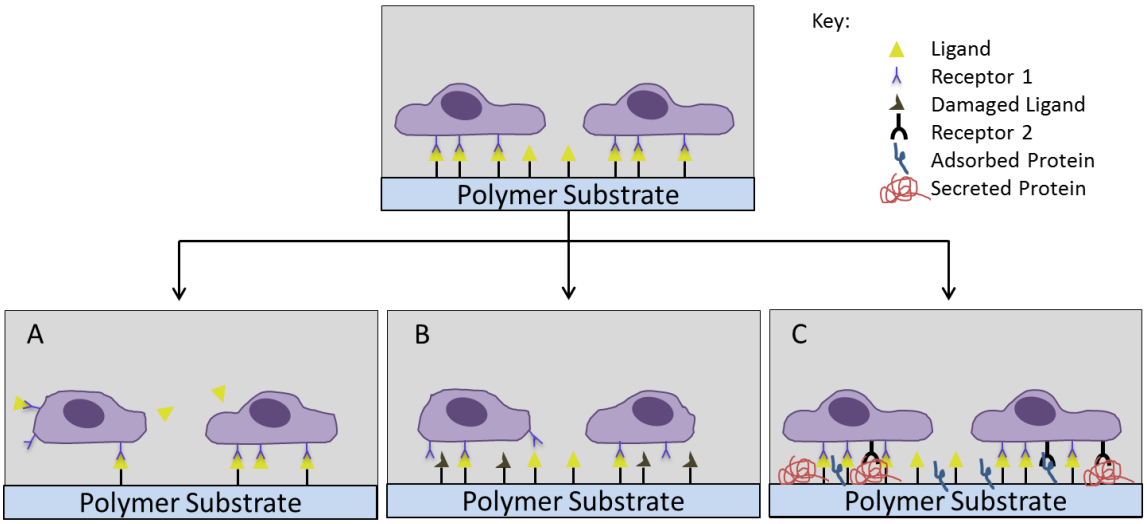

Figure 2.10.2. Over time, the cell-material interface can be dynamically altered through (A) removal of a cell-adhesive ligand from the surface, (B) degradation/denaturation of the ligand, and (C) fouling over time due to secreted or adsorbed molecules.

CHAPTER 3. SYNTHETIC, CHEMICALLY-DEFINED POLYMER-COATED MICROCARRIERS FOR THE EXPANSION OF HUMAN MESENCHYMAL STEM CELLS

Elements of this chapter have been published as:

John D. Krutty, Andrew D. Dias, Junsu Yun, William L. Murphy, and Padma Gopalan (2019). Synthetic, chemically-defined polymer-coated microcarriers for the expansion of human mesenchymal stem cells. *Macromolecular Biosciences.*

doi: 10.1002/mabi.201800299

3.1 PREFACE

In the previous chapter, we discussed the role of natural and synthetic biological coatings and polymers in cell culture. In this work, we introduce a chemically defined copolymer coating that was developed in our lab as a 2D crosslinkable mat. The copolymer is designed using reactive monomers to allow it to resist nonspecific cell adhesion while including reactive moieties to make it stable and tailorable to different biological applications. Here, a method is developed to apply this copolymer to 3D surfaces irrespective to their shape and size. We demonstrate its utility on 3D surfaces by coating microcarriers for the scaled-up expansion of human mesenchymal stem cells (hMSC). Copolymer coated microcarriers resist cell adhesion until functionalization with an integrin-binding peptide, enabling hMSC to adhere and grow while retaining their hMSC-like phenotype.

3.2 ABSTRACT

Mesenchymal stem cells (MSC), also called marrow stromal cells, are adult cells that have attracted much interest for their potential uses in therapeutic applications. There is a pressing need for scalable culture systems, due to the large number of cells needed for clinical treatments – up to millions of MSCs per kilogram of patient body weight. Here, we apply a tailorable thin polymer coating - poly(poly(ethelene glycol) methyl ether methacrylate-*ran*-vinyl dimethyl azlactone-*ran*-glycidyl methacrylate) [P(PEGMEMA-*r*-VDM-*r*-GMA); PVG] - to the surface of commercially available polystyrene (PS) and glass microcarriers to create chemically defined surfaces for large scale cell expansion. These chemically defined microcarriers create a reproducible surface that does not rely on the adsorption of xenogenic serum proteins to mediate cell adhesion. Specifically, this coating method anchors PVG copolymer through ring opening nucleophilic attack by amine residues on poly-L-lysine (PLL) that is pre-adsorbed to the surface of microcarriers. Importantly, this anchoring reaction preserves the monomer VDM reactivity for subsequent functionalization with an integrin-specific RGD peptide to enable cell adhesion and expansion via a one-step reaction in aqueous media. MSCs cultured on PVG-coated microcarriers achieve six-fold expansion - similar to the expansion achieved on PS microcarriers - and retain their ability to differentiate after harvesting.

3.3 INTRODUCTION

Mesenchymal stem cells (MSCs), also referred to as marrow stromal cells, are adult cells capable of differentiation down multiple cell lineages[1-5] and have demonstrated immunosuppressive and anti-inflammatory properties.[6] These traits make MSCs a target for potential therapeutic applications, with 500 ongoing or completed clinical trials as of 2016.[7]

Millions of MSCs per kilogram of patient are generally used for clinical applications,[8] underscoring a pressing need for scalable culture systems. In order to reduce the time and cost associated with the expansion of MSCs for clinical applications, innovation on the traditional, two-dimensional cell culture flasks has resulted in improved culture systems such as cellstack plates, bioreactors, and microcarriers [9]. Microcarriers are one system currently used for MSC expansion – 100-300 μm beads provide a surface for cell adhesion and are subsequently kept in suspension in a bioreactor. The constant mixing in the bioreactor provides gas and nutrient exchange that improves upon the diffusion limits that plague traditional cell culture. Microcarrier systems can produce relevant cell numbers – hundreds of millions of cells in a culture system – and show promise for scale-up to meet industrial lot size requirements, and offer improvements over traditional, two-dimensional cell culture including a high surface area, uniformity, and lower media and resource requirements.[10]

Microcarriers for cell culture may exist as a bare material or have a functional coating. Bare microcarriers are mainly made of polymers including poly(hydroxyethyl methacrylate) (PHEMA)[11], polystyrene (PS)[12-14], polyacrylamide (PA)[15, 16], poly(L-lactic acid) (PLLA)[17], and poly(lactic-co-glycolic acid) (PLGA).[18] Coatings for microcarriers consist of charged molecules, peptides (e.g. Corning Synthemax®, CellBIND®), or proteins (e.g. collagen, gelatin, Cultispher-S) that facilitate cell adhesion, typically with no potential for further customization or tailoring. Additional commercially available microcarriers include dextran-based Cytodex I, II, and III (GE Healthcare), Sigma-Solohill (collagen- or recombinant protein-coated), and Cultispher® (Percell Biolytica AB).

Commercially available versions of microcarriers are effective at up to 10-fold expansion of MSCs.[8, 12, 19-21] Despite the improvements they represent over tissue culture flasks, currently

commercially available microcarriers suffer from drawbacks similar to those that plague traditional cell culture methods, including the inability to provide a chemically defined surface for cell culture. A chemically defined surface can create a cell culture environment with homogeneous presentation of adhesive signals and repeatability that does not rely on the batch-to-batch variability[22] of natural protein matrices or adsorbed serum proteins, which can effect cell behavior and lineage determination.[23-25] A microcarrier that presents a cell-adhesive peptide on a chemically defined surface would potentially provide cell adhesion and expansion seen in commercially available microcarriers while also minimizing non-specific adsorption of proteins present in cell culture media. This innovation represents step towards the creation of a xeno-free cell culture system for the expansion of MSCs. Xenogenic components of cell culture media, like fetal bovine serum (FBS), can introduce variability to the cell culture media.[26, 27] Additionally, the use of cells that have been cultured in media containing FBS has been reported to create an immunological response to FBS proteins.[28, 29]

Here, we present a method to convert existing microcarriers into chemically defined microcarriers by coating them with a copolymer. We recently developed and validated the chemically defined synthetic copolymer coating, poly (polyethylene glycol methyl ether methacrylate – *ran* – vinyl dimethyl azlactone – *ran* – glycidyl methacrylate) [P(PEGMEMA-*r*-VDM-*r*-GMA), hereafter referred to as PVG] in 2D, spin-coated onto flat substrates. When functionalized with the cell adhesive peptide sequence Arg-Gly-Asp (RGD) this surface is suitable for MSC adhesion and expansion.[30-32] Peptide conjugation through ring-opening of the VDM monomer was optimized to 1mM in phosphate buffered saline (PBS) solution at room temperature. The reported reaction efficiency is ~ 70%.[31,32] We present a method here to covalently anchor the PVG copolymer to amine groups presented on the surface of existing PS-

based microcarriers to create a chemically defined, customizable microcarrier. These PVG-coated microcarriers resist nonspecific protein adsorption and prevent the adhesion of cells. The coated microcarriers can then be functionalized with integrin-specific RGD peptide to restore adhesion and expansion of MSCs.

3.4 RESULTS

3.4.1. PVG Coating of Multiwell Plates

In our previous work we have shown that the PVG copolymer can be crosslinked to create a coating on a range of planar substrates including PS substrate, and the coating is stable under typical cell culture conditions.[30-32] On the planar substrate, control of the coating thickness and uniformity was achieved through spin rate and polymer concentration during spin coating. However, spin coating is not a viable option on the 3D microcarrier surfaces. Hence, to have a uniform coating on spherical microcarriers, we developed a process that used an anchoring layer to react with the epoxy groups in the PVG. The anchoring layer is a poly-L-lysine (PLL) layer which presents primary amines that readily react with the epoxy groups in the PVG. Using this method, the PVG copolymer coating was applied to both 2D and 3D polystyrene (PS) substrates as described in the Materials and Methods section (**Figure 3.9.1**, **Figure 3.9.2a**). We prepared the analogous 2D surfaces in order to analyze the elemental content and reactivity of the anchored PVG. PVG layer was applied to a silicon wafer via the sequential anchoring process (**Figure 3.9.2a)**. The silicon from the substrate provides an internal standard for absolute quantification of the elemental nitrogen content resulting from the overlying coating. After each stepwise addition of a nitrogen-containing material (PLL, PVG, RGD Peptide), the ratio of [atomic % nitrogen / atomic % silicon] increased, which confirms the successful addition

of a nitrogen-containing layer (**Figure 3.9.2b**). Monitoring the water contact angle of the surface after each layer addition also provides a second means of verifying the chemistry. Starting with a planar PS surface, the water contact angle measurement decreased after PLL and PVG were added to the coating, which is representative of a more hydrophilic surface (**Figure 3.9.2c, Supplemental Figure S3.10.2**). The average water contact angle of 52.7° on a PVG-coated surface was consistent with previously reported value of 59° for a 30nm thick PVG coating, and 52° for 6nm thick PEG brushes[32]. Finally, we used PM-IRRAS to determine the mode of anchoring between the PVG and PLL layers. The two possibilities are that the reaction between PVG and PLL occurs by nucleophilic ring opening of the VDM ring by the primary amines in PLL, or the VDM stays largely intact and the anchoring occurs by ring opening to the GMA groups in PVG (**Figure 3.9.2d**). The PM-IRRAS studies require a gold coated glass substrate, on which PLL does not readily adsorb. Hence, we first deposited a carboxylic acid-terminated self-assembled monolayer (SAM) of hexa(ethylene glycol) dodecane thiol (See Methods section). These SAMs then reacted with PLL through EDC/NHS chemistry to bind PLL to the surface. The intact oxazoline ring present in VDM shows an absorbance at 1818 cm^{-1}. PLL-functionalized SAMs (blue line) show no peak at 1818 cm^{-1}, while PVG-functionalized surfaces (green line) show a peak centered at 1818 cm^{-1}. This suggests that the PLL-PVG reaction is predominantly occurring through the ring-opening of the epoxide in the GMA side chain under the conditions employed, leaving the the VDM ring largely intact for further functionalization with peptides. Additionally, SAMs that were reacted with PVG but not PLL showed no detectable peak at 1818cm^{-1}, which provided further evidence that the anchoring of PVG to the surface is PLL-dependent. The lack of a peak at 915 cm^{-1} indicates that there is no intact epoxide on these surfaces[33], providing further evidence for the proposed mechanism. (full spectra in

Supplemental Figure S3.10.3, 800-1200 cm^{-1} spectra in **Supplemental Figure S3.10.4**). Finally, we analyzed whether PLL will desorb from the surface of PVG coated microcarriers. We prepared microcarriers using a fluorescently tagged PLL and incubated in cell culture media for seven days. The media fluorescence did not increase above the baseline, indicating a non-significant desorption of PLL from the microcarrier surface (**Supplemental Figure S3.10.5**). The PVG-coated microcarriers were reacted with a fluorescent SDP ester, to confirm the presence of the PVG coating via fluorescence microscopy (**Figure 3.9.2e**). In the absence of the PLL layer, the PVG coating did not attach to the microcarrier and hence did not fluoresce (**Supplemental Figure S3.10.1**). These results also suggest that the presence of PVG was not due to adsorption of the PVG layer to the microcarrier, since the microcarriers did not fluoresce in the absence of the anchoring layer.

3.4.2 Cell Attachment to Microspheres

We used the sequential anchoring method to create PLL- and PVG-coated PS microspheres. The PVG-coated microcarriers were then split into three groups: unmodified PVG, PVG functionalized with an integrin-binding RGD, and PVG functionalized with a scrambled version of the RGD peptide (RDG, scram). MSCs seeded onto microcarriers at a density of 10,000 cells cm^{-2} attached and grew for 24 hours, at which point they were either fixed and fluorescently stained or lysed and analyzed for DNA content using the CyQuant® Proliferation Assay kit. Representative images of the prepared microcarriers (**Figure 3.9.3a**), stained for actin and nuclei, showed adhesion to the surface of the PS, PLL (not shown), and RGD-functionalized microcarriers, while the PVG and scramble RDG-functionalized (not shown) conditions showed aggregates of cells adhered to one another but were not associated with a microcarrier.

MSCs grown for 24h in the PS, PLL and RGD-functionalized conditions exhibited a significantly higher cell number than cells grown on the PVG and scramble-functionalized conditions (**Figure 3.9.3b**). The non-adherent PVG and scramble conditions maintained a DNA content similar to that of the number of cells that were seeded.

3.4.3 Cell Expansion and Differentiation on Microspheres

To study the potential for expansion of MSCs in microcarrier culture, we seeded hMSCs onto PS, PLL-coated, and PVG-coated microcarriers functionalized with RGD. The number of cells increased in these conditions, as opposed to the PVG-coated and scramble peptide-coated microcarriers, in which the number of cells did not change over the course of seven days (**Figure 3.9.4a**). PS, PLL-coated and PVG-RGD microcarriers all achieved 6x expansion by 4 days, at which point the cell density was high enough to form cell-and-microcarrier aggregates – large clumps in which multiple microcarriers were held together by a mass of MSCs (**Figure 3.9.4b**).

Additionally, MSCs did not adhere to PVG-coated glass microcarriers, but expanded on RGD-functionalized PVG-coated glass microcarriers, demonstrating the versatility of the sequential anchoring application of PVG (**Supplemental Figure S3.10.6**). To test whether MSCs that had been cultured on PVG-RGD coated microcarriers retained their potential to differentiate down multiple lineages, hMSCs were harvested from microcarriers with trypsin and mechanical agitation after 7 days of culture, then induced to either osteogenic or adipogenic differentiation. The differentiated cells stained positive for mineral deposits or lipid droplets, respectively, suggesting that hMSCs retained their capacity to differentiate to both osteoblasts and adipocytes, respectively, after expansion on microcarriers (**Figure 3.9.5a,c**). Cells cultured on all microcarrier conditions showed similar levels of lipid droplet or mineral deposition post-differentiation (**Figure 3.9.5b,d**). The ability of hMSCs to differentiate post culture on PVG-

RGD microcarriers suggests that PVG-coated microcarrier culture does not cause a substantial loss of multipotency in hMSCs.

3.5 DISCUSSION AND CONCLUSION

The large number of clinical trials focused on using human cells in general and hMSCs in particular[8] underscores the need for cost effective, scalable, chemically defined and reproducible cell culture methods. Previously, we have reported on a PEG-based, functionalizable coating for 2D surfaces, PVG[30-32]. In order to meet the needs of scalable cell manufacturing, here, we have developed a sequential anchoring mechanism to create PVG-coated microcarriers. The PVG coating permits on-demand functionalization with desired peptides in a one-step, aqueous reaction. We functionalized PVG-coated microspheres with an RGD-containing peptide and a scrambled version of the peptide. We have shown evidence for the mechanism of this application using fluorescence microscopy, XPS and PM-IRRAS, which together suggest that the PVG is present on the surface of the microcarriers, chemically bound to the surface, and presents intact VDM rings for efficient conjugation of peptides.

hMSCs attached readily to RGD-functionalized microcarriers at levels similar to the commercially available PS microcarriers but did not attach to PVG-coated microcarriers functionalized with a scrambled version of this peptide. Twenty-four hours post-seeding, the DNA content in these non-adherent conditions indicated that the cells that had been seeded remained in culture (**Figure 3.9.3b**). However, cells in these conditions attached poorly and formed aggregates that were not attached to microcarriers (**Figure 3.9.3a**). These aggregates would be expected to have the same amount of DNA as the number of seeded cells but would not be expected to survive and grow. As expected, the cells grown on blank PVG-coated and PVG-

coated + RDG (scramble) functionalized microcarriers did not expand over time (**Figure 3.9.4**). Overall hMSC expansion on PVG-coated + RGD functionalized microcarriers was less than expansion on the uncoated PS microcarriers after 7 days, but expansion on the PS, PLL-coated, and PVG-coated + RGD functionalized microcarriers were comparable after 4 days. The decrease in MSC proliferation on PVG-coated + RGD and PLL-coated microcarriers after 4 days can potentially be attributed to higher levels of microcarrier aggregation (**Figure 3.9.4b**). This decrease in cell expansion across all conditions could be due to aggregation of the microcarriers, which was substantial starting at day 4, especially in PVG-coated microcarriers compared to PS or PLL microcarriers. This increased aggregation may be driven by cells adhering to multiple microcarriers at once, forming a cluster. These clusters potentially reduce the amount of available surface area for cell growth, increasing the contact between cells leading tocontact inhibition of proliferation, which halts the cell cycle and reduces cell division. To overcome this plateau in expansion, future studies will seek to optimize factors including microcarrier diameter, PVG concentration, and adhesion peptide density to maintain cell adhesion while reducing aggregation.

The ability to functionalize PVG coated microcarriers with the desired peptides opens opportunities for driving growth of multiple cell types through the incorporation of peptides that react with different cell receptors. For example, microcarriers can be tailored for specific cell types using attachment peptides (e.g., IKVAV) or growth factor sequestering peptides to drive cell proliferation. Additionally, the incorporation of biologically active peptides to the PVG surface is simple and does not require harsh solvents – the reaction consists of an hour-long incubation with a cysteine-containing peptide at room temperature – lending to its ease of use and eliminating the need for activation steps or harsh solvent conditions. The concentration of

peptides needed for functionalization is very low, 1mM, which will keep the cost of production low for large scale applications such as those required for clinical applications. PVG coated microcarriers also represent a chemically defined surface that does not rely on the adsorption of serum proteins to enable cell adhesion. While MSCs were cultured in media containing FBS for this work, this surface represents a xeno-free culture surface and a step towards a completely xeno-free culture system. We are not aware of any other microcarrier for cell culture that is tailorable to unique applications in an aqueous, one-step process. As such, this development represents an important innovation in the field which could increase the ease with which this technology is adopted. Additionally, these PVG-coated microcarriers remain capable of facilitating MSC adhesion after 1 month of storage, making them suitable for long-term use (**Supplemental Figure S3.10.7**). In this work, we demonstrated the addition of cell attachment functionality which supported hMSC multilineage differentiation capacity after expansion, suggesting that these microcarriers are a relevant platform for expanding cells while maintaining hMSC functionality.

3.6 EXPERIMENTAL SECTION

3.6.1 PVG coating of microcarriers*:* Untreated polystyrene microcarriers with diameter of 125-212 μm (Corning, Corning, NY) were weighed and incubated in 0.01wt% 70,000-150,000 Da poly-L-lysine (Sigma-Aldrich, Milwaukee, WI) for 1 hour. PLL adsorbs to polystyrene largely though hydrophobic interactions and its use is common in cell culture applications[34-36]. Microcarriers were then washed twice with dH_2O and once with EtOH. Microcarriers were placed in a 10mg mL^{-1} solution of PVG polymer in EtOH and allowed to react overnight. Microcarriers at this state were stored in EtOH at -20°C for up to 1 month.

3.6.2 Stability of PLL: First, poly-L-lysine hydrobromide (MW 70,000-100,000) (Sigma Aldrich) was dissolved in 0.1M bicarbonate buffer at a concentration of 10mg mL-1. Alexa Fluor 488 SDP Ester (Thermo Fisher, Waltham, MA) was added to the PLL solution according to manufacturer recommendations. Briefly, SDP ester was dissolved at 10mg mL-1 in dimethyl formamide. The SDP ester solution was slowly added to the PLL solution to achieve a final concentration of 1 mg mL-1. The reaction was allowed to proceed overnight under dark conditions. The reaction products were purified using a Slide-a-Lyzer dialysis kit with a pore size of 2000 molecular weight cutoff, dialyzed against distilled water overnight. The purified product was dissolved in water to create a 0.01 wt% solution. A dilution series of 0.01 wt% solution was used to measure the florescence intensity and construct the standard curve. The 0.01 wt% solution was used to create PVG-coated microcarriers as described previously. These microcarriers were incubated at 37°C and 5% CO2 for 1, 2, 4, or 7 days in αMEM + 10% FBS, at which point samples of the supernatant were taken and analyzed for fluorescence at an excitation/emission of 485/528 using a BioTek Synergy HTX (BioTek, Winooski, VT) plate reader.

3.6.3 Peptide Immobilization*:* PVG-coated microcarriers were washed twice with PBS and reacted with Cys-Gly-Gly-Gly-Arg-Gly-Asp-Ser-Pro (CGGGRGDSP, "RGD"), Cys-Gly-Gly-Gly-Arg-Asp-Gly-Ser-Pro (CGGGRDGSP, "scramble") peptides (Genscript). Microcarriers were incubated in 1mM peptide solutions in 1x phosphate buffered saline (PBS) (Fisher Scientific) for 1 hr at room temperature according to the procedure in Schmitt et al. (2015, 2016).

The microcarriers were then rinsed twice with PBS and sanitized in 70% ethanol for 30 minutes before use in cell culture.

3.6.4 Water Contact Angle*:* Polystyrene substrates were modified with PVG copolymer according to the procedure noted in th *PVG coating of microcarriers* section above. Water contact angle measurements were used to confirm the change in surface properties after modifying PS surfaces with PLL, PVG, and the RGD peptide. Measurements were taken using a Dataphysics OCA 15 Plus instrument with an automatic liquid dispenser. Static water contact angles were measured using 5μL of deionized water in four different places on each sample. Two angles were taken for each droplet and are reported as the average plus or minus the standard deviation.

3.6.5 XPS*:* Elemental analysis of PVG functionalization of 2D surfaces was done using X-ray Photoelectron Spectroscopy (XPS). Measuments were taken using a Thermo Scientific Model K-Alpha XPS instrument with monochromatic Al Kα radiation (1486.7 eV). Survey spectra and high-resolution spectra were acquired using analyzer pass energies of 200 and 50 eV, respectively. Single point analysis was done on three separate points with a spot size of 400 μm for each point. Data was collected and analyzed in the Avantage XPS software package. Peak fitting was done with Gaussian/Lorentzian peak shapes and a Shirley/Smart background.

3.6.6 PM-IRRAS*:* Self-assembled monolayers (SAMs) of carboxylic acid-terminated hexa(ethylene glycol) dodecane thiol at a concentration of 1mM in EtOH (ProChimia Surfaces, Gdansk area, Poland) were formed on gold substrates (1000 Å, EMF Corporation, TA134), 1x1".

The carboxylic acid was activated into a reactive ester using a solution of N-(3-Dimethylaminopropyl)-N'-ethylcarbodiimide (EDC, 100mM) (Sigma Aldrich) and N-hydroxy succinimide (NHS, 250 mM) (Sigma Aldrich). 0.1wt% poly-L-lysine in distilled water was covalently bound to the surface through its N-terminal amine. PVG (10 mg mL^{-1} in EtOH) was placed on the surface and allowed to react overnight. Samples were rinsed three times with 200 proof ethanol (Pharmaco-Aaper) and dried under N_2. The samples were then placed at an incident angle of 83° in a Nicolet iS50 Fourier transform IR spectrophotometer equipped with a photoelastic modulator (PEM-90, Hinds Instruments, Hilsoboro, OR), a synchronous sampling demodulator (SSD-100, GWC Technologies, Madison, WI), and a liquid nitrogen cooled mercury– cadmium–telluride detector. The modulation was set at 1600 cm^{-1} and 1000 scans were obtained for each sample with a resolution of 8 cm^{-1}. The aperture was set to a size of 10 in the OMNIC software, corresponding to a spot size less than 5mm. The differential reflectance IR spectra were then normalized and converted to absorbance spectra using OMNIC software.

3.6.7 hMSC culture and cell quantification*:* MSCs were cultured in Minimum Essential Medium – Alpha modification (Corning, Corning MA) plus 10% fetal bovine serum (FBS) (Gibco, Cat. #16000-044, Dublin, Ireland). To evaluate hMSC attachment to PVG-coated and functionalized microcarriers, passage 4-6 hMSCs were seeded (10,000 cells cm^{-2}) on PS, PLL-coated, PVG-coated, RGD functionalized and scramble functionalized microcarriers, prepared as previously described. After 24 hours, the cells were either fixed, stained, and imaged or lysed for total DNA quantification using a CyQUANT® Cell Proliferation Assay Kit (Thermo Fisher Scientific, Waltham, MA). Fluorescence from the CyQUANT® assay was read at an emission of

527nm using a BioTek Synergy HTX plate reader. Cell standards were normalized to the intensities of known numbers of hMSC.

To study hMSC expansion on functionalized microcarrier surfaces, hMSCs were grown for up to a week in each of the different coating conditions. At desired time points (1, 2, 4, and 7 days), cells were lysed, and total DNA was quantified using a CyQUANT® Cell Proliferation Assay Kit, per kit instructions. Cell expansion was calculated by dividing the cell number on each day by the number of cells initially seeded on the microcarriers.

3.6.8 Fluorescent imaging*:*

MSCs*:* hMSCs were washed with 1x PBS and fixed in 10% buffered Formalin for 20-30 minutes. Cells were then permeabilized with 0.1% Triton X-100 (MP Biomedicals, Aurora, OH) in 1x PBS for 20 minutes. Cells were washed twice with PBS and blocked using 1% bovine serum albumin (BSA) (Fisher Scientific). Cells were stained for actin cytoskeleton using Alexa-Fluor^{TM} 647 Phalloidin (Thermo Fisher) and for nuclei using 4',6-Diamidine-2'-phenylindole dihydrochloride (DAPI) (Sigma Aldrich) for 30 minutes each, washing in between with PBS. Cells were imaged on an inverted microscope with DAPI, FITC, and Far Red filter cube sets.

PVG-coated microcarriers: PS microspheres were prepared by incubating in PBS or 0.1% PLL for 1h at room temperature. PVG (10mg mL^{-1} in EtOH) reacted with the surface overnight. Microcarriers were then stained with Alexa Fluor 488 5-sulfodichlorophenol (SDP) ester for 1 hour and imaged on an inverted microscope with a FITC filter cube set.

3.6.9 hMSC differentiation and analysis*:* To evaluate differentiation capacity after expansion on coated microcarriers, hMSCs were differentiated to osteoblasts and adipocytes based on

established protocols. For differentiation, hMSCs were seeded at 5000 cells·cm^{-2} on collagen-coated plates (Corning, Corning, NY) in 10% FBS in αMEM, and permitted to grow to confluence for three days. Osteogenic (OS) medium and adipogenic induction medium (AIM) were prepared. OS medium consisted of 10% FBS in αMEM with 0.1 μM dexamethasone, 10 mM β glycerol phosphate, and 50 μM ascorbic acid 2-phosphate. AIM consisted of 10% FBS in Dulbecco's Modification of Eagle's Medium (DMEM) high glucose with penicillin (100 U mL^{-1})/streptomycin (100 μg mL^{-1}), 1 μM dexamethasone, 10 μg mL^{-1} insulin, and 500 μM isomethyl isobutyl xanthine (IBMX). Media was changed every 3-4 days, and analysis was performed after 21 days of differentiation. As negative controls, cells were grown for 21 days in 10% FBS in αMEM.

Alizarin Red S stained mineral deposits from osteoblasts, and Oil Red O stained lipid droplets in adipocytes. To perform staining, cells were fixed in 10% buffered formalin solution and incubated Alizarin Red S (40 mM, pH 4.1-4.3) and washed with water three times or Oil Red O working solution for 20 minutes and washed with water until washings were clear. Working Oil Red O solution was prepared by mixing three parts stock Oil Red O solution (3 mg mL^{-1} in 99% isopropanol) with two parts distilled water and filtering with a 0.2 μm syringe filter.

3.6.10 Statistical Analysis

Experiments were carried out and repeated a total of two to three trials, with n=4 replicates per trial. Except where noted, a one-way ANOVA was conducted to determine significance, as there are multiple groups with one independent variable. A post-hoc Tukey's test was then used to determine significance between groups.

3.7 ACKNOWLEDGEMENTS

This research was funded by the National Science Foundation (NSF DMR **1709179**)

). The authors acknowledge support from staff and the use of equipment at the Materials Science Center at UW-Madison DMR-1121288 and DMR-1720415.

3.8 REFERENCES

[1] M. F. Pittenger, A. M. Mackay, S. C. Beck, R. K. Jaiswal, R. Douglas, J. D. Mosca, M. A. Moorman, D. W. Simonetti, S. Craig, D. R. Marshak. *Science* **1999**;284:143-7.

[2] X. Shen, B. Pan, H. Zhou, L. Liu, T. Lv, J. Zhu, X. Huang, J. Tian. *J. Biomed. Sci* **2017**;24:29.

[3] A. Singh, A. Singh, D. Sen. *Stem Cell Res. Ther.***2016**;7:82.

[4] G. V. Silva, S. Litovsky, J. A. R. Assad, A. L. S. Sousa, B. J. Martin, D. Vela, S. C. Coulter, J. Lin, J. Ober, W. K. Vaughn, R. V. C. Branco, E. M. Oliveira, R. He, Y.-J. Geng, J. T. Willerson, E. C. Perin. *Circulation* **2005**;111:150-6.

[5] A. Augello, C. De Bari. *Hum. Gene Ther.* **2010**;21:1226-38.

[6] G. Ren, L. Zhang, X. Zhao, G. Xu, Y. Zhang, A. I. Roberts, R. C. Zhao, Y. Shi. *Cell Stem Cell*;2:141-50.

[7] T. Squillaro, G. Peluso, U. Galderisi. *Cell Transplantation* **2016**;25:829-48.

[8] F. dos Santos, P. Z. Andrade, M. M. Abecasis, J. M. Gimble, L. G. Chase, A. M. Campbell, S. Boucher, M. C. Vemuri, C. L. da Silva, J. M. S. Cabral. *Tissue Eng., Part C* **2011**;17:1201-10.

[9] K. M. Panchalingam, S. Jung, L. Rosenberg, L. A. Behie. *Stem Cell Res. Ther.***2015**;6:225.

[10] J. Rowley, E. Abraham, A. Campbell, H. Brandwein, S. Oh. *BioProcess International* **2012**;10:16-22.

[11] H. Ayhan, A. Kozluca, E. Pişkin, I. Gurhan. *J. Bioact. Compat. Polym***1999**;14:17-30.

[12] T. R. J. Heathman, V. A. M. Glyn, A. Picken, Q. A. Rafiq, K. Coopman, A. W. Nienow, B. Kara, C. J. Hewitt. *Biotechnol. Bioeng.***2015**;112:1696-707.

[13] D. S. Mark Szczypka, Heather Woolls,Heather Brandwein. *BioProcess Int.* **2014**.

[14] D. K. Aletta Schnitzler, Janice Simler, Anthony DiLeo, Andrew Ball. *BioPharm Int.* **2012**;25.

[15] S. Reuveny, A. Mizrahi, M. Kotler, A. Freeman. *Dev. Biol. Stand.* **1983**;55:11-23.

[16] S. Reuveny, A. Mizrahi, M. Kotler, A. Freeman. *Ann. N. Y. Acad. Sci.* **1983**;413:413-5.

[17] H. Tan, J. Wu, D. Huang, C. Gao. *Macromol. Biosci.* **2010**;10:156-63.

[18] K. W. Chun, H. S. Yoo, J. J. Yoon, T. G. Park. *Biotechnol. Prog.* **2004**;20:1797-801.

[19] M. Szczypka, D. Splan, H. Woolls, H. Brandwein. *BioProcess Int.* **2014**;12:54-64.

[20] S. Frauenschuh, E. Reichmann, Y. Ibold, P. M. Goetz, M. Sittinger, J. Ringe. *Biotechnol. Prog.* **2007**;23:187-93.

[21] D. Schop, R. van Dijkhuizen-Radersma, E. Borgart, F. W. Janssen, H. Rozemuller, H. J. Prins, J. D. de Bruijn. *J. Tissue Eng. Regener. Med.* **2010**;4:524-31.

[22] C. W. Cheng, L. D. Solorio, E. Alsberg. *Biotechnol. Adv.* **2014**;32:462-84.

[23] F. M. Watt, W. T. S. Huck. *Nat. Rev. Mol. Cell Biol.* **2013**;14:467.

[24] D. S. W. Benoit, M. P. Schwartz, A. R. Durney, K. S. Anseth. *Nat. Mater.* **2008**;7:816.

[25] G. Maheshwari, G. Brown, D. A. Lauffenburger, A. Wells, L. G. Griffith. *J. Cell Sci.* **2000**;113:1677-86.

[26] Z. Xiaoyang, B. Haven, H. W. S., F. Farah, M. Michael, P. Erno. *Biotechnol. Prog.* **2006**;22:1294-300.

[27] C. Tekkatte, G. P. Gunasingh, K. M. Cherian, K. Sankaranarayanan. *Stem Cells Int.* **2011**;2011:504723.

[28] T. A. Selvaggi, R. E. Walker, T. A. Fleisher. *Blood* **1997**;89:776-9.

[29] A. Mackensen, R. Dräger, M. Schlesier, R. Mertelsmann, A. Lindemann. *Cancer Immunol. Immunother.* **2000**;49:152-6.

[30] S. K. Schmitt, W. L. Murphy, P. Gopalan. *J. Mater. Chem. B* **2013**;1:1349-60.

[31] S. K. Schmitt, D. J. Trebatoski, J. D. Krutty, A. W. Xie, B. Rollins, W. L. Murphy, P. Gopalan. *Biomacromolecules* **2016**;17:1040-7.

[32] S. K. Schmitt, A. W. Xie, R. M. Ghassemi, D. J. Trebatoski, W. L. Murphy, P. Gopalan. *Adv. Healthcare Mater.* **2015**;4:1555-64.

[33] R. Giménez, X. F. Fernández-Francos, J. M. Salla, A. Serra, A. Mantencón, X. Ramis. *Polymer.* **2015**;46(24):10637-10647.

[34] W. G. Wood, A. Gadow. *J. Clin. Chem. Clin. Biochem.* **1983**; 21:789,797.

[35] W.D Corry. *J. Colloid Interface Sci.* **1978**; 63: 151-160.

[36] D. Mazia, G. Schatten, W. Sale. *J. Cell Biol.* **1975**; 66(1) 198-200.

3.9 FIGURES

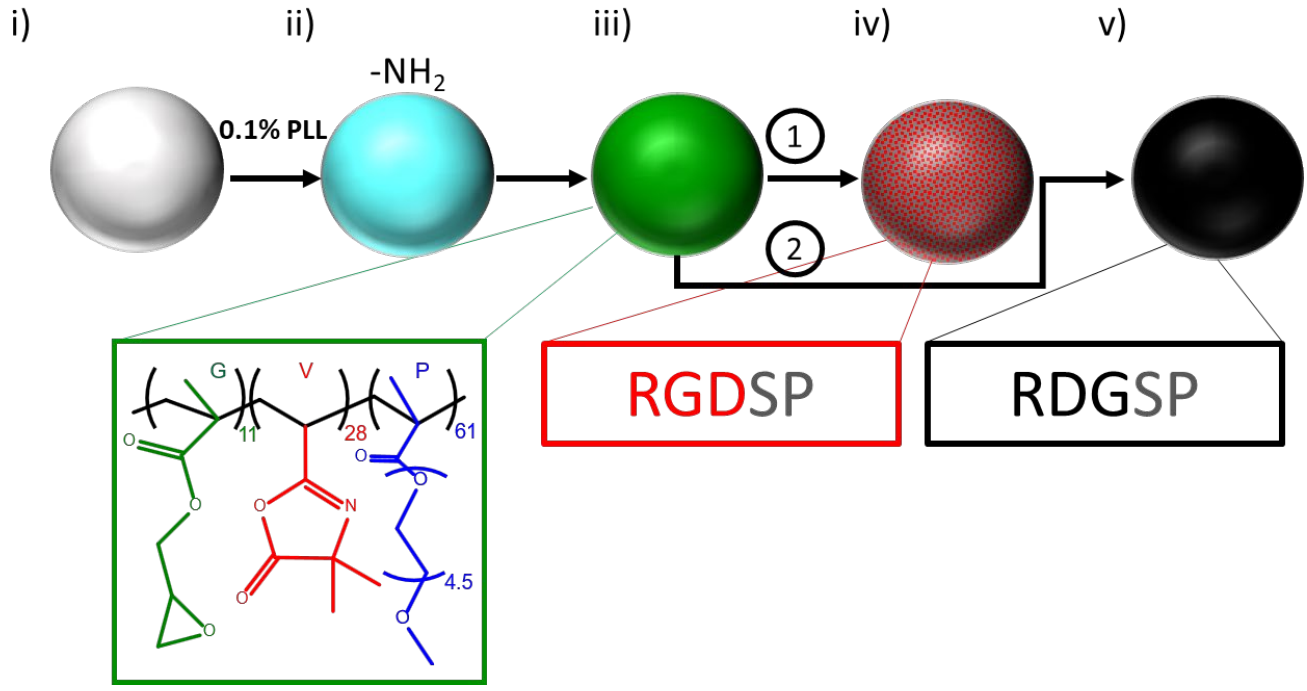

Figure 3.9.1. Schematic of coating process (i) Polystyrene microcarriers are coated in (ii) (PLL) and (iii) PVG. Desired peptides can be applied to this coating, in this example a peptide functionalized with (iv) Arg-Gly-Asp (RGD) and (v) a scrambled version of the peptide.

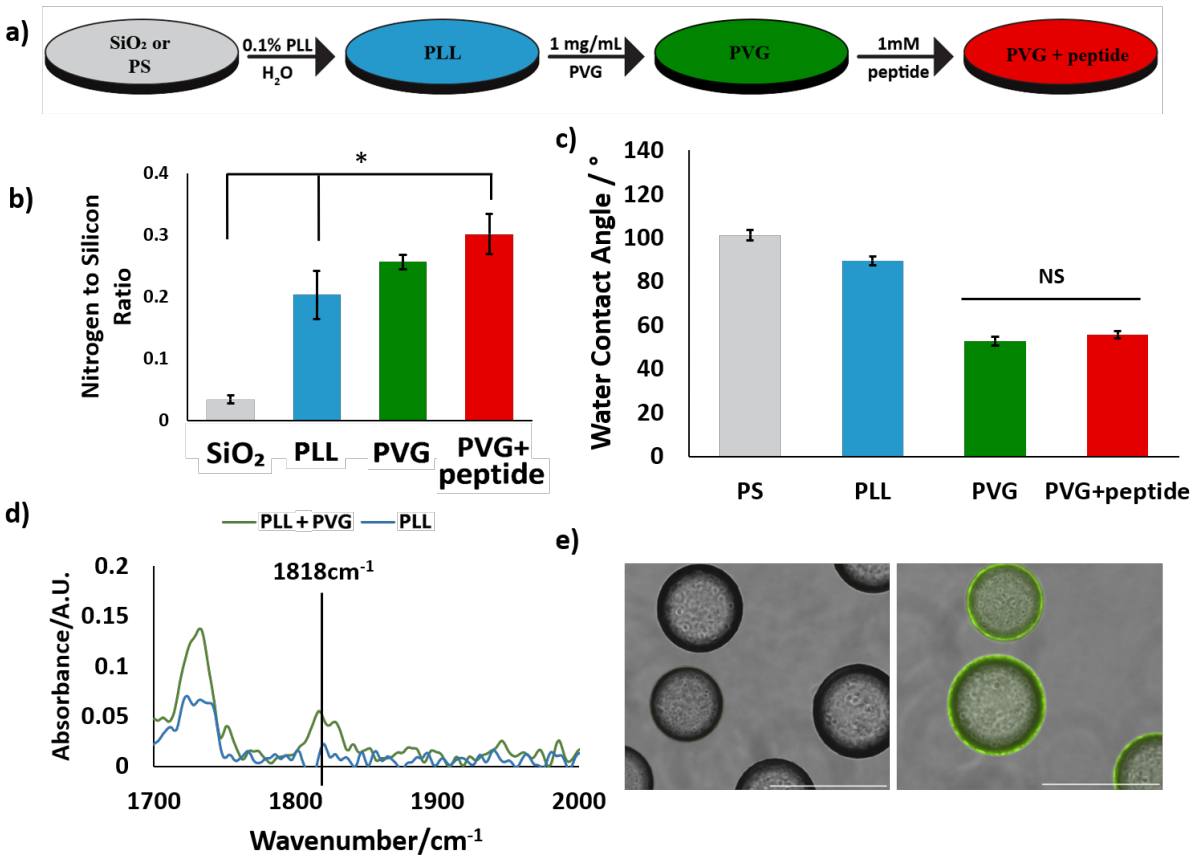

Figure 3.9.2. Characterization of the sequential anchoring PVG coating method. a) Schematic representation of sequential anchoring process on 2D surfaces. b) XPS N/Si ratio increases in each step of polymer coating process in 2D. *$p<0.05$ by one-way ANOVA. c) contact angle measurements of coated and uncoated PS samples. Significance of $p<0.05$ except where noted. d) PM-IRRAS of PVG-coated slides show intact peak at -1818 (oxazoline ring). e) Fluorescence micrograph of uncoated (left) and PVG-coated (right) microcarriers. Scale bar = 200 µm.

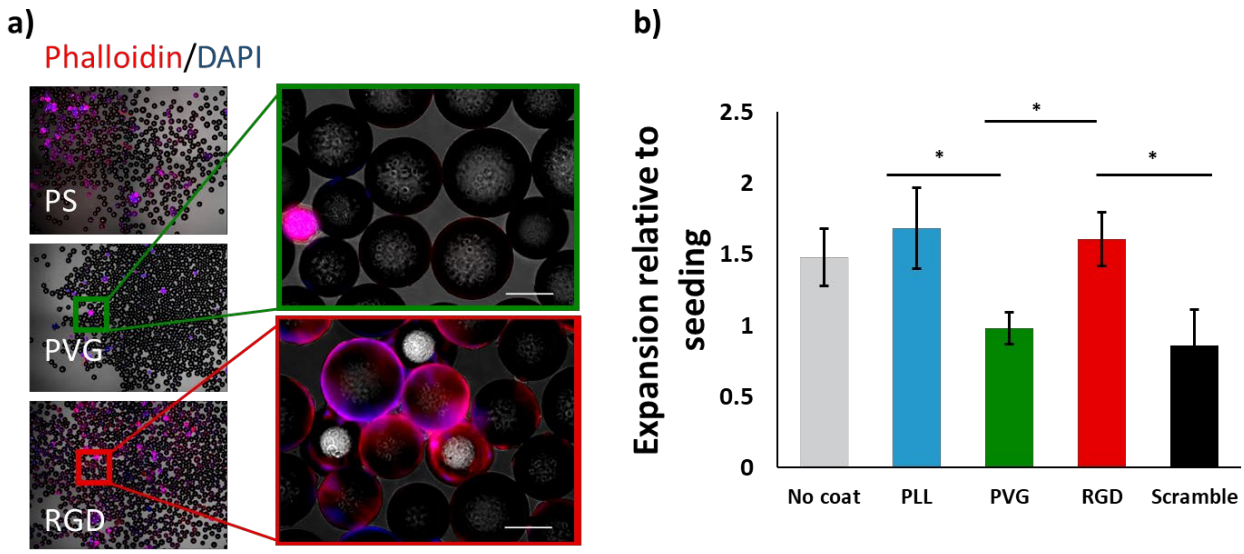

Figure 3.9.3. hMSCs attachment to microcarriers after 24h. a) Representative images of PS, PVG-coated and PVG + RGD microspheres at 4x (left) and 20x (right) Scale bar = 100µm. b) hMSC expansion relative to seeding after 24h as measured by DNA quantification. *$p < 0.05$ by ANOVA with a post-hoc Tukey's test.

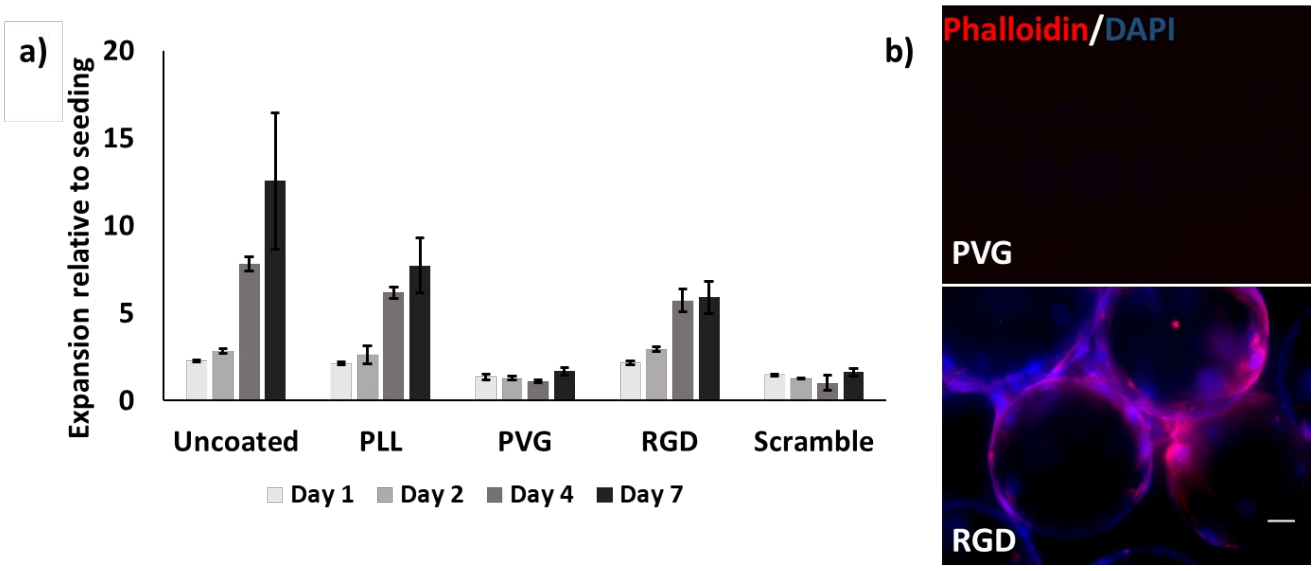

Figure 3.9.4. hMSCs readily expand on PVG coated microcarriers functionalized with RGD. a) DNA content of hMSCs expanded on microcarriers, and b) representative fluorescent max intensity projection of hMSCs with nuclei stained with DAPI (blue) and rhodamine phalloidin (red) after 7 days of growth on PVG-RGD microcarriers. Error bars are one standard deviation. Scale bar = 16μm.

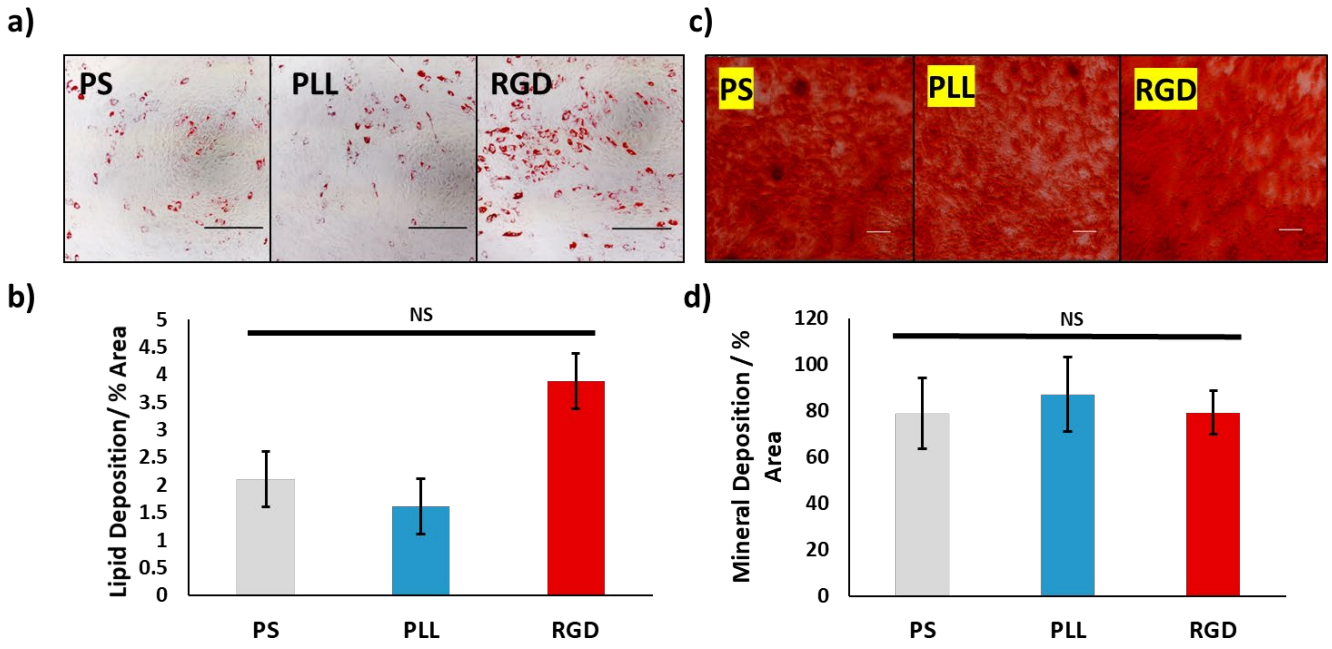

Figure 3.9.5. hMSCs expanded on microcarriers for 7 days appear to retain osteogenic and adipogenic differentiation capacity after harvesting. a) Micrograph of Oil Red O staining for lipid droplets on MSCs differentiated to the adiopogenic lineage. b) Quantification of lipid deposition. c) Alizarin Red S staining for mineral deposits on expanded MSCs that were differentiated to the osteogenic lineage. d) Quantification of mineral deposition. Scale bar = 100um.

3.10 SUPPLEMENTAL FIGURES

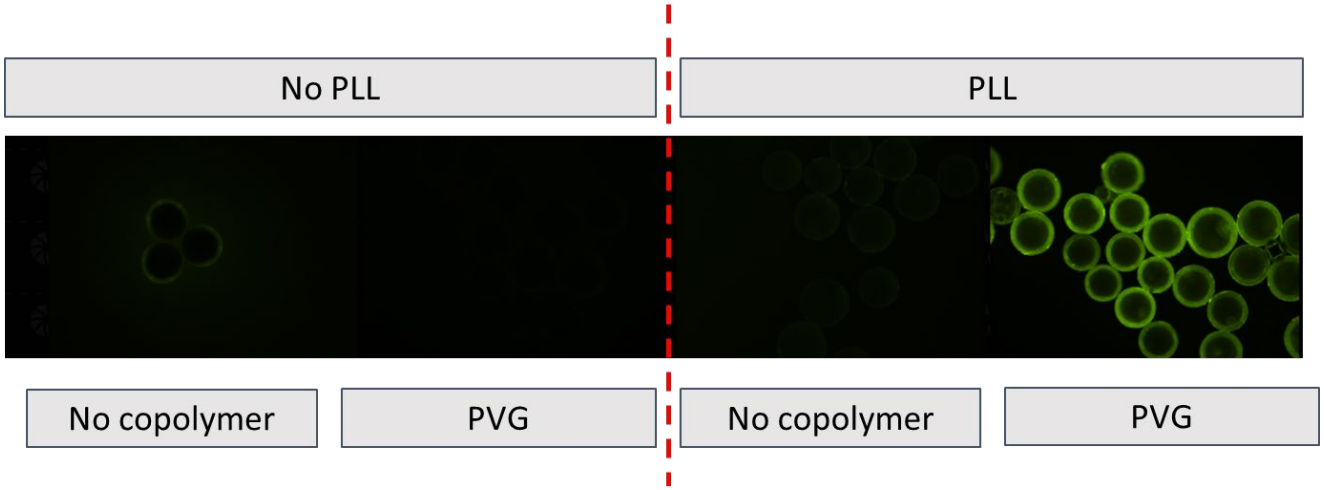

Supplemental Figure S3.10.1. PVG coating is dependent on PLL adsorption. Fluorescent images of microcarriers without PLL (left) or with PLL adsorption (right).

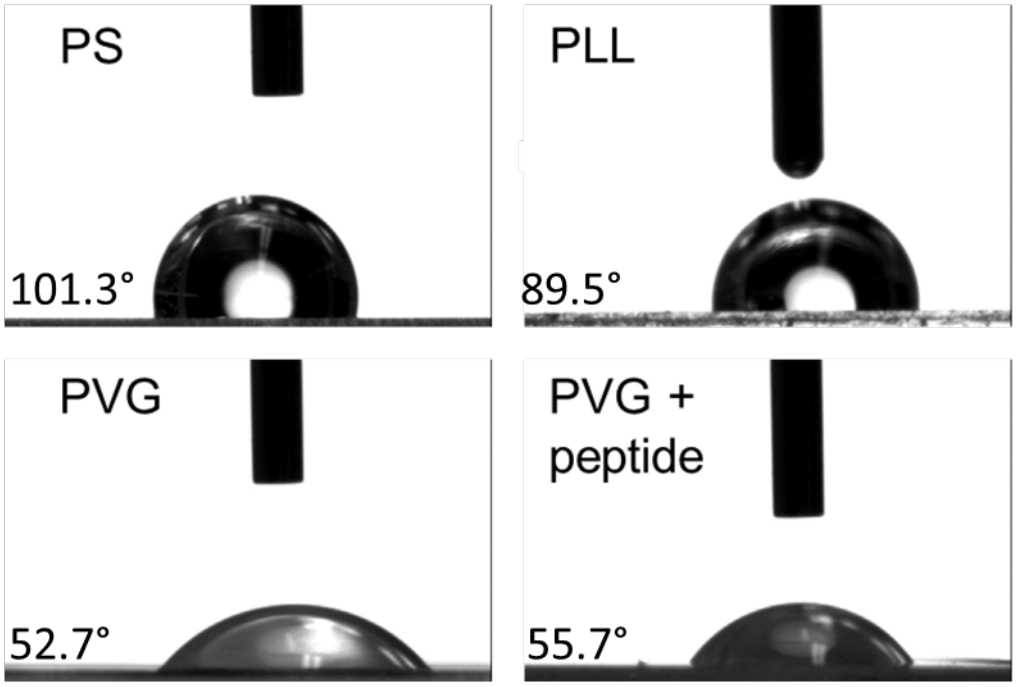

Supplemental Figure S3.10.2. Representative images of contact angle measurements on modified 2D polystyrene. Contact angle measured with 5uL dH_2O.

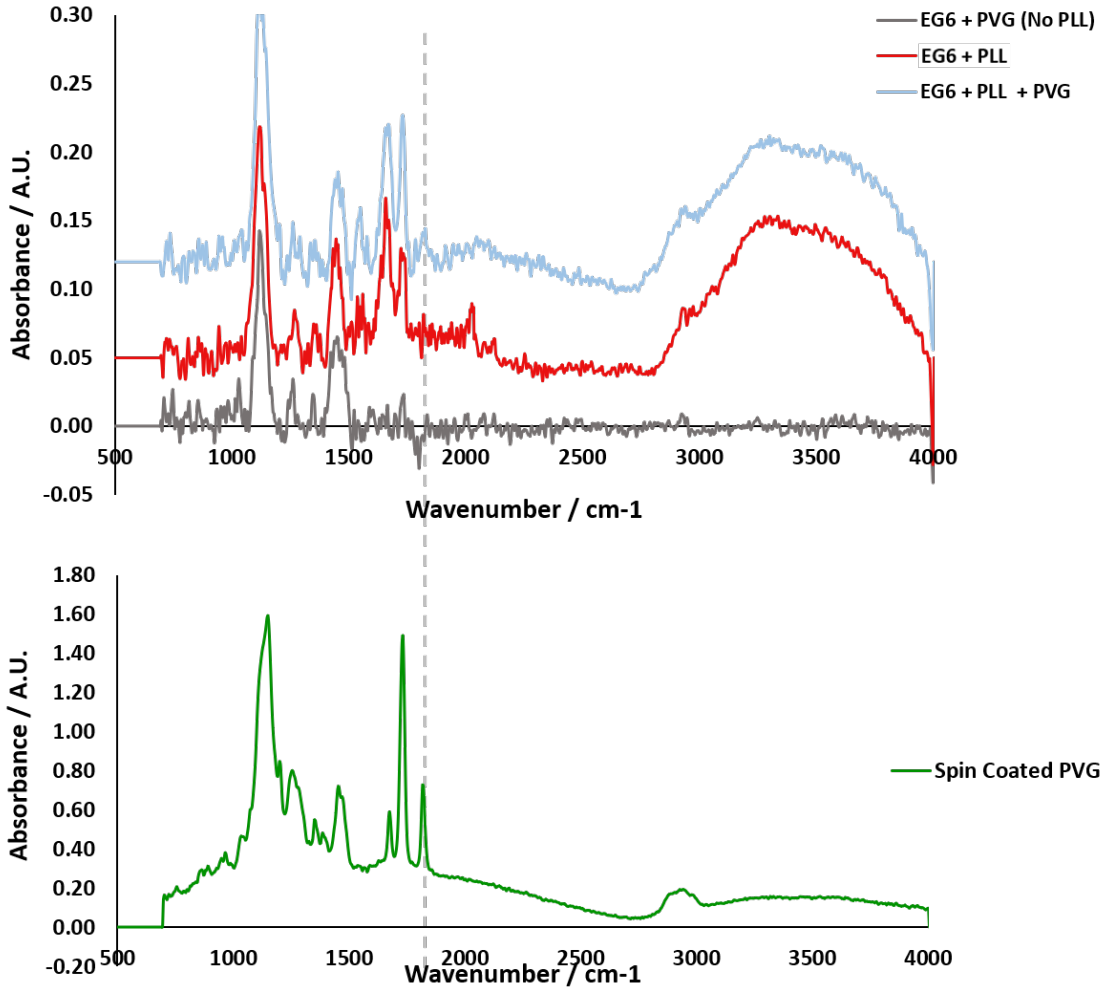

Supplemental Figure S3.10.3. PM-IRRAS spectra of PVG coating on SAMs of EG6 prepared with or without PLL (top). Peak at 1818 cm^{-1} represents the intact oxazoline peak of VDM. Spin coated PVG on a gold-coated glass slide (bottom) represents a positive control.

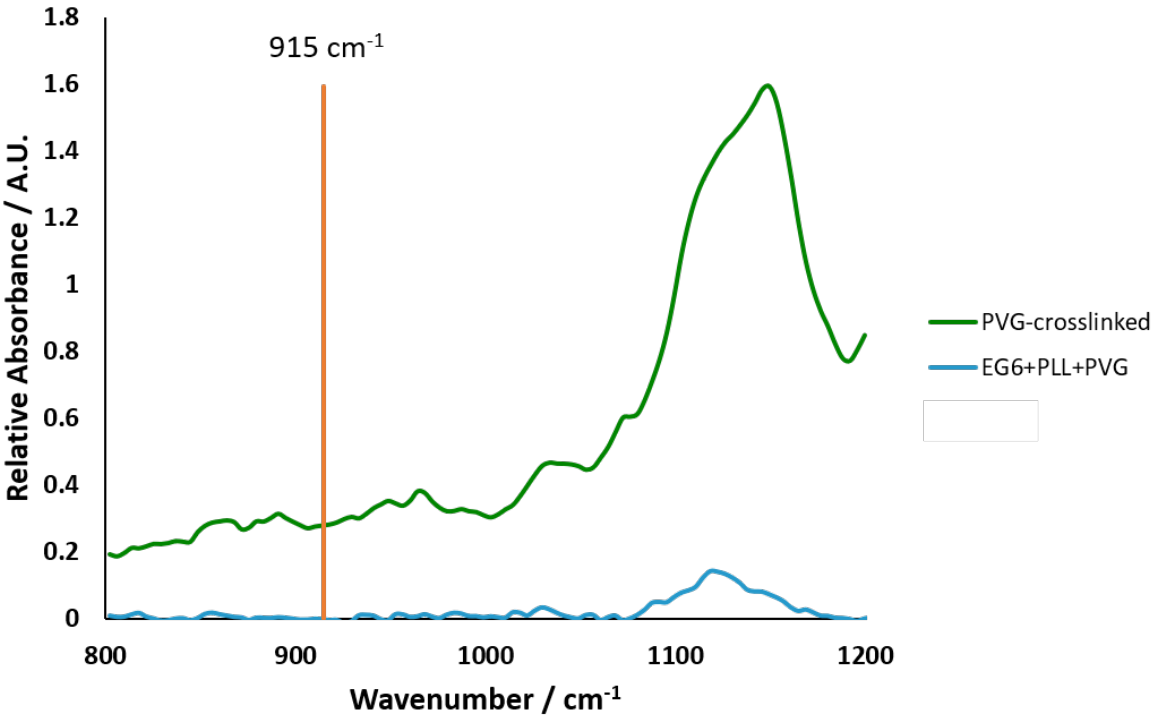

Supplemental Figure S3.10.4. PM-IRRAS spectra of PVG coating on SAMs of EG6 prepared with or without PLL (top). Absence of peak at 915 cm^{-1} represents lack of an epoxide stretch, indicating that the copolymer is not adsorbed to the surface with an intact epoxide ring.

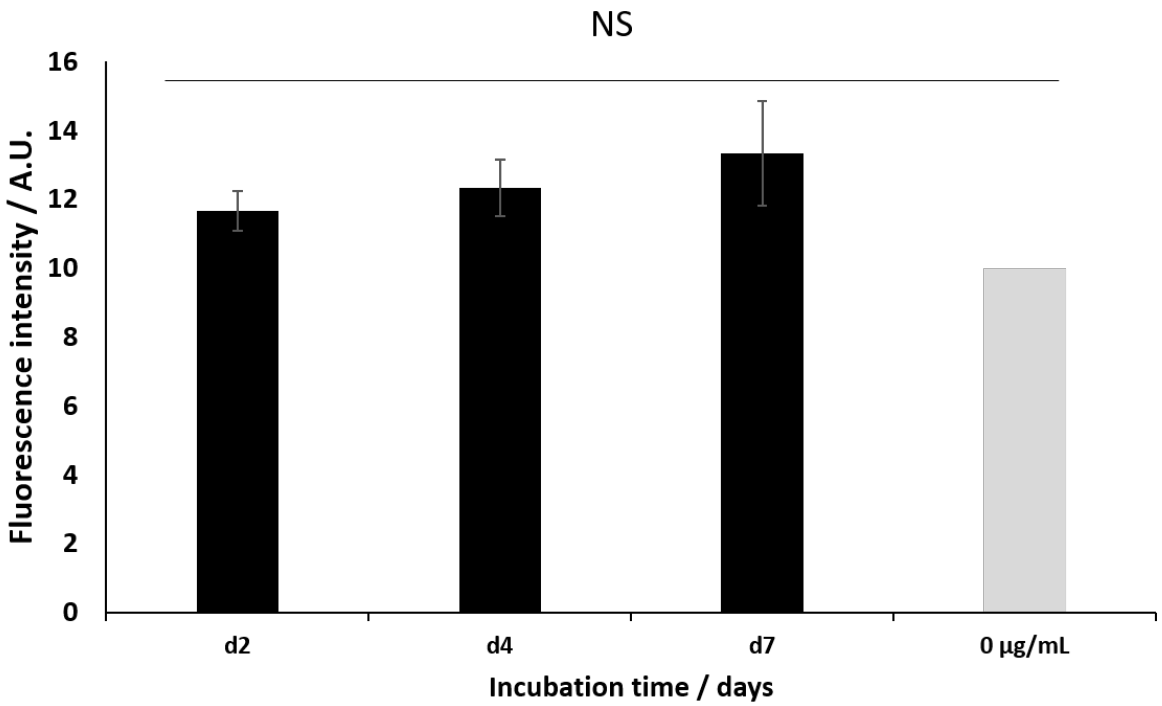

Supplemental Figure S3.10.5. Fluorescence intensity of media after incubation with fluorescent-PLL + PVG coated microcarriers. The fluorescence intensity does not significantly increase over seven days, indicating that PLL desorption from the surface is minimal. $p = 0.45$ by one way ANOVA, n=3 replicates

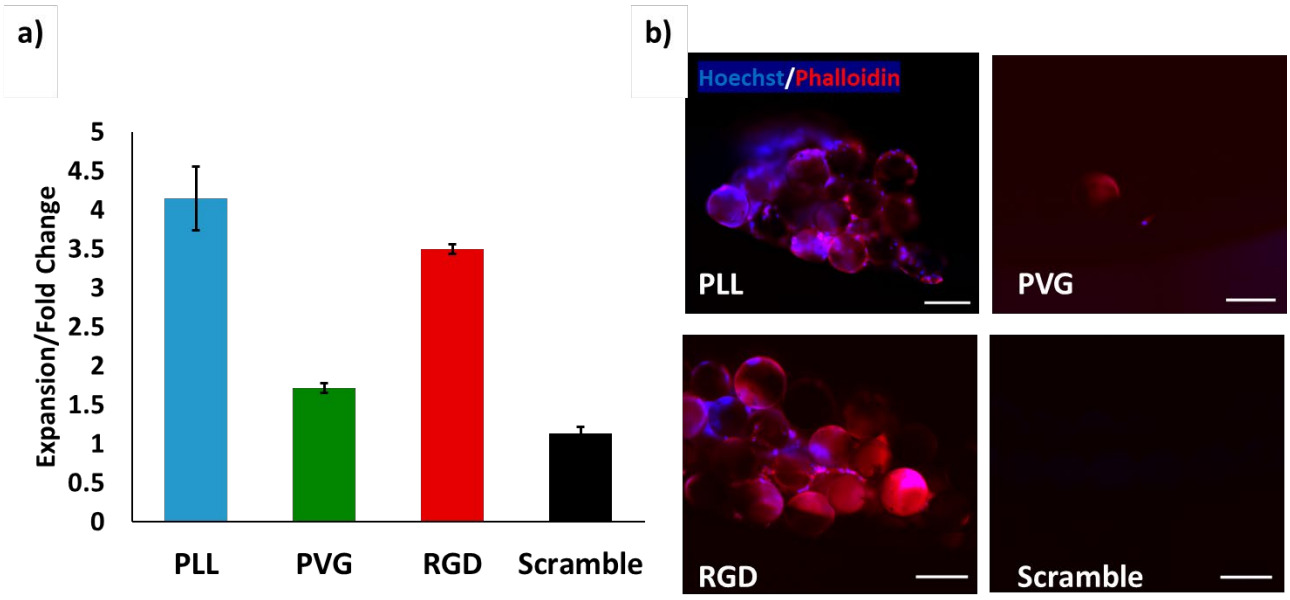

Supplemental Figure S3.10.6. PVG coating enables cell expansion on glass microspheres. a) Expansion of MSCs after 7 days of culture as measured by DNA quantification and b) Fluorescent micrography of cells stained for nuclei (blue) and the actin cytoskeleton (red). Scale bars = 200 μm.

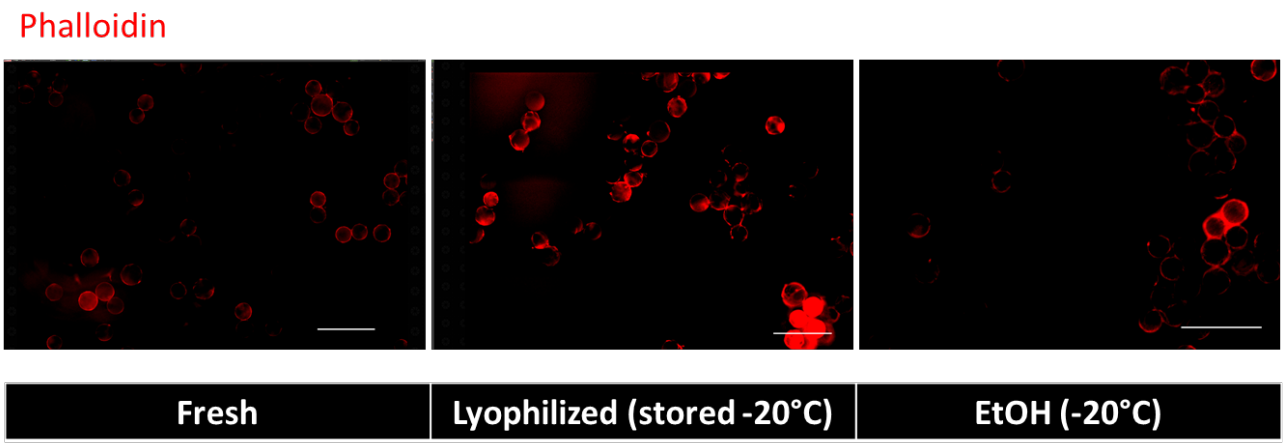

Supplemental Figure S3.10.7. PVG-coated microcarriers maintain functionality after 30d of storage at -20°C. Fluorescent micrographs of MSCs stained for actin cytoskeleton (red) on PVG + RGD microcarriers prepared after 30 days of storage. Scale bar = 500 μm.

CHAPTER 4. XENO FREE BIOREACTOR CULTURE OF HUMAN MESENCHYMAL STROMAL CELLS ON CHEMICALLY DEFINED MICROCARRIERS

4.1 PREFACE

In Chapter 3, we introduced a novel process for applying a synthetic polymer coating to biomaterials of different shapes and sizes. We characterized the material and confirmed its presence and effect on glass and polystyrene surfaces and ensured that it retains the ability to react with biologically relevant peptides. We then demonstrated that the coating creates a "chemically defined" surface by resisting the adsorption of serum proteins. We showed the coating's utility in cell culture applications through its use in small-scale microcarrier culture in serum containing media. Our results indicated that PVG coated microcarriers with no functionalization resist the adhesion of hMSC in serum-containing media. We are then able to restore adhesion through the use of an integrin-specific RGD peptide, which enables cells to expand in number on the microcarriers. In this chapter, we further refine the coating procedure using flat surfaces. These improved coating conditions allow us to address challenges facing the widespread adaptation of microcarriers for hMSC biomanufacturing, demonstrating a scalable, xeno-free cell culture system that enables efficient, enzyme-free separation of cells and microcarriers.

4.2 ABSTRACT

Human mesenchymal stromal cells (hMSC), also called mesenchymal stem cells, are adult cells that have demonstrated their potential in therapeutic applications, highlighted by their ability to differentiate down different lineages, modulate the immune system, and produce biologics. There is a pressing need for scalable culture systems for hMSC due to the large number of cells needed for clinical applications. Most current methods for expanding hMSC fail to meet the requirements of a cell culture system that can provide a reproducible cell product in clinically relevant numbers without the use of serum-containing media or harsh enzymes. In this work, we apply a tailorable, thin, synthetic polymer coating - poly(poly(ethylene glycol) methyl ether methacrylate-*ran*-vinyl dimethyl azlactone-*ran*-glycidyl methacrylate) [P(PEGMEMA-*r*-VDM-*r*-GMA); PVG] - to the surface of commercially available polystyrene (PS) microcarriers to create chemically defined surfaces for large scale cell expansion. These chemically defined microcarriers create a reproducible surface that does not rely on the adsorption of xenogeneic serum proteins to mediate cell adhesion, enabling their use in xeno-free culture systems. Specifically, this work demonstrates the improved adhesion of hMSC to coated microcarriers over PS microcarriers in xeno-free media and describes their use in a readily scalable, bioreactor-based culture system. Additionally, these surfaces resist the adsorption of media-borne and cell-produced proteins, which result in integrin receptor-specific cell adhesion throughout the culture period. This feature allows the cells to be efficiently passaged from the substrate using a chemical chelating agent (EDTA) in the absence of cleavage enzymes, an improvement over other microcarrier products in the field. Bioreactor culture of hMSC on these microcarriers results in the production of 5-6 million cells over four days from a scalable, xeno-free environment.

4.3 INTRODUCTION

Human mesenchymal stromal cells (hMSC), also called mesenchymal stem cells, are a relevant cell type for many therapeutic and research applications due to their immunosuppressive potential[1-3], ability to differentiate down multiple lineages[4-9], and biologics production[10-12]. In the last 15 years, these cells have been the subject of over 900 clinical trial s in the U.S., with over 100 trials conducted per year since 2015 (clinicaltrials.gov). As the demand for hMSC and other cell types continues to rise, there is a pressing need for reproducible, cost effective manufacturing methods to create cells. Some innovations have been made to facilitate the production of cells at scale, including large tissue culture flasks, cellstack plates, bioreactors, and microcarriers[13]. Microcarriers are solid, 100-300 μm diameter beads that enable cell adhesion before being cultured in suspension in a stirred bioreactor. The constant mixing in a microcarrier-containing bioreactor introduces enhanced gas and nutrient exchange and therefore can be scaled up to very large vessels and to manufacture large numbers of cells. They provide a higher surface area for cell growth and require fewer resources, and as such are one of the leading target systems for cell manufacture[14]. Microcarriers for cell culture may exist as a bare material or have a functional coating. Bare microcarriers are mainly made of polymers including poly(hydroxyethyl methacrylate) (PHEMA)[15], polystyrene (PS)[16-18], polyacrylamide (PA)[19, 20], poly(L-lactic acid) (PLLA)[21], and poly(lactic-co-glycolic acid) (PLGA)[22], and stimuli-responsive materials[23] including poly(N-isopropylacrylamide) (pNIPAAm)[24]. Coatings for microcarriers consist of charged molecules, peptides (e.g. Corning Synthemax®, CellBIND®), or proteins (e.g. collagen, gelatin, Cultispher-S) that facilitate cell adhesion, typically with no potential for further customization or tailoring. Additional commercially available microcarriers include dextran-based Cytodex I, II,

and III (GE Healthcare), Sigma-Solohill (collagen- or recombinant protein-coated), and Cultispher® (Percell Biolytica AB).

Typical cell production methods are dependent on many xenogeneic solid and soluble components such as fetal bovine serum[25, 26], collagen, Matrigel and others. As research into cell-based therapeutics advances, there is a growing body of evidence suggesting that there are many drawbacks to the inclusion of xenogeneic components. Animal-derived products suffer from high cost, issues with production, and large batch-to-batch variation[25, 27] which can introduce large variability into cell culture and have deleterious effects on the cell as the end product[28-30]. Additionally, xenogeneic components may be incorporated into the cell itself, which can induce an immune response from the recipient of a cell based therapeutic and in some extreme cases has resulted in anaphylaxis[31, 32]. Synthetic cell culture materials have been developed in 2D[33-38] and 3D[39-43] to culture stem cells as well as direct stem cell fate, but in most cases are not amenable to scale up for cell production at scale.

In this work, we improve upon our previously reported[44-46] P(PEGMEMA-*r*-VDM-*r*-GMA) (PVG) coated microcarrier culture system[47] to enable microcarrier culture in scalable bioreactors in media free of xenogeneic components (xeno-free media). We first report on the utility of the coating through its application to 96-well and 384-well plates with different geometries, demonstrating its potential for coating a wide range of cell culture materials. We also improve upon the sequential anchoring method developed in[47] by increasing the concentration of the poly-l-lysine (PLL) anchoring layer, thereby creating a surface that is more capable at resisting the nonspecific adhesion of hMSC and enabling their adhesion through the inclusion of a cell adhesive Asp-Arg-Gly (RGD) containing peptide. These improved, PVG coated microcarriers are then applied to hMSC culture in xeno-free media and in bioreactors that can be readily scaled to

create therapeutically relevant numbers of hMSC without exposing them to xenogeneic components. Additionally, the chemically defined surface prevents the nonspecific adsorption of serum and cell-produced extracellular matrix (ECM) proteins and reduces batch-to-batch variation[sources]. This reduction in ECM protein adsorption tightly controls the adhesion of hMSC through the integrin-binding RGD peptide. We show that the PVG coating enables efficient, enzyme-free, ethylenediaminetetraacetic acid (EDTA) based passaging of hMSC, further reducing the cost of materials needed for cell culture over the state of the art commercially available coated microcarriers. Finally, the PVG coating is tailored to other biologically relevant functions by using a vascular endothelial growth factor (VEGF) binding peptide (VBP) to sequester soluble VEGF.

4.4 RESULTS

4.4.1. Optimizing PVG coating on Multiwell Plates

In Chapter 3, we described a sequential anchoring method enabling the stable application of PVG onto planar and three-dimensional surfaces. This application method relied on commercially available cell culture materials, including 0.01% poly-L-lysine in water, a common coating to improve cell adhesion. PLL acts as an anchoring layer, and its presentation on the surface exerts profound influence on the uniformity of the PVG coating. We tested different concentrations of the PLL anchoring layer in 96-well and 384-well tissue culture polystyrene plates (**Figure 4.9.1, Supplemental Figure S4.10.1**). When the concentration of the PLL was 0.05 wt%, the PVG coating was most effecting at resisting the nonspecific adhesion of hMSC before functionalization (**Figure 4.9.1a, c**), and enabled more complete adhesion after functionalization with an RGD-based peptide (**Figure 4.9.1b, d**). The effectiveness of each coating was quantified

using cell number/well as a measure of the well's adhesivity (**Figure 4.9.1e-f**). This optimized sequential anchoring method was used for all subsequent experiments on microcarriers in xeno-free media.

4.4.2. hMSC Adhesion to PVG-Coated Microcarriers in Xeno-Free Media

Uncoated PS microcarriers were used as control in xeno-free media. The DNA content on PS microcarriers decreased after changing the media at 24 hours, similar to the decrease seen on PVG-coated microcarriers before functionalization (**Figure 4.9.2a).** This decrease in DNA content is due to the removal of unadhered cells, indicating poor adhesion to the bare PS surface. Few cells seeded onto PS microcarriers adhered, and those that did adopted a rounded morphology indicating a non-adhesive surface (**Figure 4.9.2b**). Cell adhesion was greatly improved on RGD-functionalized, PVG-coated microcarriers, as demonstrated by large aggregates of cells with a flattened morphology (**Figure 4.9.2c**). We quantified the cell seeding efficiency of hMSC seeded on PVG-coated microcarriers using Equation 1, which yielded a seeding efficiency of 77%. These cell seeding results show that PVG coated microcarriers may enable scalable hMSC culture in xeno-free media.

4.4.3. hMSC Expansion and Enzyme-Free Passaging in Xeno-Free Media

hMSC were cultured in xeno-free media on RGD functionalized, PVG-coated microcarriers in a 125 mL stirred flask bioreactor (**Figure 4.9.3, Supplemental Figure S4.10.2**) to evaluate their potential for scale up to industrial processes. hMSC were seeded onto microcarriers at 1750 cells cm^{-2} according to manufacturers' recommendations in xeno free media and allowed to attach for up to 12 hours in static conditions, before being cultured in suspension for 7 days. 1mL samples were taken at day 1, 2, 4 and 7, cells passaged from the surface using EDTA, and nuclei stained using Hoechst 33342. To track the expansion of hMSC over time, the

cells were imaged, and nuclei counted (**Figure 4.9.4)**. Cell number increased up to day 4, at which point large aggregates of microcarriers and cells reduced expansion rate (**Supplemental Figure S4.10.3**). This is similar to the expansion pattern published in Chapter 3 in serum-containing media.

One of the advantages of PVG-coated surfaces over traditional cell culture surfaces is the ability to passage using non-enzymatic, chemical chelating agents such as EDTA. This process is gentle on the cells, contains no animal products, and has been shown on planar substrates to preserve the cell culture surface and patterned peptides[45]. In order to quantify the efficacy of EDTA passaging from PVG-coated microcarriers, 1mL samples of the microcarriers in suspension in a bioreactor were harvested on days 2, 4, and 7. hMSC were separated from the microcarriers using EDTA and stained for nuclei using Hoechst 33342 (**Figure 4.9.4**). Passaging efficiency was determined using Equation 2 and shows that 77-85% of cells were singularized and separated from the surface using EDTA, and this efficiency did not decrease as aggregates became larger over time (**Figure 4.9.4b**). As a comparison, for the cells cultured on the commercially available Corning Synthemax® microcarriers, EDTA was not an effective passaging agent (**Supplemental Figure S4.10.4**).

4.4.4. hMSC Differentiation and Immunosuppression post-microcarrier culture

hMSC are an ideal cell type for scale up and manufacturing due to their multipotency and immunosuppressive potential. In order to evaluate the potency of hMSC that had been grown in xeno-free media on PVG-coated microcarriers, cells that had been cultured in the bioreactor were differentiated down the adipogenic and osteogenic lineages. Cells were harvested from the microcarriers and seeded on collagen-I coated plates, and differentiated for 21 days and stained with the Oil Red O or Alizarin Red S, for adipogenic differentiation and osteogenic differentiation,

respectively (**Figure 4.9.6 a, b**). Cells grown on microcarriers demonstrated the capacity to differentiate down the adipogenic lineage similarly to cells that had been cultured on planar, TCPS surfaces, as measured by lipid deposition. hMSC cultured in the bioreactor did not retain the ability to produce mineral deposits that stained positive for Alizarin Red S, however (**Figure 4.9.6c, d**). The cells harvested from the bioreactor exhibited a change in physical appearance but showed no signs of positive mineral deposition.

4.5 DISCUSSION

hMSC continue to be an important cell type for potential therapeutic treatments, with over 900 clinical trials using hMSC underway or already completed. Over 500 of those trials have been filed within the last four years (clinicaltrials.gov), which demonstrates a continued interest in the cells for their therapeutic potential, even as desired trait has expanded to include immunosuppressive behavior in addition to differentiation potential. The ever-increasing interest in hMSC and other human cell types underscores the need for reproducible, scalable production methods. In our previous work in Chapter 3, we demonstrated a method for applying a chemically defined, synthetic copolymer, PVG, to the surface of three-dimensional microcarriers. We showed that these coated microcarriers enabled the potential scale up of hMSC production by demonstrating cell adhesion in a small-scale, serum-containing environment. Increasingly, studies have shown that there is a wide array of negatives associated with cell culture in the presence of xenogeneic components, ranging from inconsistency of the final product to immune responses form the patient and, in extreme cases, anaphylaxis has been reported[31, 32]. To address these issues, we have demonstrated the capability for bioreactor culture of hMSC on a tailorable, chemically defined surface in xeno-free culture media.

In order to achieve the maximum cell adhesion potential to our 3D coated microcarriers, the coating process needed to be optimized. We showed in multiwell plates that by increasing the concentration of the PLL anchoring layer, the PVG coating layer was improved (**Figure 4.9.1, Supplemental Figure S4.10.1**). The unfunctionalized, PVG coated wells prepared with a higher concentration of PLL were better able to resist the adsorption of serum proteins, which was shown by a reduction in the nonspecific adhesion of cells in serum-containing media. The improved coating was nearly 100% effective at eliminating nonspecific cell adhesion, with many wells containing zero adherent cells. This is a significant improvement over previous iterations of the sequential anchoring mechanism, as it ensures that the adhesion to the surface is mediated solely though the included RGD peptide, which enables enzyme free, EDTA-based passaging from these surfaces.

The improved coating mechanism also increases the potential of these surfaces to be tailored to specific applications outside of cell adhesion. In **Supplemental Figure S4.10.5**, we demonstrate the ability to tailor these microcarriers to additional biologically relevant applications through the functionalization with a vascular endothelial growth factor (VEGF) binding peptide (VBP). PVG coated microcarriers functionalized with VBP are capable of reducing the amount of soluble VEGF detectable in the supernatant media by ELISA. This knockdown is likely due to the sequestration of VEGF near the microcarrier surface. We hypothesize that this sequestration creates a locally high VEGF concentrations near the surface of the microcarrier, where the protein will be more readily accessible to cells. The ability to create a locally high concentration of relevant growth factors would reduce the need for soluble growth factors in the culture media, a large component of the media cost.

The relevance of polymer coated microcarriers to the process of scalable cell manufacturing lies in the improvement of the efficiency of cell culture on these surfaces. As demonstrated in **Figure 4.9.3**, uncoated PS microcarriers are incapable of enabling cell adhesion and growth in xeno-free media. The few cells that do attach to these surfaces adopt a rounded morphology, indicative of poor adhesion. This lack of adhesion is likely due to the absence of fetal bovine serum (FBS) or other xenogeneically derived serum components that enable cell adhesion through their adsorption to PS surface, similar to the process that enables adhesion to TCPS plates[48, 49]. Therefore, microcarrier culture of hMSC in xeno-free media relies on the use of coated microcarriers. The only synthetic, RGD-based coating for microcarriers that exists in the market now is Corning Synthemax® II, which enables cell adhesion and growth in xeno-free media. Currently, there are not any chemically defined or tailorable coatings for microcarriers that can be purchased through commercial sources. Additionally, the PVG coated microcarriers enable efficient passaging with the divalent cation chelating agent EDTA, which is not possible on Synthemax® II coated microcarriers (**Supplemental Figure S4.10.2**). The ability to passage cells using EDTA removes the need for harsh, enzymatic passaging methods. The removal of passaging enzymes from the cell manufacturing process would remove an expensive component of cell culture cost and simplify the material acquisition process.

Cells cultured on PVG coated, RGD functionalized microcarriers in a 125mL bioreactor in xeno-free media were able to produce between 5 and 6 million cells over four days, at a rate of more than 78,000 cells per mL of media used. This rate could be improved through the scale up to larger bioreactors and optimization of seeding density and culture conditions. Furthermore, cells could be passaged and separated from the microcarriers in an enzyme-free process, something that is not currently available using the microcarriers on the market. These cells retained their potential

for differentiation down the adipogenic lineage but did not stain positively for mineral deposition despite a visible change in cell phenotype (**Figure 5.9.6**). The mechanism behind this change is unclear, as hMSC cultured on PVG coated surfaces have been successfully differentiated down the osteogenic lineage in previous work. Future work should include analysis of the hMSC phenotype post PVG coated microcarrier culture. As a whole, the ability to scale production of hMSC in xeno-free media coupled with the potential for growth factor sequestration and customization to different cell types, these PVG coated surfaces represent an important improvement over the state of the art in the field.

4.6 EXPERIMENTAL SECTION

4.6.1 PVG copolymer synthesis

PVG copolymer was synthesized using reversible addition-fragmentation chain transfer anionic polymerization (RAFT) according to previously reported procedures (Source). Briefly, poly(ethylene glycol) methyl ether methacrylate (PEGMEMA), glycidyl methacrylate (GMA), and vinyl dimethyl azlactone (VDM) were added to a 25mL Schlenk flask. Anisole was added as a solvent to bring the reaction mixture to 13mL. The chain transfer agent (CTA) 2-cyano-2-propyl benzodithioate and the initiator 2,2'-azobis(2-methylpropionitrile) were added at a monomer : CTA : initiator ratio of 1:1. The mixture was degassed using three freeze-pump-thaw cycles. Polymerization was conducted at 70 °C for 15h and stopped by exposure to the atmosphere. The resultant polymer was precipitated in *n*-hexanes, filtered and dissolved in tetrahydrofuran (THF, Fisher Scientific). This was repeated three times to remove any unreacted monomer. The resultant polymer P(PEGMEMA-*r*-VDM-*r*-GMA) was dissolved and stored in THF. Gel permeation chromatography (GPC) yielded a Mn = 47,000 and a dispersity of 2.1. Proton nuclear

magnetic resonance spectroscopy showed the final concentration of the copolymer was 61% PEGMEMA, 29% VDM, and 10% GMA.

4.6.2 Optimization of PVG Coating on Multiwell Plates: 96-well and 384-well tissue culture polystyrene (TCPS) plates were coated with PVG copolymer via the sequential anchoring process via the procedure described in Krutty et al. 2019[47]. Briefly, TCPS plates were incubated in 70,000-150,000 kDa poly-L-lysine (Sigma-Aldrich, Milwaukee, WI) solutions in water at concentrations of either 0.01wt% or 0.05wt%, depending on the condition being tested, for one hour. PLL adsorbs to polystyrene largely though hydrophobic interactions and its use is common in cell culture applications[50, 51]. Each well was rinsed 2x with 300µL dH_2O and 1x with 300µL 200 proof EtOH. Finally, wells were filled with 10-50 µL of 10mg mL^{-1} PVG solution in EtOH and allowed to react overnight.

4.6.3 PVG coating of microcarriers*:* Untreated polystyrene microcarriers with diameter of 125-212 µm (Corning, Corning, NY) were weighed and incubated in 0. 05wt% 70,000-150,000 Da poly-L-lysine for 1 hour. Microcarriers were then washed twice with dH_2O and once with EtOH. Microcarriers were placed in a 10mg mL^{-1} solution of PVG polymer in EtOH and allowed to react overnight. Microcarriers at this state were stored in EtOH at -20°C for up to 1 month.

4.6.4 Peptide Immobilization*:* PVG-coated surfaces were washed twice with PBS and reacted with Cys-Gly-Gly-Gly-Arg-Gly-Asp-Ser-Pro (CGGGRGDSP, "RGD"), Cys-Gly-Gly-Gly-Arg-Asp-Gly-Ser-Pro (CGGGRDGSP, "scramble") peptides (Genscript). TCPS plates and microcarriers were incubated in 1mM peptide solutions in 1x phosphate buffered saline (PBS) (Fisher Scientific) for 1 hr at room temperature according to the procedure in Schmitt et al. (2015,

2016). The coated surfaces were then rinsed twice with PBS and sanitized in 70% ethanol for 30 minutes before use in cell culture.

4.6.5 hMSC culture:

Serum-containing medium: hMSC (Lonza PT-2501 Lot # 0000684888) were cultured in Minimum Essential Medium – Alpha modification (Corning, Corning MA) plus 10% fetal bovine serum (FBS) (Gibco, Cat. #16000-044, Dublin, Ireland). Cells were thawed from LN2 storage and seeded onto T175 TCPS plates at 2800 cells cm^{-2}. Cells were incubated at 37°C and 5% CO_2 and manipulated under sterile conditions. Media was changed after 24 hours, then every 2-3 days. Cells were passaged at 70-80% confluence using 5mL Trypsin (Fisher/Hyclone, SH30236.02) at 37°C and 5% CO_2 for 5 minutes. After 5 minutes, adherent cells were loosened using gentle agitation of the plate

Xeno-free medium: hMSCs (Roosterbio, XF RoosterKit-hBM Lot 164) were cultured in RoosterNourish™ MSC-XF xeno free media (Roosterbio, Frederick, MD). Cells were thawed from LN2 storage and seeded onto T175 TCPS plates at 2800 cells cm^{-2}. Cells were incubated at 37°C and 5% CO_2 and manipulated under sterile conditions. Media was changed after 24 hours, then every 2-3 days. Cells were passaged at 70-80% confluence using 5mL TrypLE Select Enzyme (Invitrogen, Carlsbad CA) at 37°C and 5% CO_2 for 5 minutes. After 5 minutes, adherent cells were loosened using gentle agitation of the plate

4.6.6 hMSC adhesion on multiwell plates: To evaluate hMSC attachment to PVG-coated and functionalized surfaces, passage 4-6 hMSC were seeded (10,000 cells cm^{-2}) in αMEM + 10% FBS on PS, PLL-coated, PVG-coated, RGD functionalized and scramble functionalized TCPS plates,

prepared as previously described. After 24 hours, the cells were fixed, stained for nuclei and actin cytoskeleton, and imaged.

4.6.7 Microcarrier suspension culture in 24-well plates: To study hMSC attachment and expansion on functionalized microcarrier surfaces, hMSC were grown for up to a week in either αMEM + 10% FBS or RoosterNourish MSC-XF media. Passage 4-6 cells were seeded in 500µL media onto 10 cm^2 of microcarriers in an Ultra-Low Adhesion 24-well plates (Corning). A cell seeding density of 10,000 hMSC cm^{-2} was used with each of the following surface functionalizations: PS, PVG-coated, PVG + RGD peptide, or PVG + scramble peptide. At desired time points (1, 2, 4, and 7 days), cells were either fixed and stained or lysed, and total DNA was quantified using a CyQUANT® Cell Proliferation Assay Kit, per kit instructions.

4.6.8 Microcarrier suspension culture in stirred flask bioreactors: 715mg of PVG + RGD coated microcarriers were added to 30mL of αMEM + 10% FBS or RoosterNourish™ media in a 125 mL, non-treated, PS disposable spinner flask (Corning). 1.5 x 10^6 cells were seeded onto the microcarriers and the working volume was brought to 67mL (approximately one half of the bioreactor's capacity). A static incubation period of 4h to 12h was used to encourage cell adhesion before starting the stirring process. For all cell expansion and cell phenotype quantification data, a 12h static incubation period was used. The bioreactor was then placed on a magnetic stir plate in the incubator (37°C, 5% CO_2) and agitated at a rate of 60rpm. One half volume media changes (approx. 33mL) were performed after 24 and 72 hours.

4.6.9 Fluorescent imaging: hMSC were washed with 1x PBS and fixed in 10% buffered Formalin solution for 20-30 minutes. Cells were then permeabilized with 0.1% Triton X-100 (MP Biomedicals, Aurora, OH) in 1x PBS for 20 minutes. Cells were washed twice with PBS and

blocked using 1% bovine serum albumin (BSA) (Fisher Scientific). Cells were stained for actin cytoskeleton using Alexa-Fluor™ 647 Phalloidin (Thermo Fisher) and for nuclei using 4',6-Diamidine-2'-phenylindole dihydrochloride (DAPI) (Sigma Aldrich) or Hoechst 33342 for 30 minutes each, washing in between with PBS. Cells were imaged on an inverted microscope with DAPI, FITC, and Far Red filter cube sets.

4.6.10 Cell passaging and quantification: hMSC nuclei were counted to determine cell number, seeding efficiency, and passaging efficiency.

hMSC Passaging: hMSC were passaged using Versene, a 1x ethylenediaminetetraacetic acid solution (EDTA, Invitrogen). EDTA lifts cells from surfaces through the chelation of Ca^{2+} and Mg^{2+} ions, which are an important component of integrin receptor binding.

hMSC seeding efficiency and quantification: Representative samples were removed from the bioreactor in 3x1mL samples on day 1, 2, 4, and 7. hMSC nuclei were stained using 2 µM Hoechst 33342 (Thermo Fisher), a cell membrane permeable fluorescent stain. Samples were allowed to settle for 30 minutes before being imaged in phase and fluorescence, and adherent cells were quantified using Equation [1]:

[1] $$Seeding\ efficiency\ = \frac{Microcarrier\ Adjacent\ Nuclei}{Total\ Nuclei} * 100\%$$

Where Microcarrier Adjacent Nuclei are defined as nuclei belonging to cells that are attached to microcarriers as visualized in the phase microscope images.

hMSC passaging and passaging efficiency: hMSC were lifted from the microcarrier surface using either TrypLE or EDTA. Microcarriers were removed from the bioreactor in 1mL samples, rinsed with PBS, and incubated in the passaging solution for 4 minutes at 37°C and 5% CO_2, agitated

through gentle pipetting, and returned to the incubator for another 4 minutes. Samples were stained using Hoechst 33342, then placed in a multi-well plate and allowed to settle for 30 minutes before being. Samples were imaged in phase and fluorescence, and passaging efficiency was quantified using Equation [2]:

$$[2] \qquad Passaging\ efficiency\ = \frac{Unassociated\ Nuclei}{(Unassociated\ Nuclei + Microcarrier\ Adjacent\ Nuclei)} * 100\%$$

where Unassociated Nuclei are defined as those nuclei belonging to cells that are not adhered to the surface of a microcarrier as visualized in the phase microscope images.

hMSC expansion on microcarriers: Cells were grown on microcarriers in a stirred flask bioreactor as described in **Section 4.6.7**, and passaged as described earlier in this section. Microcarriers were then separated from the nonadherent cells using a cell strainer (Corning Falcon) with a pore size of 100 μm. Samples were stained using Hoechst 33342, then placed in a multi-well plate and allowed to settle for 30 minutes before imaging. Samples were imaged in phase and fluorescence, where number of nuclei was used as a proxy for total cell number.

4.6.9 hMSC differentiation and immunosuppression analysis*:* To evaluate differentiation capacity after expansion on coated microcarriers, hMSC were differentiated to osteoblasts and adipocytes based on established protocols. For differentiation, hMSC were seeded at 5000 cells·cm^{-2} on collagen-coated plates (Corning, Corning, NY) in 10% FBS in αMEM, and permitted to grow to confluence for three days. Osteogenic (OS) medium and adipogenic induction medium (AIM) were prepared. OS medium consisted of 10% FBS in αMEM with 0.1 μM dexamethasone, 10 mM β glycerol phosphate, and 50 μM ascorbic acid 2-phosphate. AIM consisted of 10% FBS in Dulbecco's Modification of Eagle's Medium (DMEM) high glucose with penicillin (100 U mL^{-1})/streptomycin (100 μg mL^{-1}), 1 μM dexamethasone, 10 μg mL^{-1} insulin, and 500 μM isomethyl

isobutyl xanthine (IBMX). Media was changed every 3-4 days, and analysis was performed after 21 days of differentiation. As negative controls, cells were grown for 21 days in 10% FBS in αMEM.

Alizarin Red S stained mineral deposits from osteoblasts, and Oil Red O stained lipid droplets in adipocytes. To perform staining, cells were fixed in 10% buffered formalin solution and incubated Alizarin Red S (40 mM, pH 4.1-4.3) and washed with water three times or Oil Red O working solution for 20 minutes and washed with water until washings were clear. Working Oil Red O solution was prepared by mixing three parts stock Oil Red O solution (3 mg mL^{-1} in 99% isopropanol) with two parts distilled water and filtering with a 0.2 μm syringe filter.

4.6.11 hMSC differentiation and immunosuppression analysis: PS microcarriers were coated with PVG copolymer as described previously. Microcarriers were incubated in a 1μg/mL solution of VEGF in PBS + 1% FBS, which was necessary to stabilize the protein in solution.

4.6.12 Statistical Analysis

Experiments were carried out and repeated a total of two to three trials, with n=3-4 replicates per trial. Except where noted, a one-way ANOVA was conducted to determine significance, as there are multiple groups with one independent variable. A post-hoc Tukey's test was then used to determine significance between groups.

4.7 ACKNOWLEDGEMENTS

This research was funded by the National Science Foundation (NSF DMR **1709179**). The authors acknowledge support from staff and the use of equipment at the Materials Science Center at UW-Madison DMR-1121288 and DMR-1720415. Additional support was provided by the Wisconsin Alumni Research Foundation Accelerator Program.

4.8 REFERENCES

[1] B. Follin, M. Juhl, S. Cohen, A. E. Pedersen, J. Kastrup, A. Ekblond. *Tissue engineering Part B, Reviews* **2016**;22:1-26.

[2] K. Le Blanc, L. C. Davies. *Immunology Letters* **2015**;168:140-6.

[3] X. Chen, M. A. Armstrong, G. Li. *Immunology and Cell Biology* **2006**;84:413-21.

[4] M. F. Pittenger, A. M. Mackay, S. C. Beck, R. K. Jaiswal, R. Douglas, J. D. Mosca, M. A. Moorman, D. W. Simonetti, S. Craig, D. R. Marshak. *Science* **1999**;284:143-7.

[5] X. Shen, B. Pan, H. Zhou, L. Liu, T. Lv, J. Zhu, X. Huang, J. Tian. *Journal of Biomedical Science* **2017**;24:29.

[6] A. Singh, A. Singh, D. Sen. *Stem Cell Research & Therapy* **2016**;7:82.

[7] G. V. Silva, S. Litovsky, J. A. R. Assad, A. L. S. Sousa, B. J. Martin, D. Vela, S. C. Coulter, J. Lin, J. Ober, W. K. Vaughn, R. V. C. Branco, E. M. Oliveira, R. He, Y.-J. Geng, J. T. Willerson, E. C. Perin. *Circulation* **2005**;111:150-6.

[8] A. Augello, C. De Bari. *Human Gene Therapy* **2010**;21:1226-38.

[9] G. Chamberlain, J. Fox, B. Ashton, J. Middleton. *Stem Cells* **2007**;25:2739-49.

[10] G. Baek, H. Choi, Y. Kim, H.-C. Lee, C. Choi. *STEM CELLS Translational Medicine* **2019**;8:880-6.

[11] A. I. Caplan, J. E. Dennis. *Journal of Cellular Biochemistry* **2006**;98:1076-84.

[12] S. Rani, A. E. Ryan, M. D. Griffin, T. Ritter. *Molecular Therapy* **2015**;23:812-23.

[13] K. M. Panchalingam, S. Jung, L. Rosenberg, L. A. Behie. *Stem Cell Research & Therapy* **2015**;6:225.

[14] J. Rowley, E. Abraham, A. Campbell, H. Brandwein, S. Oh. *BioProcess International* **2012**;10:16-22.

[15] H. Ayhan, A. Kozluca, E. Pişkin, I. Gurhan. *Journal of Bioactive and Compatible Polymers* **1999**;14:17-30.

[16] T. R. Heathman, V. A. Glyn, A. Picken, Q. A. Rafiq, K. Coopman, A. W. Nienow, B. Kara, C. J. Hewitt. *Biotechnol Bioeng* **2015**;112:1696-707.

[17] M. Szczypka, D. Splan, H. Woolls, H. Brandwein. *BioProcess International* **2014**;12:54-64.

[18] D. K. Aletta Schnitzler, Janice Simler, Anthony DiLeo, Andrew Ball. *BioPharm International* **2012**;25.

[19] S. Reuveny, A. Mizrahi, M. Kotler, A. Freeman. *Developments in biological standardization* **1983**;55:11-23.

[20] S. Reuveny, A. Mizrahi, M. Kotler, A. Freeman. *Annals of the New York Academy of Sciences* **1983**;413:413-5.

[21] H. Tan, J. Wu, D. Huang, C. Gao. *Macromolecular Bioscience* **2010**;10:156-63.

[22] K. W. Chun, H. S. Yoo, J. J. Yoon, T. G. Park. *Biotechnology Progress* **2004**;20:1797-801.

[23] A. K. A. S. Brun-Graeppi, C. Richard, M. Bessodes, D. Scherman, O.-W. Merten. *Journal of Controlled Release* **2011**;149:209-24.

[24] M. R. Kim, J. H. Jeong, T. G. Park. *Biotechnology Progress* **2002**;18:495-500.

[25] Z. Xiaoyang, B. Haven, H. W. S., F. Farah, M. Michael, P. Erno. *Biotechnology Progress* **2006**;22:1294-300.

[26] C. Tekkatte, G. P. Gunasingh, K. M. Cherian, K. Sankaranarayanan. *Stem Cells International* **2011**;2011:504723.

[27] C. W. Cheng, L. D. Solorio, E. Alsberg. *Biotechnology Advances* **2014**;32:462-84.

[28] F. M. Watt, W. T. S. Huck. *Nat Rev Mol Cell Biol* **2013**;14:467-73.

[29] D. S. W. Benoit, M. P. Schwartz, A. R. Durney, K. S. Anseth. *Nature Materials* **2008**;7:816.

[30] G. Maheshwari, G. Brown, D. a. Lauffenburger, a. Wells, L. G. Griffith. *Journal of cell science* **2000**;113 (Pt 1:1677-86.

[31] A. Mackensen, R. Dräger, M. Schlesier, R. Mertelsmann, A. Lindemann. *Cancer immunology, immunotherapy : CII* **2000**;49:152-6.

[32] J. L. Spees, C. A. Gregory, H. Singh, H. A. Tucker, A. Peister, P. J. Lynch, S.-C. Hsu, J. Smith, D. J. Prockop. *Molecular Therapy* **2004**;9:747-56.

[33] S. Choi, W. L. Murphy. *Langmuir* **2008**;24:6873-80.

[34] S. R. Chastain, A. K. Kundu, S. Dhar, J. W. Calvert, A. J. Putnam. *Journal of Biomedical Materials Research Part A* **2006**;78A:73-85.

[35] M. L. Guo, J. H. Chen, Y. J. Zhang, K. Chen, C. F. Pan, S. Z. Yao. *Biosensors & Bioelectronics* **2008**;23:865-71.

[36] J. Lahann, M. Balcells, T. Rodon, J. Lee, I. S. Choi, K. F. Jensen, R. Langer. *Langmuir* **2002**;18:3632-8.

[37] M. T. Bernards, G. Cheng, Z. Zhang, S. Chen, S. Jiang. *Macromolecules* **2008**;41:4216-9.

[38] S. Tugulu, H. A. Klok. *Biomacromolecules* **2008**;9:906-12.

[39] M. P. Lutolf, P. M. Gilbert, H. M. Blau. *Nature* **2009**;462:433-41.

[40] A. M. Kloxin, A. M. Kasko, C. N. Salinas, K. S. Anseth. *Science* **2009**;324:59-63.

[41] Y. Qiu, J. J. Lim, L. Scott Jr, R. C. Adams, H. T. Bui, J. S. Temenoff. *Acta Biomaterialia* **2011**;7:959-66.

[42] M. J. Wilson, S. J. Liliensiek, C. J. Murphy, W. L. Murphy, P. F. Nealey. *Soft Matter* **2012**;8:390-8.

[43] C. A. DeForest, K. S. Anseth. *Annual Review of Chemical and Biomolecular Engineering* **2012**;3:421-44.

[44] S. K. Schmitt, A. W. Xie, R. M. Ghassemi, D. J. Trebatoski, W. L. Murphy, P. Gopalan. *Advanced healthcare materials* **2015**;4:1555-64.

[45] S. K. Schmitt, W. L. Murphy, P. Gopalan. *Journal of Materials Chemistry B* **2013**;1:1349-60.

[46] S. K. Schmitt, D. J. Trebatoski, J. D. Krutty, A. W. Xie, B. Rollins, W. L. Murphy, P. Gopalan. *Biomacromolecules* **2016**;17:1040-7.

[47] J. D. Krutty, A. D. Dias, J. Yun, W. L. Murphy, P. Gopalan. *Macromolecular Bioscience* **2019**;19:1800299.

[48] L. Vroman. **1962**.

[49] X. D. Zhu, H. S. Fan, Y. M. Xiao, D. X. Li, H. J. Zhang, T. Luxbacher, X. D. Zhang. *Acta Biomaterialia* **2009**;5:1311-8.

[50] W. D. Corry. *Journal of Colloid and Interface Science* **1978**;63:151-60.

[51] D. Mazia, G. Schatten, W. Sale. *The Journal of Cell Biology* **1975**;66:198-200.

4.9 FIGURES

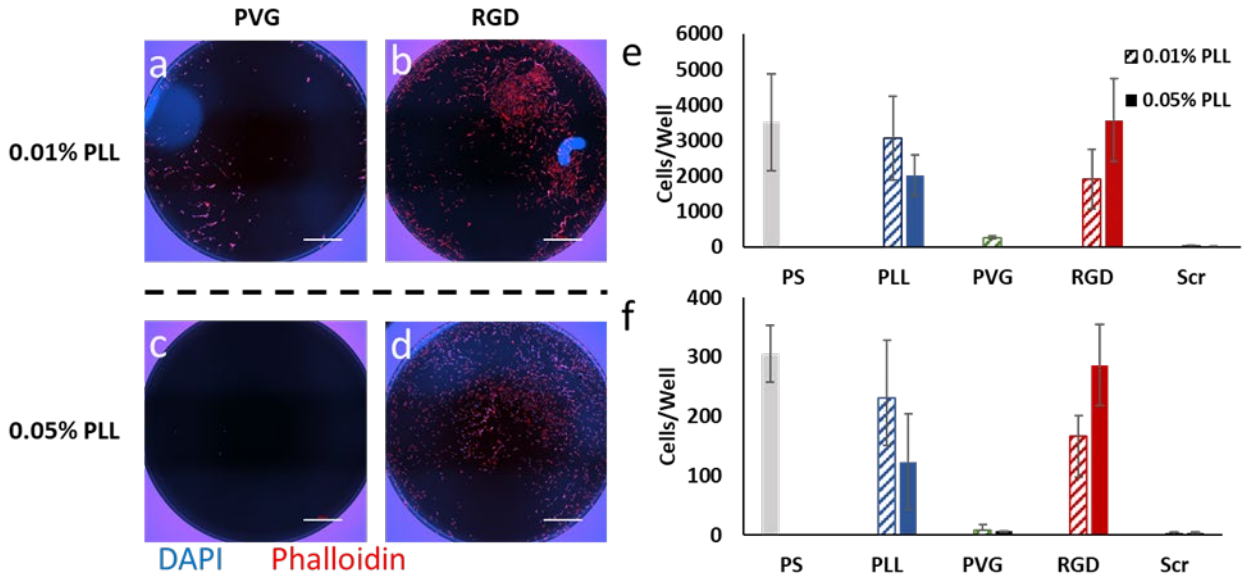

Figure 4.9.1 Increasing the PLL content during the sequential anchoring process improves application of PVG copolymer to multiwell plates. a-b) 0.01% and c-d) 0.05% PLL solutions were used to create PVG-coated 96 well plates. a,c) Unfunctionalized PVG coated plates reduce nonspecific cell adhesion. b,d) RGD functionalization restores cell adhesion to PVG coated plates. Quantification of cell number in both e) 96 well and f) 384 well plates shows that using 0.05% PLL solutions improved resistance to nonspecific adhesion in PVG-coated wells, and improved adhesion in RGD functionalized wells. Scale bar = 1000 µm.

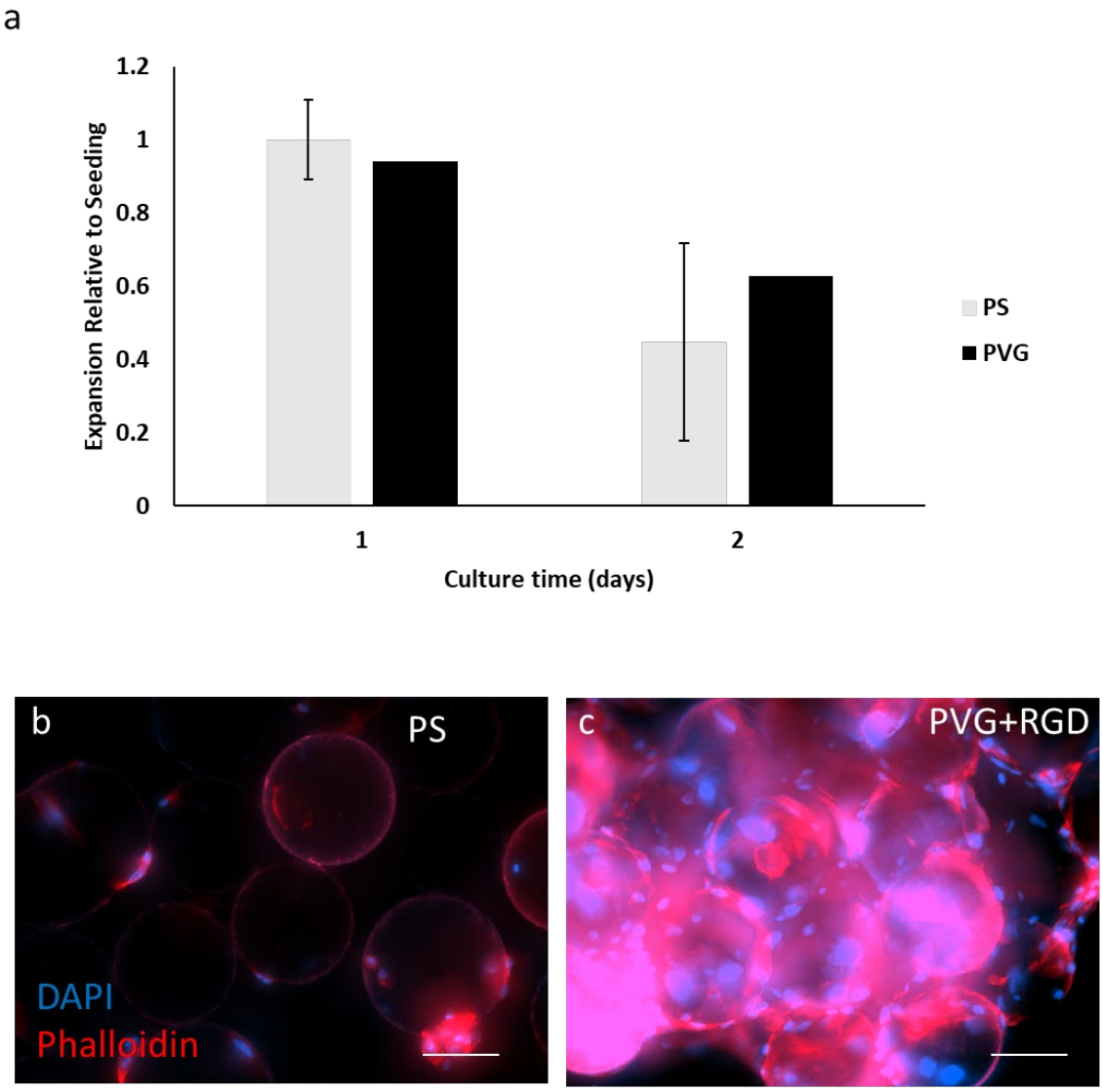

Figure 4.9.2 hMSC adhesion in xeno free media is enhanced on PVG+RGD coated microcarriers over uncoated PS microcarriers. a) DNA quantification of hMSC on microcarriers over time. The reduction in DNA content between days 1 and 2 on PS microcarriers indicates the removal of non-adherent cells during media changes. b) A low number of cells adheres to unmodified PS microcarriers. c) a large aggregate of hMSC and PVG-coated microcarriers functionalized with RGD indicates strong adhesion. Blue = DAPI, red = rhodamine phalloidin. Scale bar = 100 µm

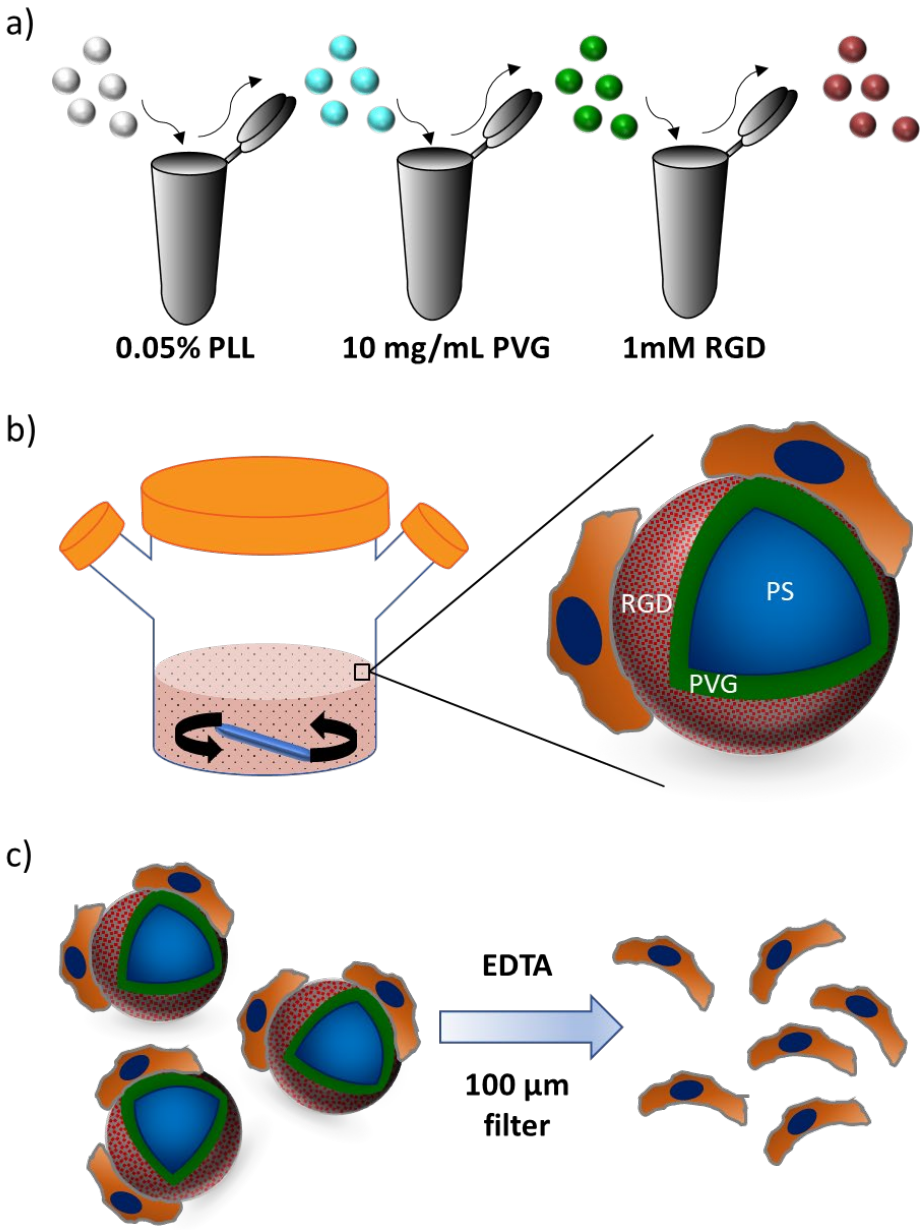

Figure 4.9.3 Xeno-free microcarrier culture at scale. a) PS microcarriers are functionalized using a sequential anchoring process of PLL adsorption, followed by PVG copolymer anchoring, and RGD functionalization. b) hMSC are then cultured in xeno-free media in a stirred flask bioreactor for up to 7 days. c) After 7 days, hMSC are passaged using EDTA and separated from the microcarriers using a cell strainer with a pore size of 100 µm.

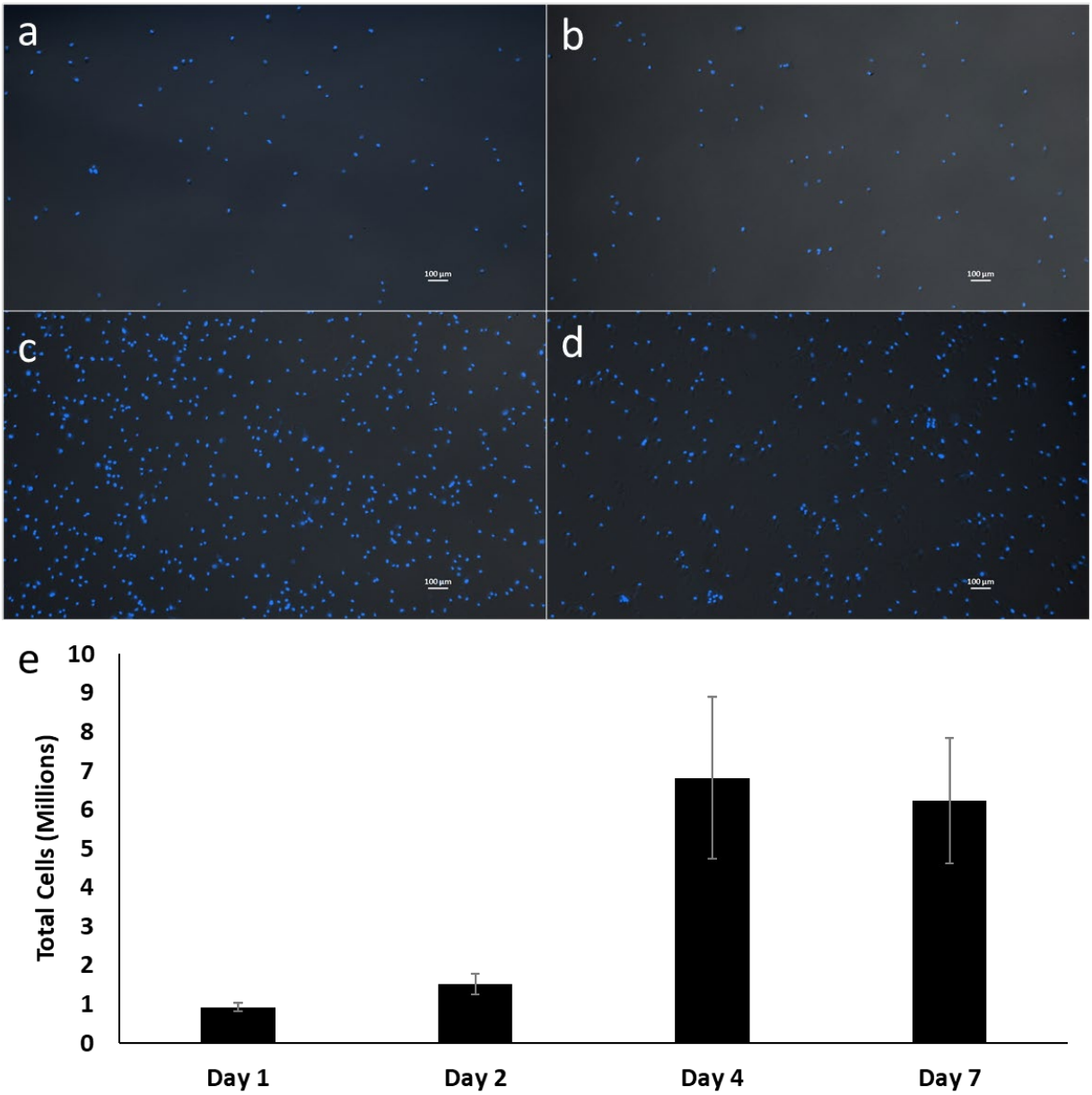

Figure 4.9.4 hMSC expansion on RGD-functionalized, PVG-coated microcarriers suspended in 125mL bioreactors in xeno-free media. hMSC were cultured on PVG+RGD microcarriers for 1, 2, 4, or 7 days (a-d, respectively), at which point a 1mL sample was removed from the bioreactor. Cells were passaged using EDTA and separated from the microcarriers and stained using Hoechst 33342. e) Nuclei were counted and used to obtain a measure of the total cell count in the bioreactor. Scale bar = 100 µm.

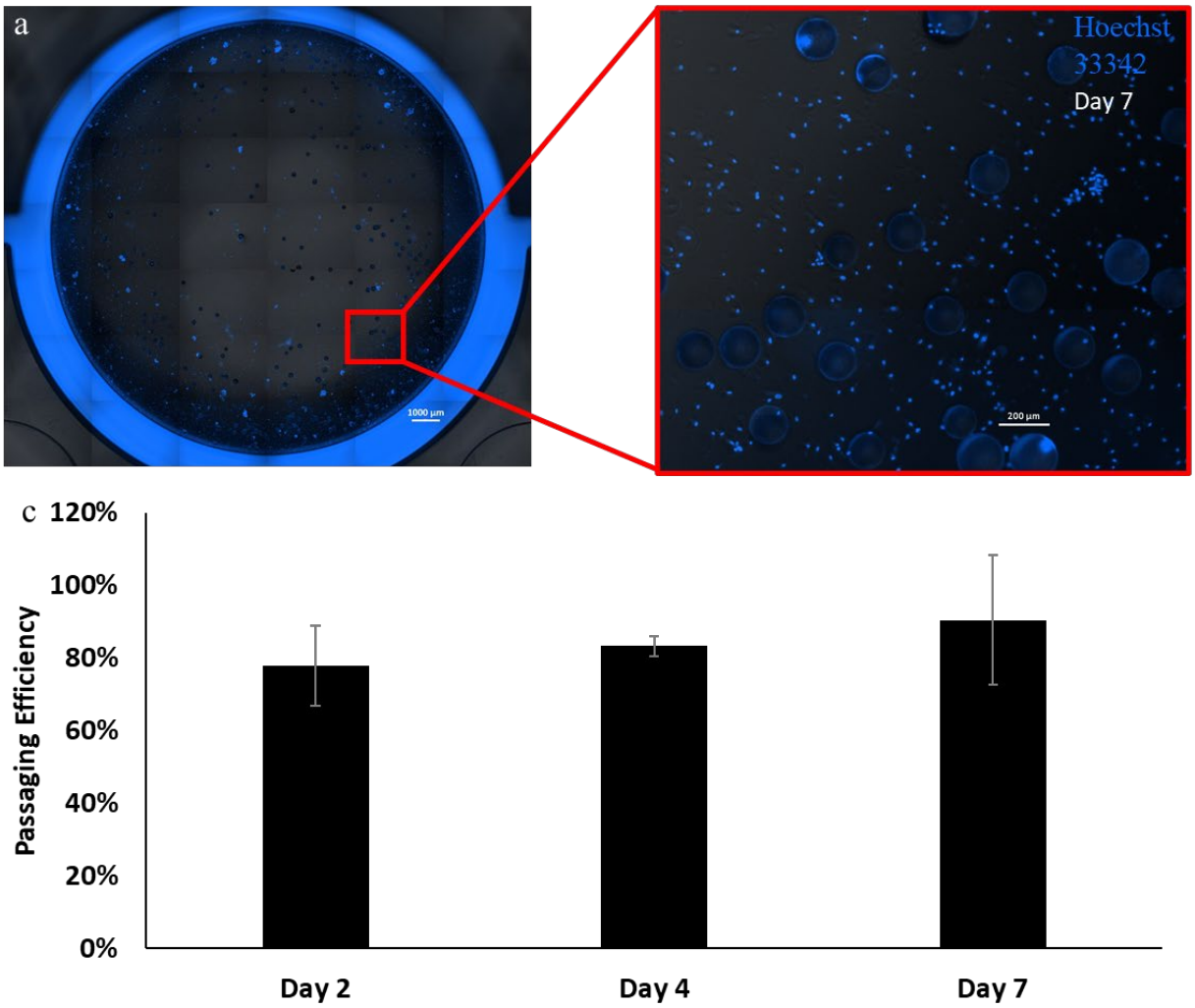

Figure 4.9.5 EDTA passaging remains effective throughout a 7-day culture period. a-b) Fluorescent micrographs of hMSC grown on PVG coated microcarriers cultured in xeno free media, and passaged using EDTA. c) Quantification of passaging efficiency (percentage of cells removed from microcarriers by EDTA) was defined as the percentage of total nuclei that were detached from microcarriers after EDTA exposure (Equation 2). Blue = DAPI, scale bars a) 1000 µm, b) 200 µm

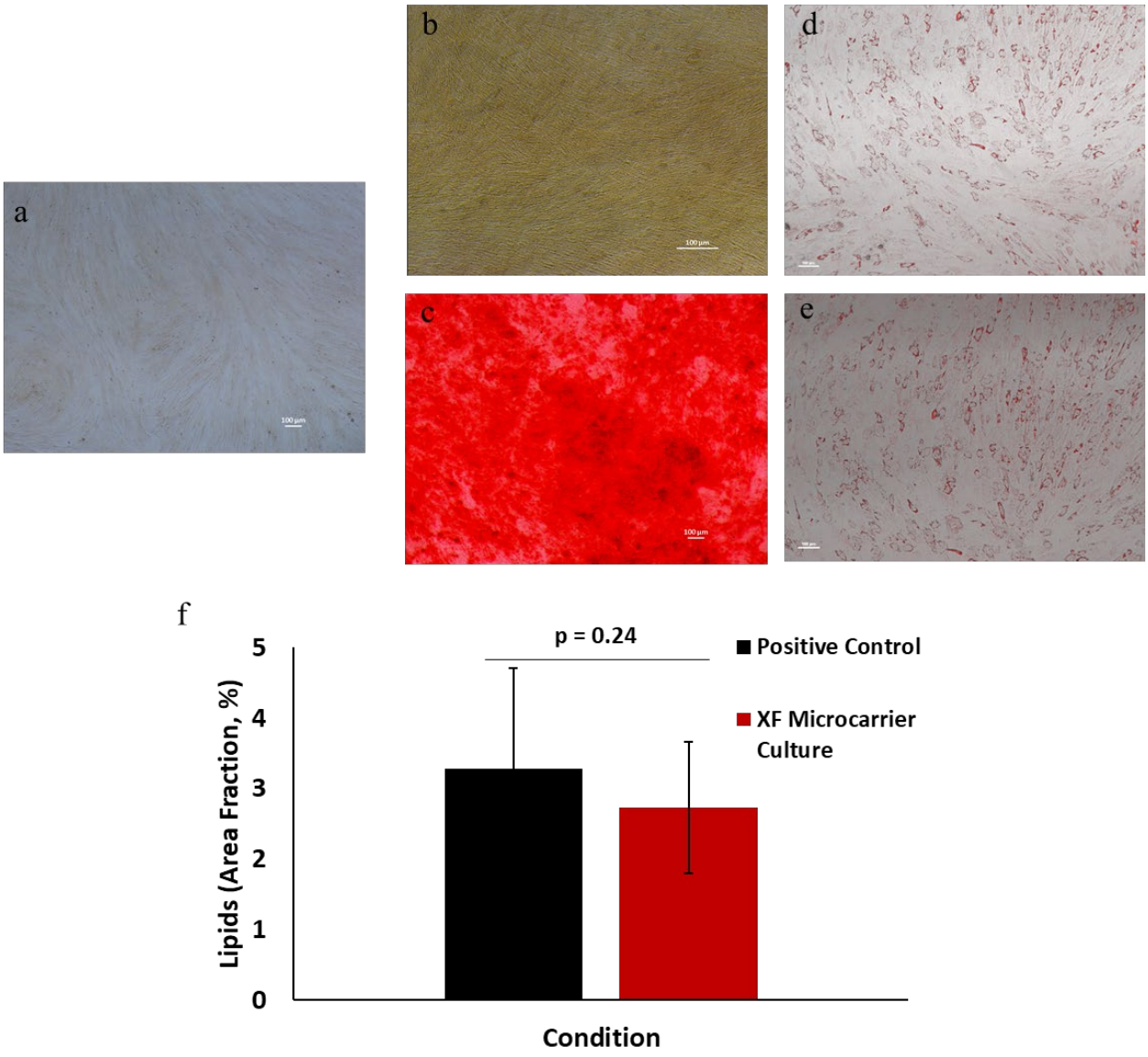

Figure 4.9.6 Differentiation of hMSC cultured in xeno-free media in a bioreactor. a) hMSC cultured in aMEM + 2% FBS as a maintenance condition and postitve control. hMSC cultured in osteogenic differentiation media after 7 days in XF bioreactor culture exhibited a change in appearance similar to cells undergoing osteogenic differentiation but did not stain positively for mineral deposition by Alizarin Red S. c) hMSC that had not been cultured in a bioreactor stained positively for mineral deposition after undergoing osteogenic differentiation. Cells differentiated down the adipogenic lineage stained positvely for lipid deposits by Oil Red O when cultured in a

bioreactor (d) or on planar surfaces (e). f) The amount of lipid deposition was not significantly changed by bioreactor culture. Scale bars = 100 μm; $p = 0.24$

4.10 SUPPLEMENTAL FIGURES

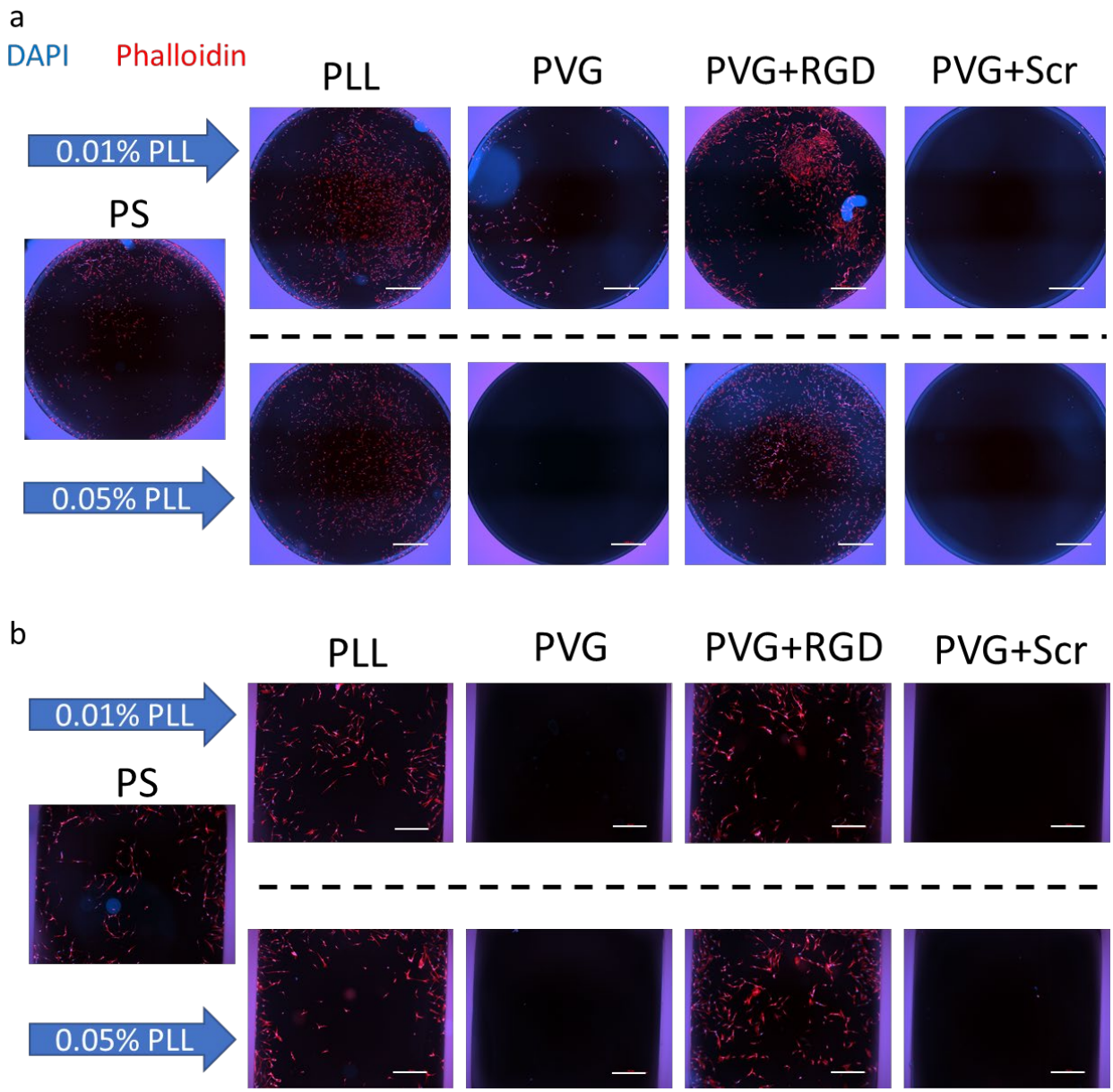

Figure 4.10.1 Increased PLL content improves the application of PVG to TCPS surfaces. Representative micrographs of hMSC grown on PVG-coated a) 96-well and b)384-well polystyrene plates. a) scale bar = 1000 µm. b) scale bar = 500 µm

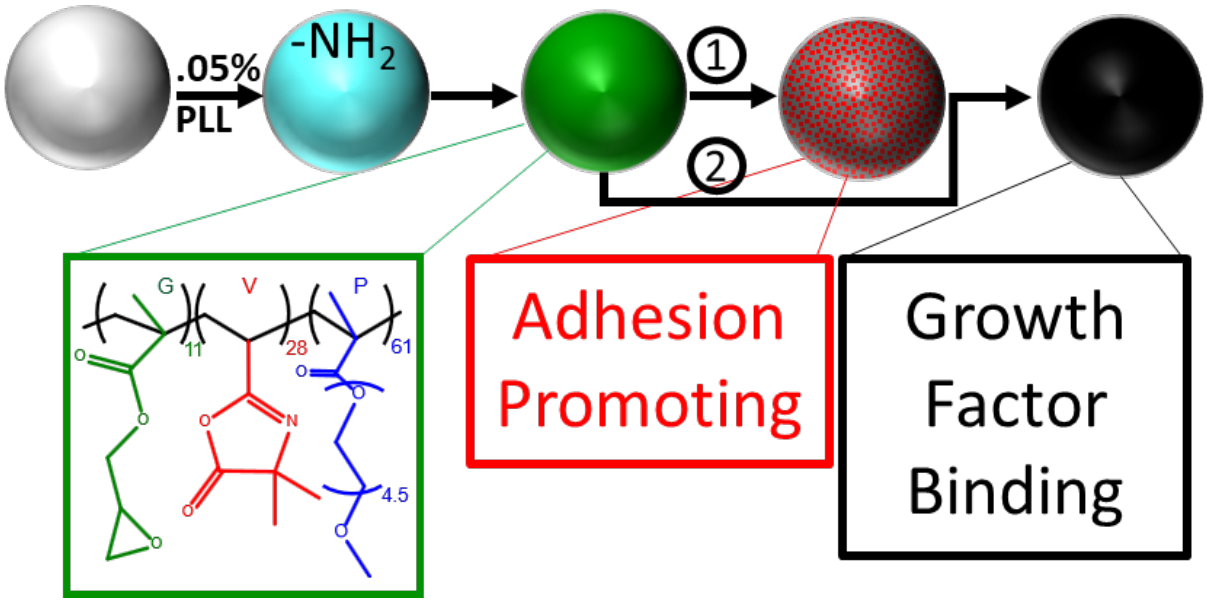

Supplemental Figure S4.10.2 Sequential anchoring of PVG copolymer onto PS microcarriers. First, 0.05% PLL is adsorbed to the surface of PS microcarriers. Next, PVG copolymer is bound to the primary amines on the surface through its epoxide group. Finally, the microcarriers can be tailored to a specific biological function such as adhesion or growth factor sequestration through N-terminal cysteine peptides.

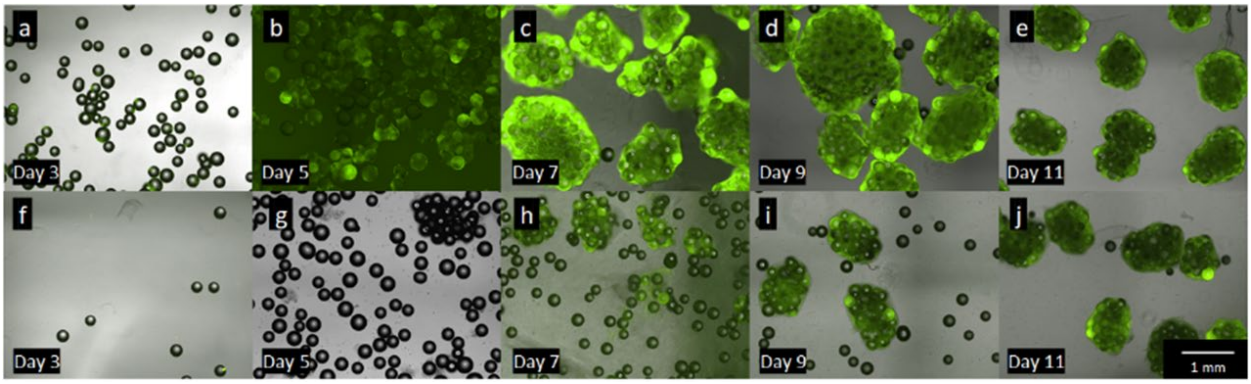

Supplemental Figure S4.10.3 15 day bioreactor culture of hMSC in xeno-free media. Microcarriers and cells begin to form large aggregates between day 5 and day 7. These aggregates continue to get larger out to day 15. Large aggregates make processing and passaging difficult and introduce cell-cell contacts which likely lead to the contact-inhibition driven decrease in cell proliferation rate after day 4. Phase and fluorescent micrographs. Green = LIVE (Calcein AM). Scale bar = 1000 µm.

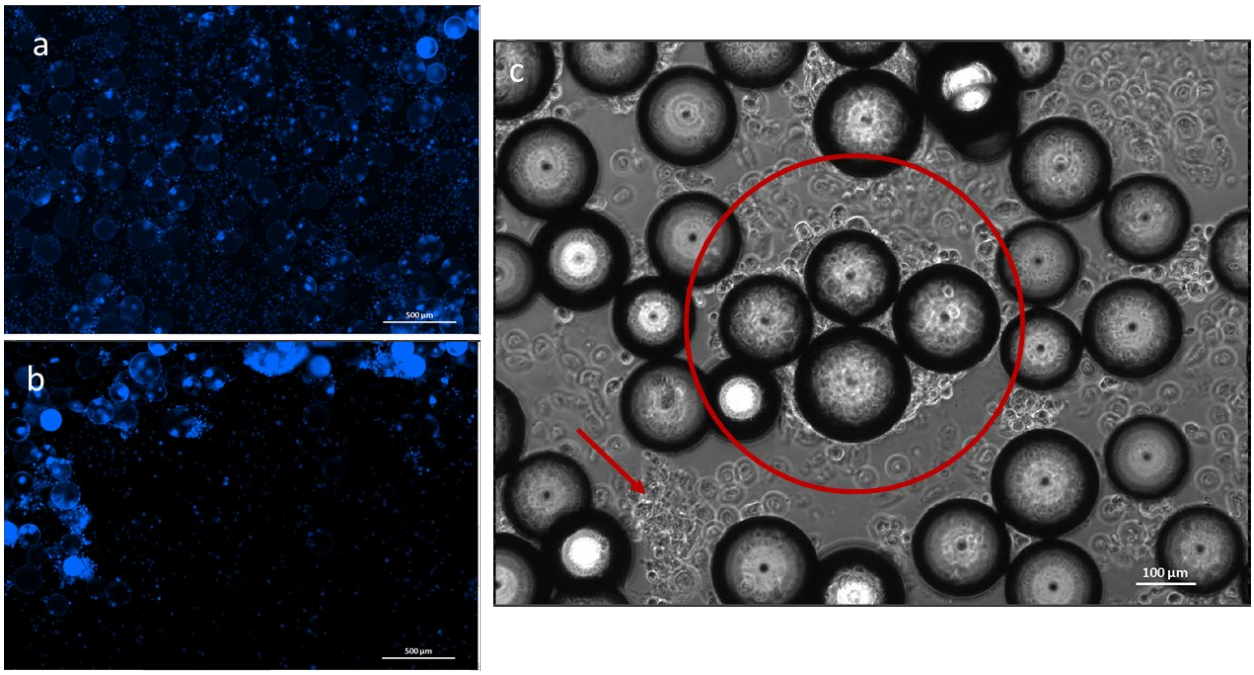

Supplemental Figure S4.10.4 EDTA passaging is insufficient to remove hMSC from Corning® Synthemax™ microcarriers. Micrographs of hMSC grown on Synthemax™ microcarriers cultured in xeno free media, and passaged using a) TrypLE or b) EDTA. c) hMSC remain in large aggregates of cells alone (arrow) and cells and microspheres (circle). Blue = DAPI, scale bars a,b) 1000 µm, c) 200 µm

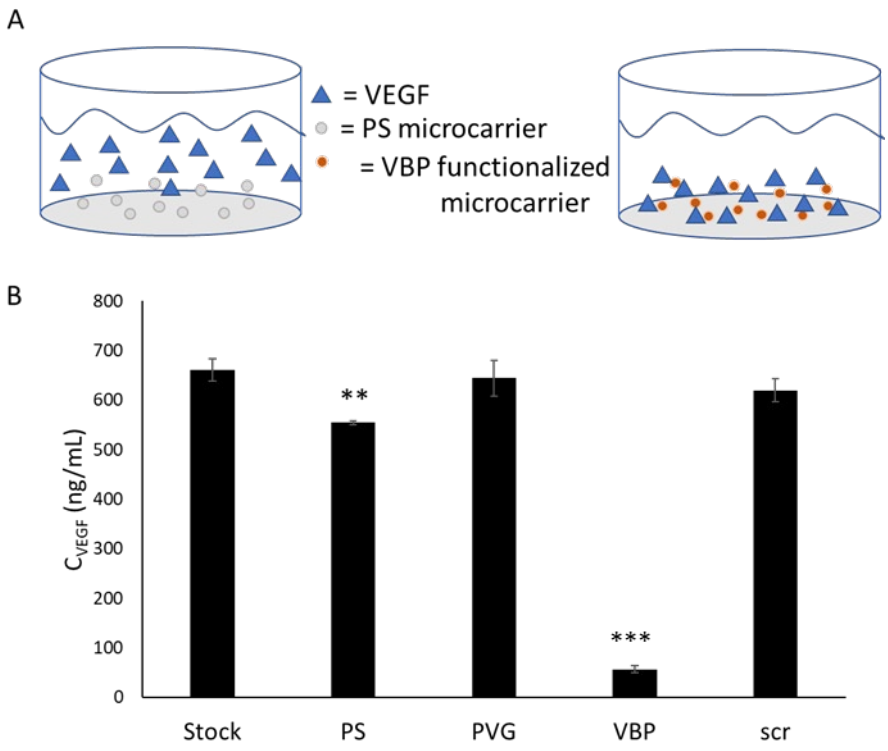

Supplemental Figure S4.10.5 VEGF Binding Peptide (VBP)-functionalized microcarriers can bind to soluble VEGF. a) VBP functionalized microcarriers bind to soluble VEGF, sequestering the protein near the culture surface. This results in b) a knockdown of soluble VEGF detectable by ELISA, where VBP functionalized microcarriers reduced significantly reduced the amount of detectable VEGF in the stock solution. **$p<0.01$; *** $p<0.001$ compared to the stock solution by one-way ANOVA with post-hoc Tukey's test.

CHAPTER 5. SURFACE-MEDIATED GROWTH FACTOR RECEPTOR BINDING THROUGH PEPTIDE HETERODIMERS

5.1 PREFACE

In Chapter 4, we described a microcarrier culture platform in xeno-free media that improved upon many aspects of the currently available cell culture materials. We developed a scalable, xeno-free, and enzyme free culture system based around the tailorable, chemically defined PVG coating. This copolymer can be used as a chemically defined surface that resists protein adsorption and cell adhesion and can be functionalized with a range of bioreactive peptides to enact a desired effect on human mesenchymal stromal cells. In this chapter, we functionalize the PVG coating with growth factor receptor binding peptides to directly influence cell behavior from the material surface. We first investigate the material chemistry to control the presentation and inter-molecular spacing of multiple growth factor receptor binding peptides. We use a novel functionalization procedure to control the spacing of two separate peptides covalently bound and verify that spacing difference using Förster resonance pairs. This chemically defined surface modulates cell signal transduction and microsphere uptake in a peptide spacing-dependent manner. Finally, we demonstrate a potential application for growth factor receptor binding materials by using VEGF receptor-binding magnetic microspheres to sort for VEGFR+ cells from a mixed population using magnetic assisted cell sorting (MACS)

5.2 ABSTRACT

Growth factors are soluble molecules that act as signaling molecules between cells, bind to receptors on the cell membrane, where their signal is transduced into the cell. This triggers a signaling cascade that results in a change in cells and cell behavior, such as survival, growth, proliferation, migration, or differentiation. In *in vitro* cell culture applications, this is typically done using expensive recombinant growth factors or a mixture of proteins sourced from animals such as FBS. Recombinant growth factors are expensive to produce and distribute, and are the highest cost associated with the *in vitro* production of human cells. Serum sourced from xenogeneic sources contain a mixture of up to tens of thousands of biologically active molecules that vary greatly from batch to batch and is dependent on livestock prices and shipping logistics that make its use an unpredictable influence on the cell manufacturing process. Additionally, xenogeneic serum has been shown to pass along xenogeneic markers onto human cells resulting in an immune response in humans. In some cases, anaphylaxis has been reported. One potential replacement for the use of xenogeneic or recombinant growth factors are peptides – short sections of amino acids – that are designed to replicate the binding of soluble growth factors and their growth factor receptors. Growth factor binding peptides have been shown to recreate the binding of multiple growth factors to their respective growth factor receptors, including vascular endothelial growth factor receptor (VEGFR), endothelial growth factor receptor, neruopilin-1 (Nrp1), fibroblast growth factor receptor, and transforming growth factor beta receptor, among others. In this work, we focus on VEGFR- and Nrp1-binding peptides and demonstrate that growth factor receptor binding peptides can affect cell behavior and cell-material interactions when the signal is presented from the surface of a biomaterial. We apply a tailorable thin, synthetic polymer coating - poly(poly(ethylene glycol) methyl ether methacrylate-*ran*-vinyl dimethyl azlactone-*ran*-

glycidyl methacrylate) [P(PEGMEMA-*r*-VDM-*r*-GMA); PVG] - to the surface of existing cell culture materials and demonstrate control over the spacing of a VEGF receptor binding peptide (VR-BP) and a Nrp1 binding peptide (CendR) on the material surface. First, we establish the ability to control peptide spacing using a novel functionalization procedure and Förster pairs to demonstrate spatial control using fluorescent imaging. Next, we show that exposure to PVG-coated, growth factor receptor binding microspheres can directly influence cell behavior, and that the nanometer-scale spacing of these growth factor receptor binding peptides can directly influence the way in which cells interact with PVG coated microspheres. Finally, we report that increasing the distance between growth factor receptor binding peptides affects both signal transduction and the rate at which cells internalize 5 μm microspheres.

5.3 INTRODUCTION

Traditional cell culture materials typically focus on the growth surface as a permissive environment enabling cell adhesion and growth. In recent years, the understanding of cell culture materials has grown to view the cell culture surface as instructive as well as permissive[1-3]; providing signals to the cells as well as enabling their growth and survival. Material chemistry[2], stiffness[2-4], and the incorporation of biologically active molecules[5] have been used to elicit a wide array of cellular responses, including differentiation[2, 4], proliferation[6], migration[7], angiogenesis[8, 9], and others. Among these biologically instructive materials are specifically engineered, synthetic cell culture materials capable of binding with specific cell receptors or receptor complexes and altering cell behavior[10, 11].

There is ample evidence of cell surface receptors forming complexes which augment their downstream signaling cascades. One illustrative previous example of biomaterials that promote receptor-receptor interactions comes from the clustering of integrins using spatial patterns of the peptide sequence RGD. Integrins diffuse laterally through the cell membrane to form clusters, which become part of focal adhesions, and are responsible for cell-substrate adhesion. There is evidence that RGD spatial patterning influences this attachment phenomenon, as well as cell adhesion and mobility[12-16]. While the clustering of integrins on cell membranes has been studied using multiple templates, complexation of growth factor receptors on surfaces has been less studied. Growth factor mimicking peptides have been shown to elicit a signaling response from many growth factor receptors, including vascular endothelial growth factor receptor (VEGFR)[17], endothelial growth factor receptor, neruopilin-1 (Nrp1), fibroblast growth factor receptor[18], and transforming growth factor beta receptor[10], among others[19]. There is prior evidence that the density of immobilized VEGFR-binding peptides on a substrate can affect signal transduction[11,

[17]. One peptide that has been previously studied is a VEGFR-binding peptide (VR-BP) that can enhance VEGF-dependent endothelial cell proliferation when immobilized at high density, and can block VEGF-dependent proliferation when immobilized at lower density.[11, 20]

Another type of receptor clustering is the interaction between growth factor receptors and their co-receptors. Growth factor receptors often have co-receptors that serve as their partners during initiation of signal transduction pathways, and a single receptor/co-receptor pair can often activate multiple signaling pathways in the cell. Thus, the receptor/co-receptor interaction represents a novel and particularly important mechanism for manipulating cell behavior. One such growth factor receptor/co-receptor pair is VEGFR and Neuropilin (Nrp). Neuropilin I and II are cell surface receptors that have pleiotropic function in many cell types, acting in the cardiovascular, neuronal and immune systems[21-24]. The formation of Nrp-VEGFR complexes[25] have been shown to influence VEGFR activation and many VEGF-dependent functions in endothelial cells[26-29]. VEGF-A_{165}, a splice variant of VEGF which includes exons 7&8, is capable of binding to both VEGFR2 and Nrp1, forming a complex at the cell surface.[30] These complexes are internalized in vesicles that are marked for dephospohrylation and destruction or recycled back to the cell surface for further signaling. Complexation of VEGFR2 with Nrp1 results in extended activation downstream signaling from VEGFR2. Indeed, Nrp1 and VEGFR2 complexation has been implicated in extracellular signal regulated kinase (ERK1/2) signaling[31], p38 Mitogen-activated protein kinase (MAPK) signaling[32], and focal adhesion kinase (FAK) phosphorylation through PLCγ[27], each of which has been shown to lead to cell cycle activation.

In this work, we describe a chemically defined copolymer surface tailored to enact spatial control of VEGFR binding peptide (VR-BP) and a Nrp1 binding peptide (CendR) on a nanometer scale. This copolymer, poly(poly(ethylene glycol) methyl ether methacrylate-*ran*-vinyl dimethyl

azlactone-*ran*-glycidyl methacrylate) [P(PEGMEMA-*r*-VDM-*r*-GMA); PVG]; has been shown to resist the nonspecific adsorption of proteins and is tailorable through N-terminal cysteine peptides. We demonstrate modulation of spacing between the two peptides using a heterobifunctional crosslinker that leverages the unique reaction chemistry that takes place between peptides and the VDM residue within PVG. Selectively quenching of the emission from a fluorescently tagged peptide by Förster resonance energy transfer (FRET) confirms this spacing. We then show that interactions between human umbilical vein endothelial cells (HUVEC) and the peptides on the PVG coating are peptide specific, ensuring that behavioral effects are due to the VR-BP and CendR peptides, and their spacing relative to one another. Finally, we show that the distance separating the two peptides on VR-BP/CendR complex surfaces controls the uptake of VR-BP/CendR microspheres as well as VEGFR2-dependent ERK signaling.

5.4 RESULTS

5.4.1. Divalent Presentation of Growth Factor Binding Peptides

The VEGF family of growth factors are proteins that function to stimulate cell proliferation, survival, angiogenesis and vasculogenesis in mammals[32-34]. One VEGF family growth factor, VEGF-A, exists in multiple isoforms. VEGF-A_{165} is a sub-8 nm protein[35] that has multiple binding loci to growth factor receptors on the cell surface. Two of these receptors are VEGFR2 (also called KDR), one of the most common VEGF targets, and Nrp1. Binding of VEGF-A_{165} to VEGFR2 causes VEGFR2 dimerization and autophosphorylation, resulting in signal transduction. VEGF-A_{165} includes exons 6 and 7 from translation, which allows it to also bind to Nrp1, forming a heterodimer of VEGFR2 and Nrp1[30, 32, 36, 37] (**Figure 5.9.1a**). VEGFR2-Nrp1 heterodimer formation results in the altered signal transduction and receptor internalization[33, 34]. In this work, we describe a functionalizable, synthetic copolymer that we leverage to present both

VEGFR2-binding and Nrp1-binding peptides at a defined distance to control growth factor receptor dimer formation (**Figure 5.9.1b**). The peptide binding chemistry used in this work is based on previous work from our group, in which a one-step reaction of VDM with N-terminal cysteine peptides was developed[38, 39]. In this process, native chemical ligation (NCL) of the adjacent N-terminal amine replaces the initial thioester bond, resulting in an amide bond linking the peptide to the PVG copolymer, and an adjacent free thiol that can be tagged using maleimide click chemistry[38] (**Figure 5.9.2a**). First, a maleimide/N-hydroxy succinimide (NHS) heterobifunctional crosslinker of defined length was bound to the free thiol (**Figure 5.9.2b**). Next, the secondary peptide was bound to the NHS terminal of the crosslinker to create the final divalent peptide pair, with the distance between peptides controlled by the length of the heterobifunctional crosslinker (**Figure 5.9.2c, d**). The control over the spacing between two molecules was demonstrated using the principle of Förster resonance energy transfer (FRET). FRET describes a phenomenon by which fluorescent molecules with overlapping excitation and emission wavelengths result in the energy transfer and fluorescent quenching of the FRET donor[40]. In this experiment, the spacing between a fluorescein-labeled peptide and a tetramethyl rhodamine (TAMRA) using the method described above. The Förster radius for fluorescein and TAMRA, the distance at which 50% of the emitted light is quenched, is 5.2 nm[40, 41]. We hypothesized that spacing conditions well outside the Förster radius at 44 nm would result in fluorescence (**Figure 5.9.3a**), while spacing within the Förster radius at 1.7 nm (**Figure 5.9.3b**) would quench the fluorescence. A baseline fluorescence measure was recorded for the unlabeled peptide and TAMRA labeled peptide, to which all other conditions were standardized (**Figure 5.9.3 c1-2, d1-2**). The fluorescein-labeled peptide fluoresced on the PVG surface in the presence of each crosslinker if TAMRA was not present (**Figure 5.9.3 c3-4, d3-4**). This fluorescence was

completely quenched when TAMRA was bound at 1.7nm (**Figure 5.9.3 c5, d5**), and only partially reduced when TAMRA was bound at 44nm (**Figure 5.9.3 c6, d6**). These results supported the hypothesis that the reaction mechanism described above provided necessary control over the molecular spacing on the surface of chemically defined PVG coatings.

5.4.2 Cell-PVG Interactions are Peptide Specific

In previous work using the PVG coating, the coating was used as a chemically defined surface to be modified with an RGD peptide to enable integrin-specific cell adhesion[38, 39, 42]. For this work, HUVEC were grown on a traditional TCPS surface. The VEGFR2-Nrp1 binding peptides were presented on the surface of PVG coated 5μm and 10μm diameter iron-modified PS (PS-Fe) beads (**Supplemental Figure S5.10.1**). This enabled the decoupling of cell adhesion and growth factor binding peptides and ensured that the effects on cell behavior could be attributed to the growth factor binding peptides. Uncoated and PVG-coated PS-Fe microspheres with either an integrin-binding RGD peptide or a VEGFR2-binding peptide (VR-BP) were used to demonstrate that the cell-microsphere interactions were peptide specific. We cultured HUVEC cells on PVG+RGD surfaces for 24 h, at which point we added the functionalized microspheres. After incubation for ten minutes, cells were harvested from the surface using EDTA, as previously reported[43]. Microspheres and microsphere-bound cells were then isolated using a strong magnet and re-seeded onto TCPS plates (**Figure 5.9.4a**). Using bare PS-Fe and PVG-coated microspheres, cells remained unbound and were not sorted into the magnetic fraction (**Figure 5.9.4b, c**). When PVG-coated microspheres were functionalized using VR-BP, bound cells were sorted into the magnetic fraction (**Figure 5.9.4d**). RGD-functionalized microspheres did not bind and sort cells into the magnetic fraction. This is likely due to the EDTA-based chelation of Ca^{2+} and Mg^{2+} cations interfering with the divalent cation-dependent integrin receptors that bind RGD[44, 45] (**Figure**

5.9.4e). The binding and release of RGD functionalized and not VR-BP functionalized microspheres in the presence of EDTA demonstrates that PVG coated surfaces can be customized with biologically active peptides, and that the cell/coating interaction is peptide specific. To demonstrate the utility of this function, VR-BP functionalized microspheres were used to positively sort VEGFR2-expressing HUVEC cells from a mixed population of HUVEC and neural progenitor cells (NPCs) (**Supplemental Figure S5.10.2**).

5.4.3. Effect of VEGFR2-Nrp1 Binding Surfaces on Endothelial Cells

Delivery of VEGFR2-Nrp1 Binding Surfaces to Endothelial Cells: First, HUVEC survival in response to treatment with either uncoated or PVG-coated PS-Fe microspheres was evaluated (**Figure 5.9.5**). HUVEC were imaged at 12-hour intervals post microsphere addition using the Live/Dead assay to assess survival over 48 hours. Uncoated 5 μm and 10 μm PS-Fe microspheres caused significant cell death over 48 hours (**Figure 5.9.5a, c**). However, HUVEC that were treated with PVG-coated microspheres did not show significant cell death, suggesting that the chemically defined PVG coating reduces cell interaction with the microspheres to limit damage to the cells (**Figure 5.9.5b, d**). Phase microscopic images of HUVEC and PVG-PS-Fe microspheres shows areas of heterogeneous microsphere density (arrows) and "drifting" effects, where the microspheres flow slightly along the bottom of the well until they encounter a cell, at which point the microspheres aggregate into a loose drift (circle).

VRBP-CendR Surfaces Reduce VEGF-based signal transduction: While VEGFR2 phosphorylation and increased ERK pathway signal transduction are reported in literature[17] as a result of soluble VR-BP peptide delivery, we were unable to recreate these results. Additionally,

soluble complexes of VR-BP and CendR were not sufficient to induce ERK signaling, nor was the stable presentation of these complexes from PVG-coated microcarriers (**Supplemental Figure S5.10.2**). HUVEC were cultured with PVG coated microspheres that were functionalized with either VR-BP alone or VR-BP and CendR peptides at variable controlled distances as described in the **Experimental Section**. HUVEC were cultured with the functionalized microspheres for 10 minutes to allow time for the microspheres to settle and bind to the receptors on the cell surface. We then lysed the HUVEC and measured signal transduction through the ERK pathway. In standard EGM2 media, the detectable phosphorylated ERK (pERK) was reduced in cell populations that had been exposed to VEGFR2/Nrp1 binding microspheres (**Figure 5.9.6a**). In a separate experiment, HUVEC that had been cultured with VR-BP/CendR microspheres were then supplemented with 100ng/mL VEGF-A_{165}. In these conditions, the reduction of pERK signaling was dependent on the spacing of VR-BP and CendR peptides. HUVEC treated with microspheres and peptides spaced using the 1.7 nm crosslinker resulted in significantly lower pERK levels than peptides spaced by 3.9 nm or 9.1 nm. This suggests that the VR-BP and CendR peptides bind to and occupy VEGFR2 and Nrp1 without initiating phosphorylation, and present competitive site inhibition to soluble VEGF proteins.

VRBP-CendR Spacing Alters Microsphere Uptake Rate: Endothelial cells in the literature have been shown to internalize microspheres up to 6 μm in diameter. PVG coated microspheres prevented HUVEC internalization in culture (data not shown). Both HUVEC and hMSC internalized VR-BP functionalized microspheres up to 10 μm in diameter[46-48]. HUVEC and hMSC were cultured in the presence of 40 ng/mL VR-BP functionalized microspheres/cell for 4h. Spacing between the VR-BP and CendR peptides was varied between samples using a

heterobifunctional crosslinker of defined length, as described previously. Cells were then imaged immediately and after 4h, using Calcein AM to visualize live cell bodies and the autofluorescence of the PS-Fe microspheres in the TAMRA channel. Internalized microspheres displaced the cell cytoplasm, resulting in a "hole" in the Calcein AM fluorescence (**Figure 5.9.7, left**). In HUVEC, the rate of microsphere internalization was 2.7 microspheres/cell using VR-BP functionalized microspheres. This uptake rate was not significantly affected by inclusion of the CendR peptide at 1.7nm, with an uptake rate of 3.0 microspheres/cell. Increasing the distance between the growth factor receptor binding peptides to 3.4 nm reduced the microsphere internalization rate from 2.7 to 0.7 microspheres/cell. HUVEC uptake of VR-BP/CendR functionalized microspheres was reduced by further increasing the peptide spacing to 9.1 nm, to 0.5 microspheres/cell (quantification in **Supplemental Figure S5.10.3**). In hMSC, the microsphere internalization rate remained high regardless of the inclusion of the CendR peptide or its spacing from VR-BP (**Figure 5.9.7, right**).

5.5 DISCUSSION

Traditional cell culture materials typically focus on the growth surface as a permissive environment enabling cell adhesion and growth. In recent years, the understanding of growth surfaces has grown to view the cell culture surface as instructive as well as permissive. Engineered, synthetic cell culture surfaces and materials are capable of binding with specific cell receptors and altering cell behavior. Certain peptides have been described in the literature that are tailored to bind to specific growth factor receptors, including VEGFR2 and Nrp1, among others. In our previous work in **Chapters 3 and 4,** we created a permissive cell culture surface that is capable of hMSC culture in serum-containing and serum-free media. In this work, we expanded upon the

existing capabilities of our PVG surfaces as well as the existing information on growth factor receptor binding materials by introducing a synthetic, chemically defined material that can also control the nanometer-scale spacing between growth factor receptor binding peptides. VEGF-A_{165} is a growth factor that is known to induce homodimers of VEGFR2 as well as heterodimers of VEGFR2 and other growth factor coreceptors, including the coreceptor Nrp1. *In vivo*, the heterodimer of VEGFR2-Nrp1 creates a signaling cascade and receptor trafficking mechanism that differs from the VEGFR2 homodimer. The well-studied nature of the VEGFR2/Nrp1 heterodimer and the literature surrounding VEGFR2- and Nrp1-binding peptides made this combination an ideal candidate to demonstrate instructive biomaterials that can induce growth factor heterodimer formation.

A mechanism by which the peptides' relative spacing could be tightly controlled needed to be created in order to interrogate the potential of growth factor receptor binding biomaterials capable of creating receptor/coreceptor heterodimers. This was designed to mimic the natural spacing created by the VEGF-A_{165} protein (**Figure 5.9.1**). Previous work by Schmitt et al. characterizing the nature of the ring opening reaction between VDM and N-terminal cysteine peptides had indicated that the NCL which occurs results in an amide bond linking the peptide to the copolymer, with an adjacent free thiol. This thiol had been shown to be reactive through a one-step click reaction with a maleimide molecule[38]. In our work, we leveraged this reactivity to append a heterobifunctional crosslinker of defined length, which was then used to attach a second peptide (**Figure 5.9.2**). This step-by-step reaction procedure, all done at room temperature in aqueous media, successfully controlled the spacing between the two peptides, as confirmed by fluorescence quenching of adjacent fluorophores on the PVG surface (**Figure 5.9.3**). This is a significant advance, as it is the first case in which growth factor receptor/coreceptor binding

peptides had been presented at a controlled distance from one another to elicit a unique response from the target cell.

The control over the relative spacing of two separate peptides on the material surface was leveraged to probe the effect of growth factor receptor spacing on cell behavior. To elicit a spacing-dependent cellular effect, we first had to ensure that the growth factor receptor binding peptides could be delivered in a controlled manner. By coating 5 μm PS-Fe microspheres with the PVG copolymer, the amount of growth factor receptor binding peptides delivered to the cells could be tightly controlled and the effects of the growth factor receptor binding peptides were decoupled from the adhesivity of the surface. Next, microspheres functionalized with RGD peptide were released from HUVEC in the presence of the divalent cation chelator EDTA, while VR-BP functionalized microspheres were not (**Figure 5.9.4**). This demonstrated that the chemically defined nature of the PVG coating enabled peptide-specific cell-material interactions. This specificity, coupled with the magnetic nature of the microspheres, lends the microspheres to a MACS sorting system that we demonstrated by selecting for a VEGFR2+ fraction of a heterogeneous mixture of cells (**Supplemental Figure S5.10.4**). In future work, a similar growth factor receptor binding microsphere may be used to both alter cell signal transduction and positively sort for the population of cells that has received the signal in a single product.

Finally, VR-BP/CendR peptide complexes were used to elucidate the effect of spacing on the signal transduction and cell behavior of HUVEC cells, which express both VEGFR2 and Nrp1. Interestingly, the VRBP peptide did not induce detectable amounts of VEGF-related signaling, either pVEGFR2 or pERK, when delivered as a soluble peptide, a soluble homodimer of varying length, a soluble heterodimer, or a bound peptide or combination of peptides. However, VR-BP presented on the surface of microspheres knocked down pERK in VEGF-stimulated samples

(**Figure 5.9.6**). This effect was also dependent on the presence of the Nrp1 binding CendR peptide and the spacing between VR-BP and CendR. This suggests that the binding of VEGFR2 to VR-BP functionalized microspheres may be enhanced though the inclusion and spacing of the CendR peptide. Additionally, internalization of the VR-BP functionalized microspheres was dependent on VR-BP/CendR spacing in HUVEC: as the crosslinker binding the two peptides was lengthened, the rate of microsphere internalization decreased substantially (**Figure 5.9.7**). This change in microsphere uptake rate was not seen in hMSC, a cell type that binds and internalizes VR-BP functionalized microspheres (**Supplemental Figure S5.10.5**) but does not express VEGFR2. In the absence of VEGFR2, there is evidence that hMSC bind to VEGF-A_{165} through the platelet derived growth factor receptor (PDGFR)[49]. It has also been shown that Nrp1 is a coreceptor for PDGFR in hMSC[50, 51], suggesting that the PDGFR/Nrp1 complex is less dependent on spacing to trigger internalization. Together with the signal transduction data, these results suggest that the controlled presentation of VR-BP and CendR peptides binds to both VEGFR2 and Nrp1, and that the closely spaced peptides bind more strongly to the receptors than those that are further apart (9.1 nm, the largest spacing used for this study, is longer than the entire VEGF-A_{165} protein on its longest axis). In future work, this may be used to create surfaces that intentionally decrease VEGF signaling. Another potential application for these materials is in controlled microparticle or nanoparticle delivery, which could be used to target a specific cell type for internalization.

This work represents a proof of concept for growth factor receptor binding materials capable of creating receptor/coreceptor heterodimers. We have shown that the PVG copolymer surface can be tailored to present multiple growth factor binding peptides in a step-by-step, aqueous process, and that the spacing between these bioactive peptides can be controlled on a nanometer scale. The interactions between endothelial cells and these surfaces were shown to be

peptide specific. Finally, we showed that the spacing of growth factor receptor and coreceptor binding peptides affects the signal transduction of cells that are bound to the surface. The concept of growth factor receptor heterodimer-forming surfaces is not one that has been thoroughly explored, and could have implications in cell culture, cell manufacturing, and drug delivery applications.

5.6 EXPERIMENTAL SECTION

5.6.1 PVG copolymer synthesis: PVG copolymer was synthesized using reversible addition-fragmentation chain transfer anionic polymerization (RAFT) according to previously reported procedures[38,39,40]. Briefly, poly(ethylene glycol) methyl ether methacrylate (PEGMEMA), glycidyl methacrylate (GMA), and vinyl dimethyl azlactone (VDM) were added to a 25mL Schlenk flask. Anisole was added as a solvent to bring the reaction mixture to 13mL. The chain transfer agent (CTA) 2-cyano-2-propyl benzodithioate and the initiator 2,2'-azobis(2-methylpropionitrile) were added at a monomer : CTA : initiator ratio of 1:1. The mixture was degassed using three freeze-pump-thaw cycles. Polymerization was conducted at 70 °C for 15h and stopped by exposure to the atmosphere. The resultant polymer was precipitated in *n*-hexanes, filtered and dissolved in tetrahydrofuran (THF, Fisher Scientific). This was repeated three times to remove any unreacted monomer. The resultant polymer P(PEGMEMA-*r*-VDM-*r*-GMA) was dissolved and stored in THF. Gel permeation chromatography (GPC) yielded a Mn = 47,000 and a dispersity of 2.1. Proton nuclear magnetic resonance spectroscopy showed the final concentration of the copolymer was 61% PEGMEMA, 29% VDM, and 10% GMA.

5.6.2 PVG coating of microspheres*:* Untreated polystyrene microcarriers with diameter of 125-212 μm (Corning, Corning, NY) were weighed and incubated in 0. 05wt% 70,000-150,000 Da

poly-L-lysine for 1 hour. Microcarriers were then washed twice with dH_2O and once with EtOH. Microcarriers were placed in a 10mg mL^{-1} solution of PVG polymer in EtOH and allowed to react overnight. Microcarriers at this state were stored in EtOH at -20°C for up to 1 month. Coated microspheres were washed 2x in PBS and 1x in EtOH before functionalization with peptides.

5.6.3 Peptide Immobilization: All functionalization reactions on microspheres were conducted in Falcon tubes on a rotating plate to ensure mixing. Peptide functionalization and use in cell culture were conducted on the same day. Immediately before use, microspheres were submerged in sterile 70% EtOH for 20-30 minutes for sanitization.

PVG-Peptide: PVG-coated surfaces were washed twice with PBS and reacted with the desired peptides. One of either Cys-Gly-Gly-Gly-Arg-Gly-Asp-Ser-Pro (CGGGRGDSP, "RGD") or Cys-Gly-Gly-Lys-Leu-Thr-Trp-Gln-Glu-Leu-Tyr-Gln-Leu-Lys-Tyr-Lys-Gly-Ile-amide (CGGKLTWQELYQLKYKGI-NH_2; "VR-BP") peptides (Genscript, Piscataway, NJ) were first bound to the surface of the PVG coated microcarriers. PVG coated microspheres were incubated in 1mM peptide solutions in 1x phosphate buffered saline (PBS) (Fisher Scientific, Hampton, NJ) for 1 hr at room temperature according to the procedure in Schmitt et al. (2015, 2016).

Addition of Crosslinker: PEGylated SMCC Crosslinker ($SM(PEG)_n$, n = 2, 8 or 24) (Thermo Fisher, Waltham, MA) was prepared in 1x PBS at a concentration of 10mM. The microspheres were allowed to react with the crosslinker for 1h at room temperature. Samples were washed 2x with PBS and 1x with EtOH before functionalization with the second peptide.

Addition of Second Peptide: The Neuropilin-1 binding C end Rule (CendR) peptide Gly-Gly-Gly-Arg-Pro-Ala-Arg-Pro-Ala-Arg (GGGRPARPAR) (Genscript) was added to the coated

microspheres at a concentration of 2mM in PBS and allowed to react for 1h at room temperature. Microspheres were rinsed 2x in PBS and 1x in EtOH before use in cell culture.

5.6.4 *In vitro* cell culture:

HUVEC: HUVEC (Lonza Cat #C2519A Lot #0000431888, Basel, Switzerland) were cultured in Endothelial Cell Growth Medium 2 (Promocell, Heidelberg, Germany). Cells were thawed from LN2 storage and seeded onto T75 TCPS plates at 3500-7000 cells cm^{-2}. Cells were incubated at 37°C and 5% CO_2 and manipulated under sterile conditions. Media was changed after 24 hours, then every 2-3 days. Cells were passaged at 70-80% confluence using 5mL TrypLE Select (Invitrogen, Carlsbad, CA) at 37°C and 5% CO_2 for 5 minutes. After 5 minutes, adherent cells were loosened using gentle agitation of the plate

hMSC: hMSC (Roosterbio, XF RoosterKit-hBM Lot 164) were cultured in RoosterNourish™ MSC-XF xeno free media (Roosterbio, Frederick, MD). Cells were thawed from LN2 storage and seeded onto T175 TCPS plates at 2800 cells cm^{-2}. Cells were incubated at 37°C and 5% CO_2 and manipulated under sterile conditions. Media was changed after 24 hours, then every 2-3 days. Cells were passaged at 70-80% confluence using 5mL TrypLE (Invitrogen) at 37°C and 5% CO_2 for 5 minutes. After 5 minutes, adherent cells were loosened using gentle agitation of the plate

5.6.5 Fluorescent imaging:

Live Imaging: Living and Live/Dead cells were imaged in the appropriate media supplemented with Calcein AM (Thermo Fisher, Waltham, MA), Ethidium Homodimer -1 (Thermo Fisher) or CellTracker™ living cell fluorescent dyes (Thermo Fisher). Cells were imaged on an inverted microscope with DAPI, FITC, and Far Red filter cube sets.

Fixed Cells: were washed with 1x PBS and fixed in 10% buffered Formalin solution for 20-30 minutes. Cells were then permeabilized with 0.1% Triton X-100 (MP Biomedicals, Aurora, OH) in 1x PBS for 20 minutes. Cells were washed twice with PBS and blocked using 1% bovine serum albumin (BSA) (Fisher Scientific). Cells were stained for actin cytoskeleton using Alexa-Fluor^{TM} 647 Phalloidin (Thermo Fisher) and for nuclei using 4',6-Diamidine-2'-phenylindole dihydrochloride (DAPI) (Sigma Aldrich) or Hoechst 33342 for 30 minutes each, washing in between with PBS. Cells were imaged on an inverted microscope with DAPI, FITC, and Far Red filter cube sets.

Fluorescence Quenching: Fluorescence quenching was measured on a Nikon TE300 inverted microscope with excitation and emission filter wheels. The Nikon FITC filter with an excitation wavelength of 513-556nm and emission wavelength of 467-498nm was used. Each patterned spot was imaged using the 20x objective and fluorescence intensity was measured in a straight line across the center of the spot and averaged. Four spots per condition were measured and averaged to create the reported fluorescence levels.

Confocal: Confocal microscopy was conducted on a Zeiss LSM880 confocal microscope with Airyscan. Imaging conditions were selected using the Zeiss-4 color confocal fluorescence setting. Images were generated by creating a 3D rendering of z-stack slices using the Zeiss ZEN software.

5.6.6 HUVEC Viability in Response to Microspheres: HUVEC were seeded in 96 well plates at a cell density of 5000 cells cm^{-2} and allowed to adhere overnight. Uncoated and PVG-coated microspheres were added to the cell culture media after 24h of culture. Cells were stained using LIVE/Dead according to the above procedure and imaged at 12h intervals for 48h. Living and dead

cells were counted based on their respective fluorescence and the percentage of living cells was determined.

5.6.7 Determination of Signal Transduction: HUVEC were cultured as described previously and seeded at a cell density of 10,000 cells cm^{-2}. At 24h, cells were treated with VEGF-A_{165} (R&D Systems, Minneapolis, MN) and some combination of PVG-coated microspheres, VR-BP functionalized microspheres, and VR-BP and CendR complex functionalized microspheres. Cells were incubated in the presence of microspheres for 10 minutes at 37 °C and 5% CO_2, at which point they were lysed using Pierce RIPA buffer (Thermo Fisher) and 1% Halt^{TM} Protease and Phosphatase Inhibitor (Thermo Fisher). Cell lysate was stored at -80 °C until ready for use. Cell lysate was thawed on ice and centrifuged at 8000xG for 10 minutes to remove stray microparticles and solid cell debris. ELISA for human phosphorylated VEGFR2 (R&D Systems) and Total/phosphorylated ERK (Abcam ab176660, Cambridge, UK) were conducted according to manufacturers' recommendations. Colorimetric absorbance at 540nm was measured using an automatic plate reader and recorded.

4.6.8 Microsphere internalization: HUVEC and hMSC were cultured according to the procedure reported above. Cells were seeded at 10,000 cells cm^{-2} and allowed to adhere overnight. At 24h, PVG coated VR-BP functionalized microspheres were added to the culture, and cells were incubated at 37 °C and 5% CO_2 for 10 minutes. At this point (t=0) cells were incubated with Caclein AM and imaged using FITC and TAMRA filter cubes, with live cells fluorescing green and microspheres fluorescing red due to inherent autofluorescence. Cells were subsequently imaged at 1h, 4h and 24h. Internalized microspheres displaced the cytoplasm, resulting in a blank circle within the fluorescent cell. Internalized microspheres were counted in representative images of 3 wells per condition.

5.6.9 Magnetic microsphere sorting:

4.6.12 Statistical Analysis

Experiments were carried out and repeated a total of two to three trials, with n=3-4 replicates per trial. Except where noted, a one-way ANOVA was conducted to determine significance, as there are multiple groups with one independent variable. A post-hoc Tukey's test was then used to determine significance between groups.

5.7 ACKNOWLEDGEMENTS

This research was funded by the National Science Foundation (NSF DMR **1709179**).

The authors acknowledge support from staff and the use of equipment at the Materials Science Center at UW-Madison DMR-1121288 and DMR-1720415.

5.8 REFERENCES

[1] F. M. Watt, W. T. S. Huck. *Nat Rev Mol Cell Biol* **2013**;14:467-73.

[2] M. Lanniel, E. Huq, S. Allen, L. Buttery, P. M. Williams, M. R. Alexander. *Soft Matter* **2011**;7:6501-14.

[3] A. J. Engler, S. Sen, H. L. Sweeney, D. E. Discher. *Cell* **2006**;126:677-89.

[4] S. Saha, L. Ji, J. J. de Pablo, S. P. Palecek. *Journal of Cellular Physiology* **2006**;206:126-37.

[5] G. Agmon, K. L. Christman. *Current Opinion in Solid State and Materials Science* **2016**;20:193-201.

[6] T. Hoshiba, H. Lu, N. Kawazoe, G. Chen. *Expert Opinion on Biological Therapy* **2010**;10:1717-28.

[7] S. P. Palecek, J. C. Loftus, M. H. Ginsberg, D. A. Lauffenburger, A. F. Horwitz. *Nature* **1997**;385:537-40.

[8] E. H. Nguyen, W. L. Murphy. *Biomaterials* **2018**;181:53-66.

[9] E. H. Nguyen, M. R. Zanotelli, M. P. Schwartz, W. L. Murphy. *Biomaterials* **2014**;35:2149-61.

[10] L. Li, J. R. Klim, R. Derda, A. H. Courtney, L. L. Kiessling. *Proceedings of the National Academy of Sciences* **2011**;108:11745-50.

[11] J. T. Koepsel, E. H. Nguyen, W. L. Murphy. *Integrative Biology* **2012**;4:914-24.

[12] G. Maheshwari, G. Brown, D. a. Lauffenburger, a. Wells, L. G. Griffith. *Journal of cell science* **2000**;113 (Pt 1:1677-86.

[13] M. Arnold, E. A. Cavalcanti-Adam, R. Glass, J. Blümmel, W. Eck, M. Kantlehner, H. Kessler, J. P. Spatz. *ChemPhysChem* **2004**;5:383-8.

[14] W. A. Comisar, N. H. Kazmers, D. J. Mooney, J. J. Linderman. *Biomaterials* **2007**;28:4409-17.

[15] J. E. Frith, R. J. Mills, J. J. Cooper-White. *Journal of Cell Science* **2012**;125:317-27.

[16] X. Wang, S. Li, C. Yan, P. Liu, J. Ding. *Nano Letters* **2015**;15:1457-67.

[17] L. D. D'Andrea, G. Iaccarino, R. Fattorusso, D. Sorriento, C. Carannante, D. Capasso, B. Trimarco, C. Pedone. *Proceedings of the National Academy of Sciences of the United States of America* **2005**;102:14215-20.

[18] M. D. Ballinger, V. Shyamala, L. D. Forrest, M. Deuter-Reinhard, L. V. Doyle, J.-x. Wang, L. Panganiban-Lustan, J. R. Stratton, G. Apell, J. A. Winter, M. V. Doyle, S. Rosenberg, W. M. Kavanaugh. *Nature Biotechnology* **1999**;17:1199-204.

[19] D. P. Bottaro, E. Fortney, J. S. Rubin, S. A. Aaronson. *Journal of Biological Chemistry* **1993**;268:9180-3.

[20] L. Cai, C. B. Dinh, S. C. Heilshorn. *Biomaterials Science* **2014**;2:757-65.

[21] H.-F. Guo, C. W. Vander Kooi. *Journal of Biological Chemistry* **2015**;290:29120-6.

[22] X. Li, M. W. Parker, C. W. Vander Kooi. *Biomolecular concepts* **2014**;5:157-66.

[23] H. Takamatsu, N. Takegahara, Y. Nakagawa, M. Tomura, M. Taniguchi, R. H. Friedel, H. Rayburn, M. Tessier-Lavigne, Y. Yoshida, T. Okuno, M. Mizui, S. Kang, S. Nojima, T. Tsujimura, Y. Nakatsuji, I. Katayama, T. Toyofuku, H. Kikutani, A. Kumanogoh. *Nat Immunol* **2010**;11:594-600.

[24] F. Nakamura, M. Tanaka, T. Takahashi, R. G. Kalb, S. M. Strittmatter. *Neuron* **1998**;21:1093-100.

[25] X. Zhang, A. A. Lanahan, M. Simons. *Cell Cycle* **2013**;12:2163-4.

[26] H. Gerhardt, C. Ruhrberg, A. Abramsson, H. Fujisawa, D. Shima, C. Betsholtz. *Developmental Dynamics* **2004**;231:503-9.

[27] B. Herzog, C. Pellet-Many, G. Britton, B. Hartzoulakis, I. C. Zachary. *Molecular Biology of the Cell* **2011**;22:2766-76.

[28] T. Kawasaki, T. Kitsukawa, Y. Bekku, Y. Matsuda, M. Sanbo, T. Yagi, H. Fujisawa. *Development* **1999**;126:4895.

[29] S. Takashima, M. Kitakaze, M. Asakura, H. Asanuma, S. Sanada, F. Tashiro, H. Niwa, J.-i. Miyazaki, S. Hirota, Y. Kitamura, T. Kitsukawa, H. Fujisawa, M. Klagsbrun, M. Hori. *Proceedings of the National Academy of Sciences of the United States of America* **2002**;99:3657-62.

[30] S. Koch, Laurens A. van Meeteren, E. Morin, C. Testini, S. Weström, H. Björkelund, S. Le Jan, J. Adler, P. Berger, L. Claesson-Welsh. *Developmental Cell* **2014**;28:633-46.

[31] M. Simons. *Physiology (Bethesda)* **2012**;27:213-22.

[32] M. Simons, E. Gordon, L. Claesson-Welsh. *Nat Rev Mol Cell Biol* **2016**;17:611-25.

[33] A. Lanahan, X. Zhang, A. Fantin, Z. Zhuang, F. Rivera-Molina, K. Speichinger, C. Prahst, J. Zhang, Y. Wang, G. Davis, D. Toomre, C. Ruhrberg, M. Simons. *Developmental Cell* **2013**;25:156-68.

[34] A. A. Lanahan, K. Hermans, F. Claes, J. S. Kerley-Hamilton, Z. W. Zhuang, F. J. Giordano, P. Carmeliet, M. Simons. *Developmental Cell* **2010**;18:713-24.

[35] Y. A. Muller, H. W. Christinger, B. A. Keyt, A. M. de Vos. *Structure* **1997**;5:1325-38.

[36] M. W. Parker, P. Xu, X. Li, C. W. Vander Kooi. *The Journal of biological chemistry* **2012**;287:11082-9.

[37] A. Fantin, B. Herzog, M. Mahmoud, M. Yamaji, A. Plein, L. Denti, C. Ruhrberg, I. Zachary. *Development* **2014**;141:556-62.

[38] S. K. Schmitt, D. J. Trebatoski, J. D. Krutty, A. W. Xie, B. Rollins, W. L. Murphy, P. Gopalan. *Biomacromolecules* **2016**;17:1040-7.

[39] S. K. Schmitt, A. W. Xie, R. M. Ghassemi, D. J. Trebatoski, W. L. Murphy, P. Gopalan. *Advanced healthcare materials* **2015**;4:1555-64.

[40] Y. Sun, C. Rombola, V. Jyothikumar, A. Periasamy. *Cytometry Part A* **2013**;83:780-93.

[41] D. A. Hiller, J. M. Fogg, A. M. Martin, J. M. Beechem, N. O. Reich, J. J. Perona. *Biochemistry* **2003**;42:14375-85.

[42] J. D. Krutty, A. D. Dias, J. Yun, W. L. Murphy, P. Gopalan. *Macromolecular Bioscience* **2019**;19:1800299.

[43] S. K. Schmitt, W. L. Murphy, P. Gopalan. *Journal of Materials Chemistry B* **2013**;1:1349-60.

[44] K. Zhang, J. Chen. *Cell adhesion & migration* **2012**;6:20-9.

[45] J. P. Xiong, T. Stehle, B. Diefenbach, R. Zhang, R. Dunker, D. L. Scott, A. Joachimiak, S. L. Goodman, M. A. Arnaout. *Science (New York, NY)* **2001**;294:339-45.

[46] R. E. Serda, J. Gu, J. K. Burks, K. Ferrari, C. Ferrari, M. Ferrari. *Cytometry Part A : the journal of the International Society for Analytical Cytology* **2009**;75:752-60.

[47] R. E. Serda, J. Gu, R. C. Bhavane, X. Liu, C. Chiappini, P. Decuzzi, M. Ferrari. *Biomaterials* **2009**;30:2440-8.

[48] P. Kolhar, S. Mitragotri. *Advanced Functional Materials* **2012**;22:3759-64.

[49] C. Pfister, H. Pfrommer, M. S. Tatagiba, F. Roser. *British Journal of Cancer* **2012**;107:1702-13.

[50] S. G. Ball, C. Bayley, C. A. Shuttleworth, C. M. Kielty. *The Biochemical journal* **2010**;427:29-40.

[51] S. G. Ball, C. A. Shuttleworth, C. M. Kielty. *The Journal of cell biology* **2007**;177:489-500.

5.9 FIGURES

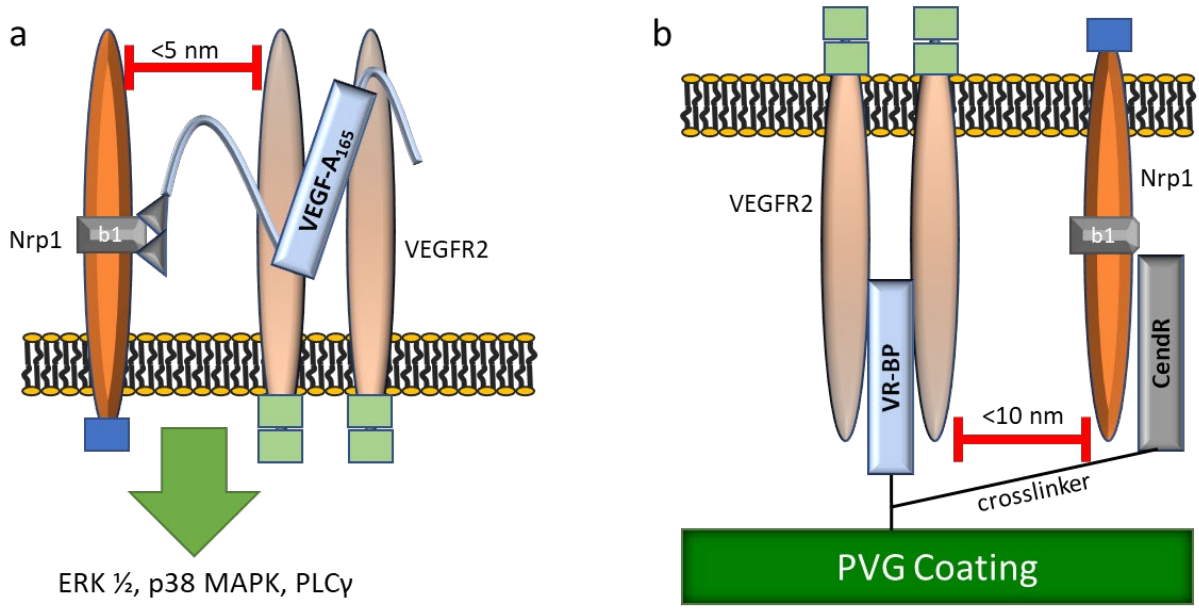

Figure 5.9.1 a) Extracellular complex formation of Nrp1, VEGF-A_{165}, and VEGFR2. VEGF-A_{165} acts as a "bridge" between the two receptors, mediating complex formation. The VEGF Homology Domain, exons 2-5 of VEGF, bind to VEGFR2, inducing dimerization. Exons 6 and 7 (grey) bind to the co-receptor Nrp1. The intracellular Nrp1 domain (blue square) is also necessary for complex formation with VEGFR2. B) Surface-mediated formation of the VEGFR2-Nrp1 complex using VEGFR2- and Nrp1-binding peptides, with peptide spacing controlled by a heterobifunctional crosslinker of defined length.

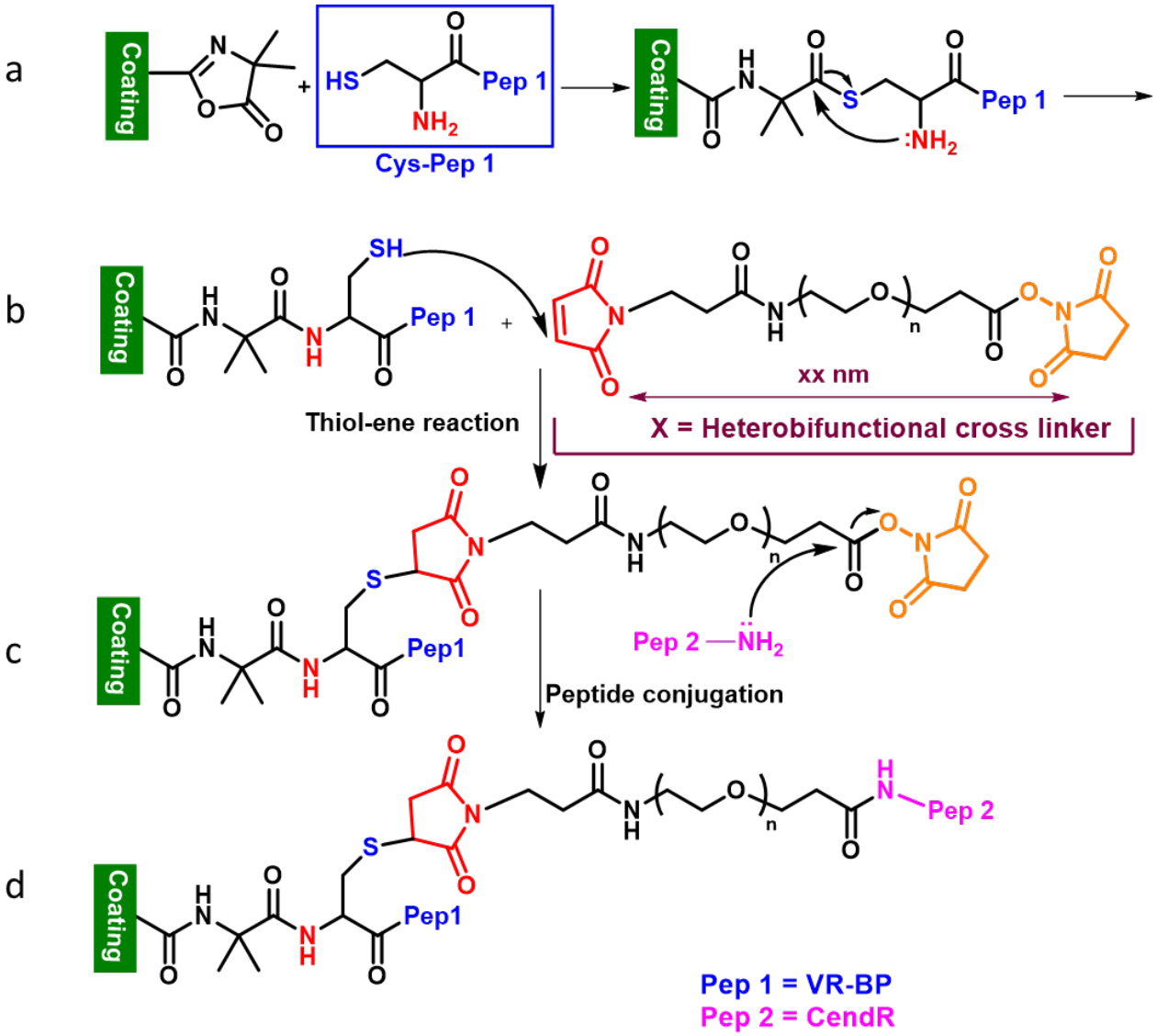

Figure 5.9.2. Schematic of VEGFR2 and Nrp-1 binding peptide complex on the surface of PVG coating. a) VR-BP is bound to the PVG coating via its N-terminal cysteine residue; the resulting native chemical ligation results in an amide bond and free thiol. b) The free thiol is bound to the maleimide end of the crosslinker through a thiol-ene reaction. c) The Nrp-1 binding CendR peptide binds to the NHS-ester end of the crosslinker. d) The spacing of the two peptides can be controlled by adjusting the number monomers in the oligo(ethylene glycol) crosslinker.

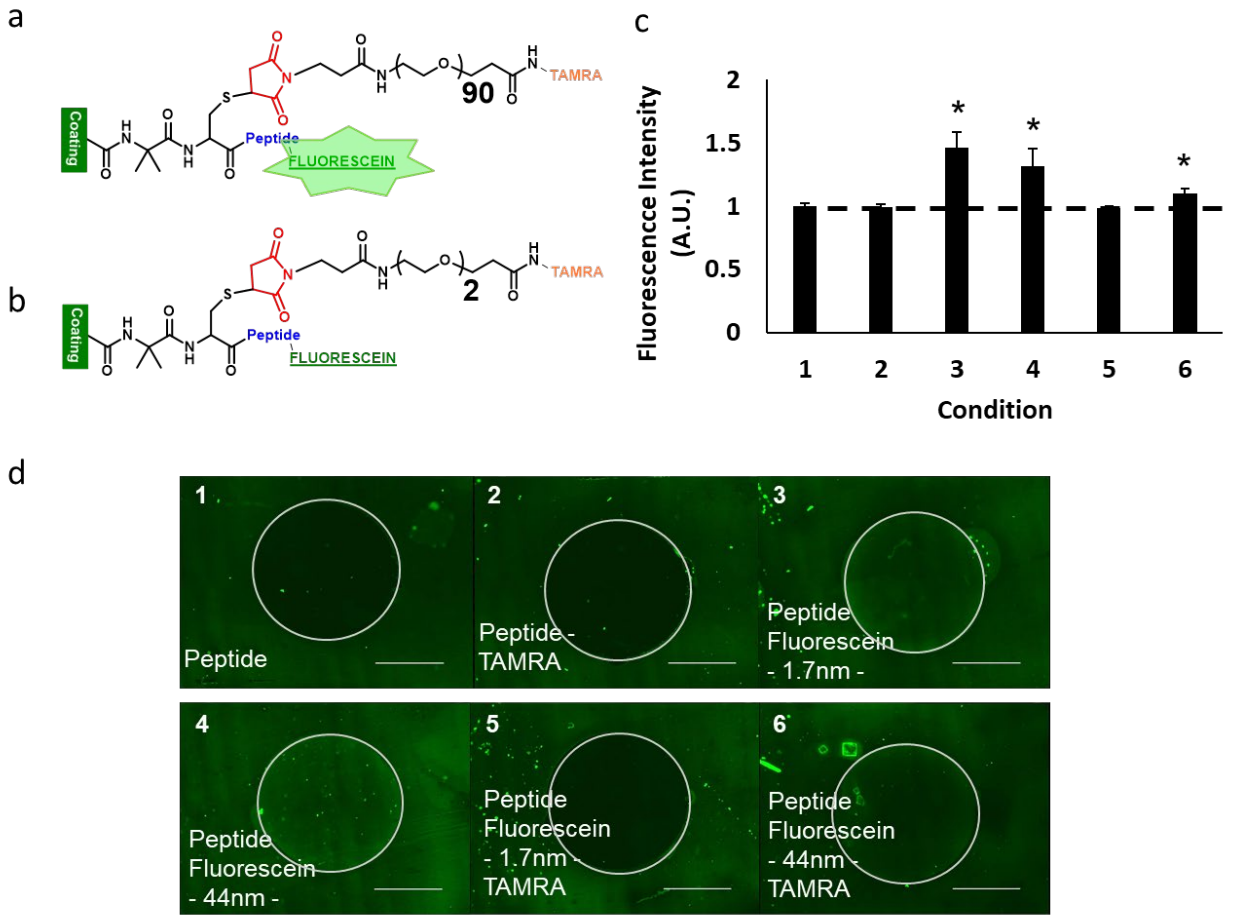

Figure 5.9.3. Fluorescence quenching of FRET pair fluorophores. Schematic of fluorescent (a) and quenched (b) fluorophores bound to the copolymer surface with spacing molecules of varying length. c-d) Fluorescein-labeled peptides increased fluorescence on PVG surface. This fluorescence is quenched and returns to control levels when bound to TAMRA at 1.6nm. Fluorescein spaced at 44nm from TAMRA shows significantly lower fluorescence intensity than fluorescein alone, but significantly higher intensity than 1.6nm. *$p < 0.05$; Scale bar = 500 μm

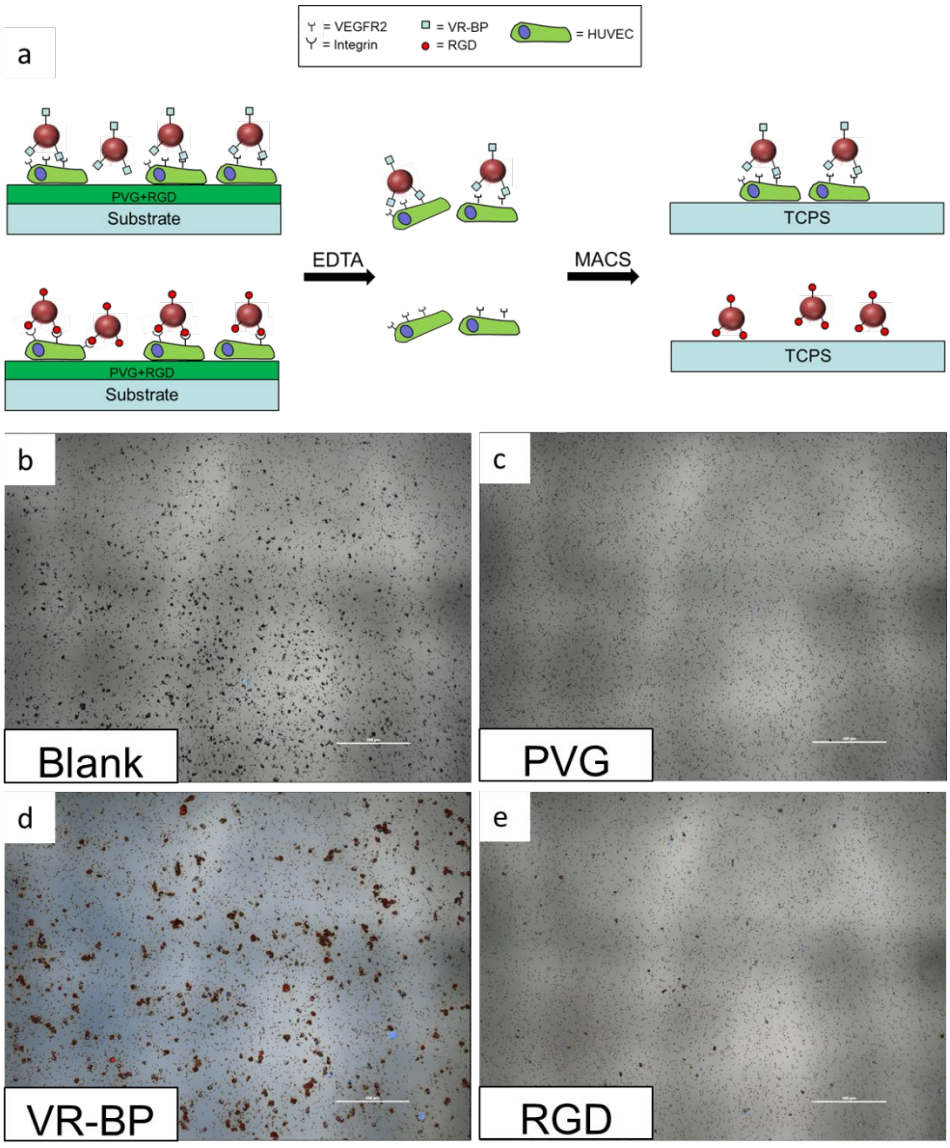

Figure 5.9.4. a) Schematic demonstrating receptor-binding specificity of functionalized, PVG-coated microspheres. VEGFR2 remains bound to VR-BP in the presence of EDTA (top) and are sorted into the magnetic fraction, while Ca^{2+} and Mg^{2+} dependent integrins release from RGD functionalized microspheres (bottom). b-e) Representative images of the magnetic fractions of b) uncoated; c) PVG coated; d) VR-BP functionalized and e) RGD functionalized PS-Fe microspheres. Red = CellTracker™ Red, Blue = Hoechst 33342. Scale bar = 500µm.

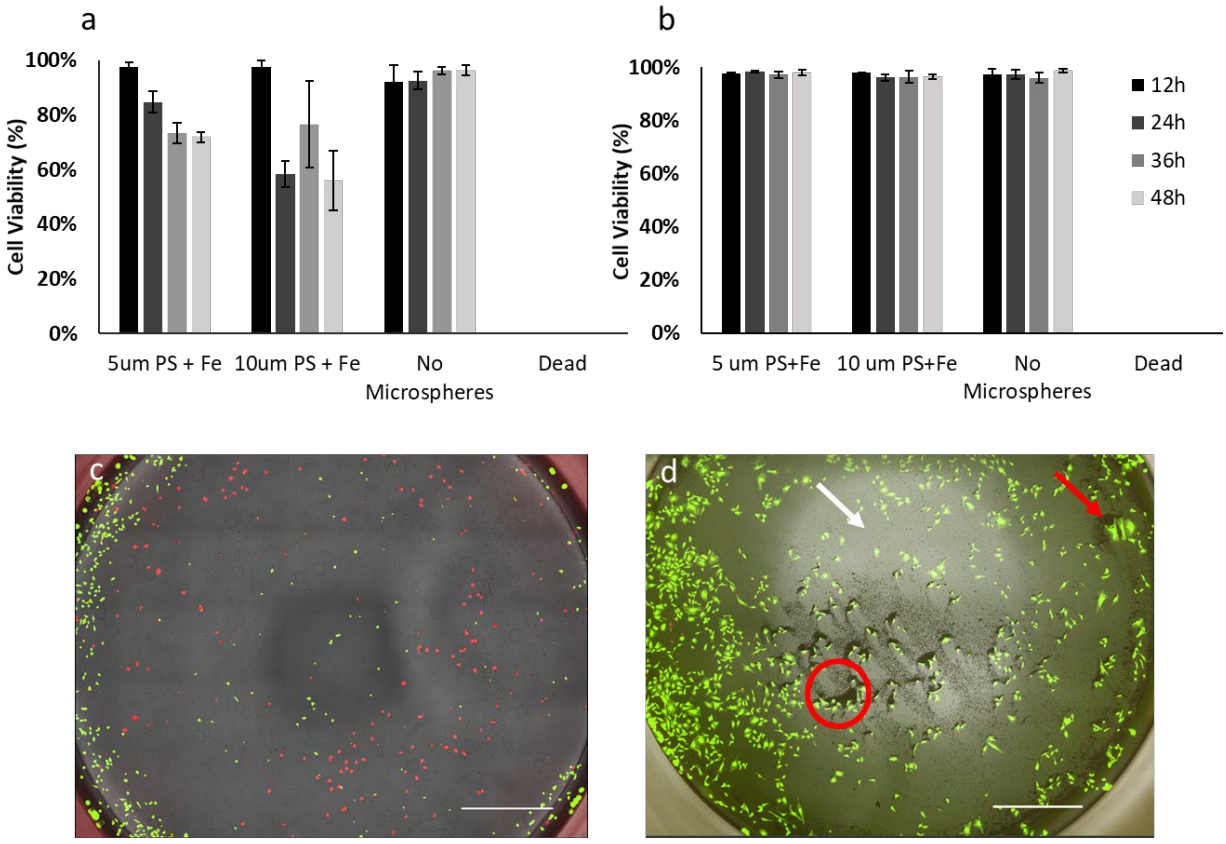

Figure 5.9.5. a) HUVEC viability decreases in presence of 5 µm and 10 µm Fe-modified PS microcarriers over the course of 48 hours. b) Cell viability is restored to normal levels when PVG coating is applied to microspheres. c-d) Live/Dead fluorescent micrograph of HUVEC in presence of c) uncoated and d) PVG coated Fe-PS microcarriers. Areas of high microcarrier concentration (red arrow), low concentration (white arrow), and drifting effects (red circle) are highlighted. Green = Calcein AM, Red = Ethidium homodimer. Scale bar = 1000 um.

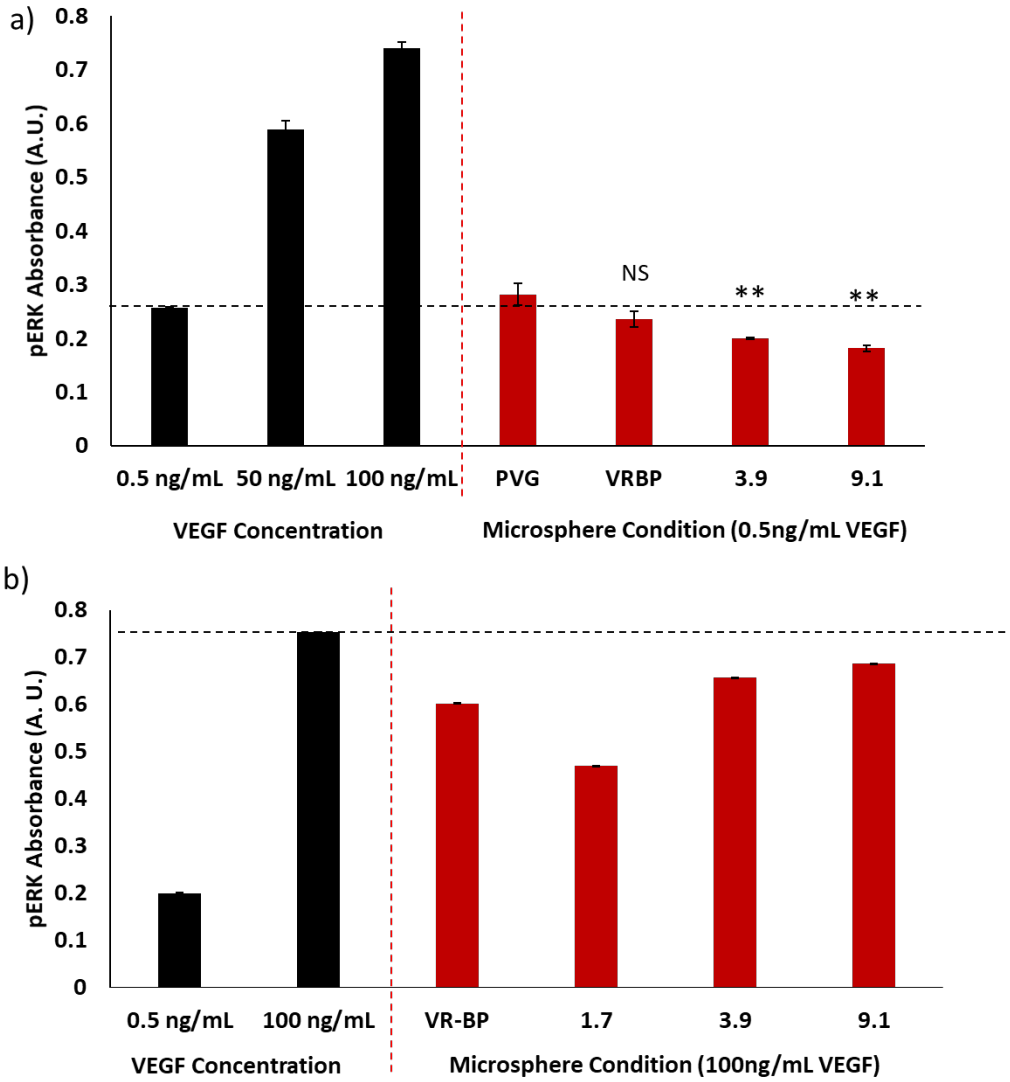

Figure 5.9.6. Treatment with VR-BP/CendR microspheres decreases VEGF-dependent ERK signal transduction in a spacing-dependent manner. a) In EGM2 media (0.5ng/mL VEGF-A_{165} for cell survival), treatment for 10 min with VRBP/CendR complex forming microspheres reduces the level of detectable pERK slightly from the control. b) In media supplemented with 100 ng/mL VEGF-$_{A165}$, the length of the crosslinker binding VR-BP and CendR is shown to have an effect on detectable pERK levels. VEGF-dependent signal transduction is reduced by ~60% when HUVEC

are bound to VR-BP/CendR peptides separated by the 1.7 nm crosslinker, with the effect being reduced by crosslinkers of greater length.

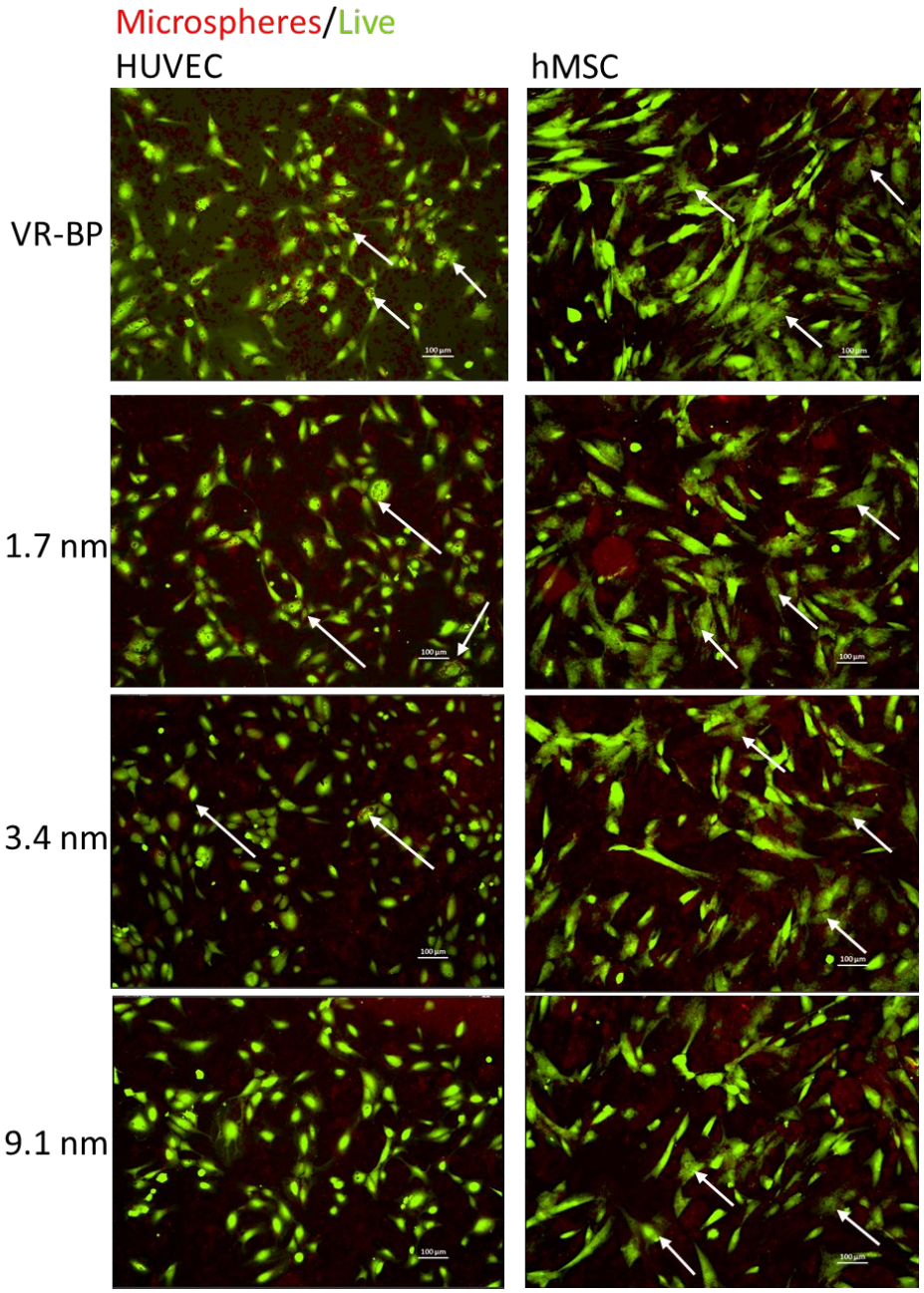

Figure 5.9.7. Representative images showing HUVECs (left) and hMSC (right) internalized 5 µm, PVG+VR-BP microspheres at a rate of X microspheres/cell over 4 hours (white arrows). Addition of the Nrp1 binding peptide CendR at a defined spacing (left) reduced cellular uptake in HUVEC

but not in hMSC. Green = Live (Calcein AM), Red = PS+Fe microsphere autofluorescence. Scale bar = 100 um.

5.10 SUPPLEMENTAL FIGURES

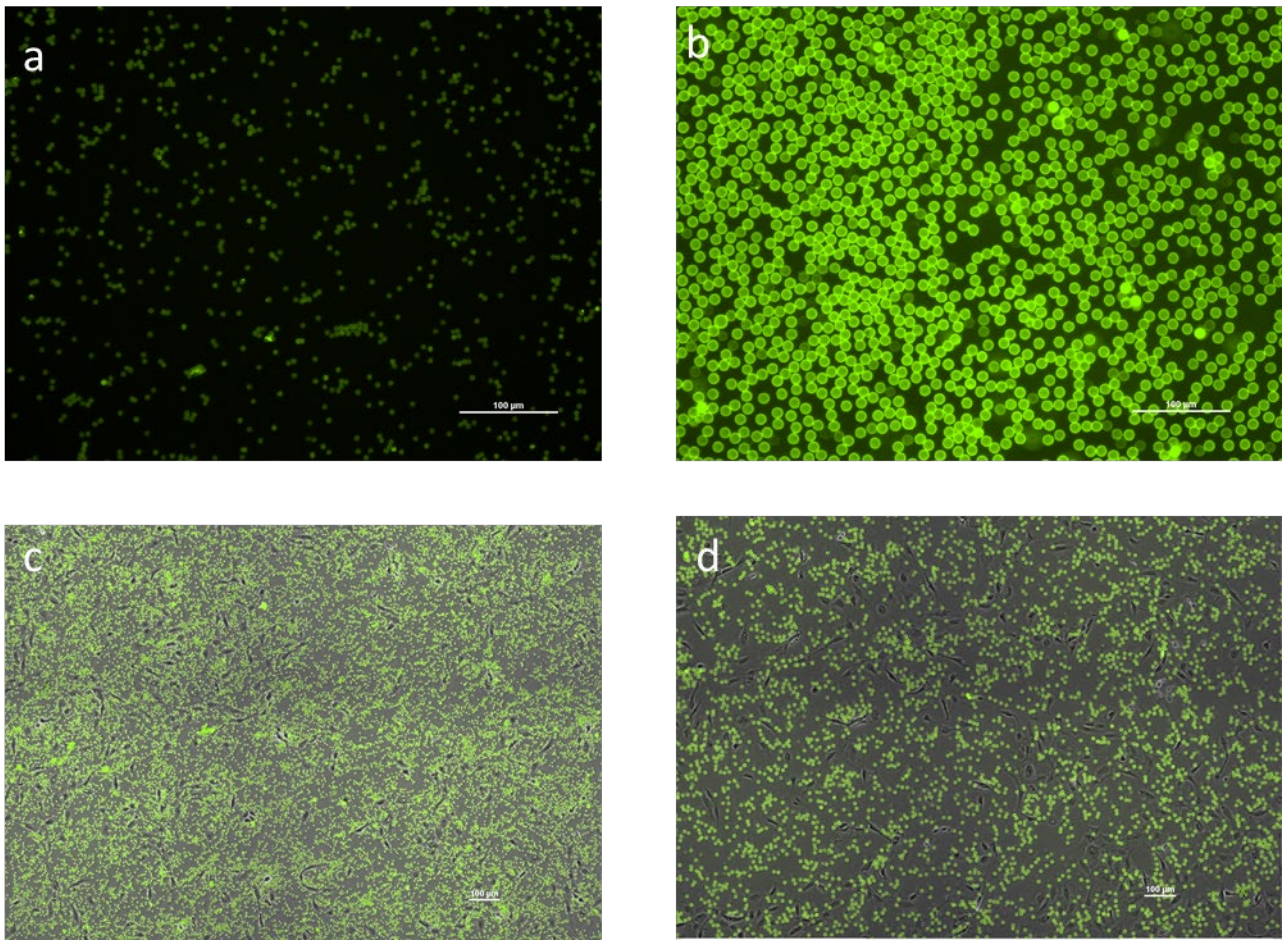

Supplemental Figure S5.10.1. PVG-coated microspheres of a,c) 5 µm or b,d) 10 µm diameter were prepared using FITC-tagged PLL. Fluorescent microspheres a-b) alone and c-d) in the presence of HUVEC cells. Scale bar = 100 µm.

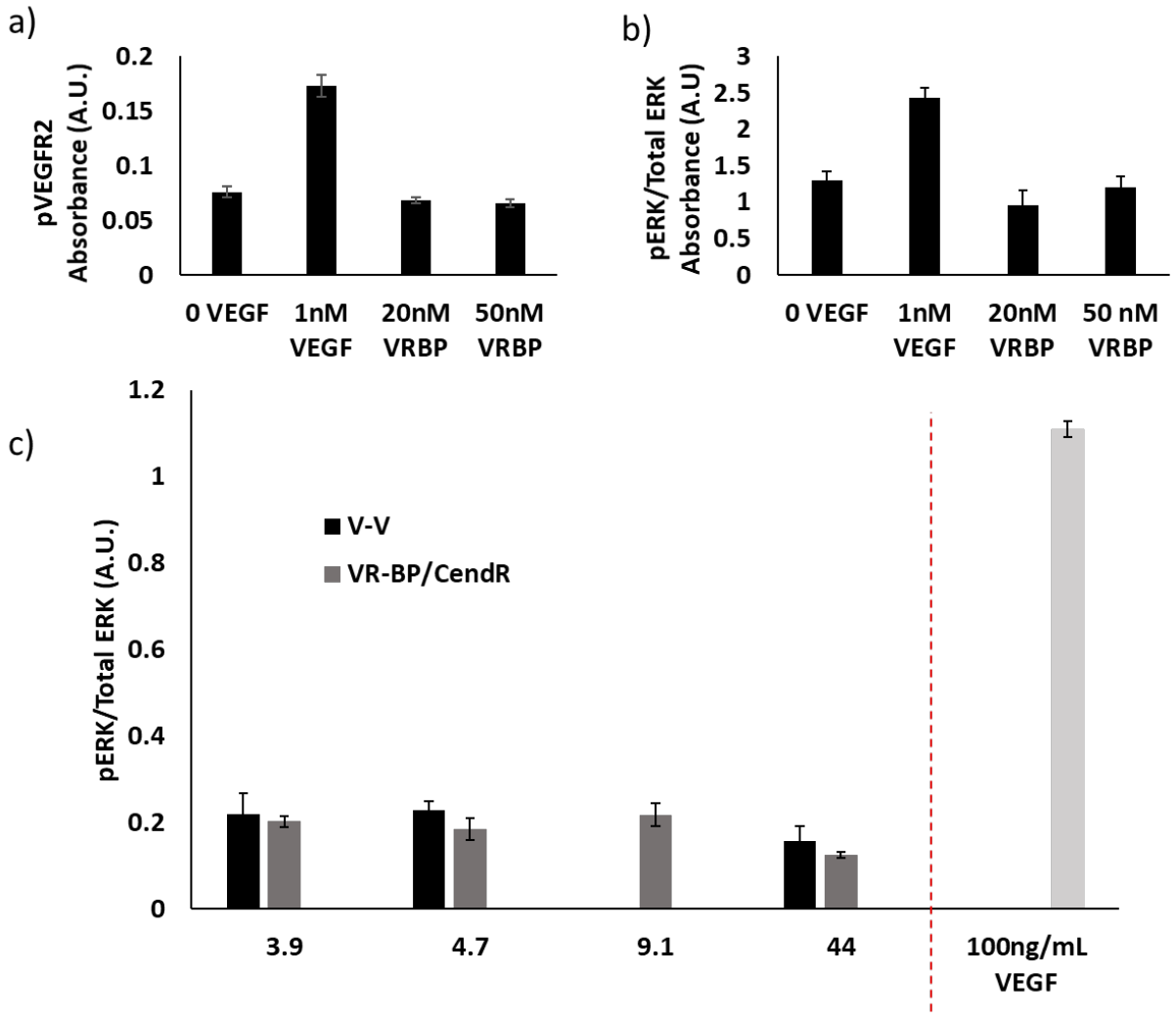

Supplemental Figure S5.10.2. VEGFR2 signaling is not affected by soluble delivery of VR-BP. Soluble VR-BP peptide was delivered to cells at 1, 10, and 50 ng/mL and did not induce a) pVEGFR2 or b) pERK/Total ERK signaling, detected by ELISA. c) 100 ng/mL Soluble VR-BP complexed with either a second VR-BP peptide (black bars) or a CendR peptide (dark grey) did not have a induce detectable levels of pERK.

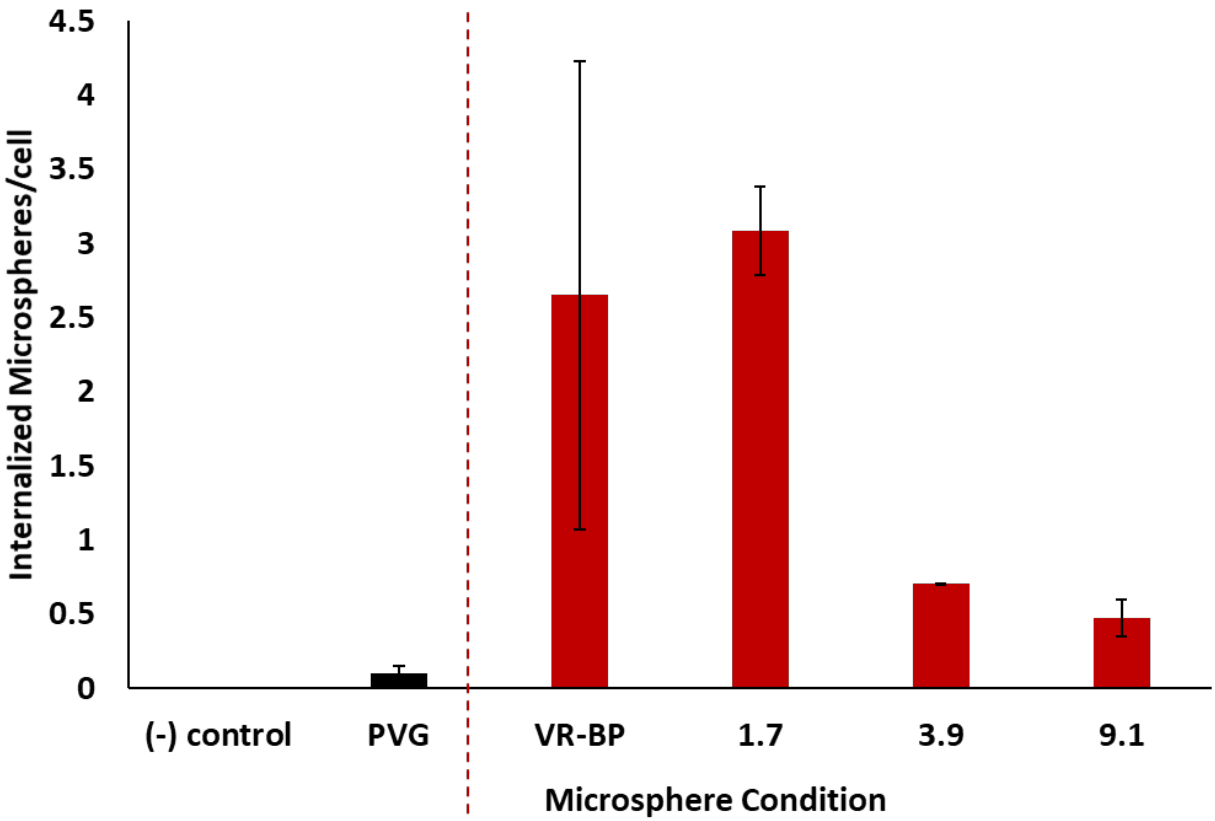

Supplemental Figure S5.10.3. Quantification of microsphere uptake shows a decrease in internalized microspheres/cell in HUVEC with an increase in peptide spacing. VR-BP and CendR peptides spaced by 9.1nm show negligible cell uptake. This trend is not mirrored in hMSC, which uptake microspheres at a high rate regardless of peptide presentation.

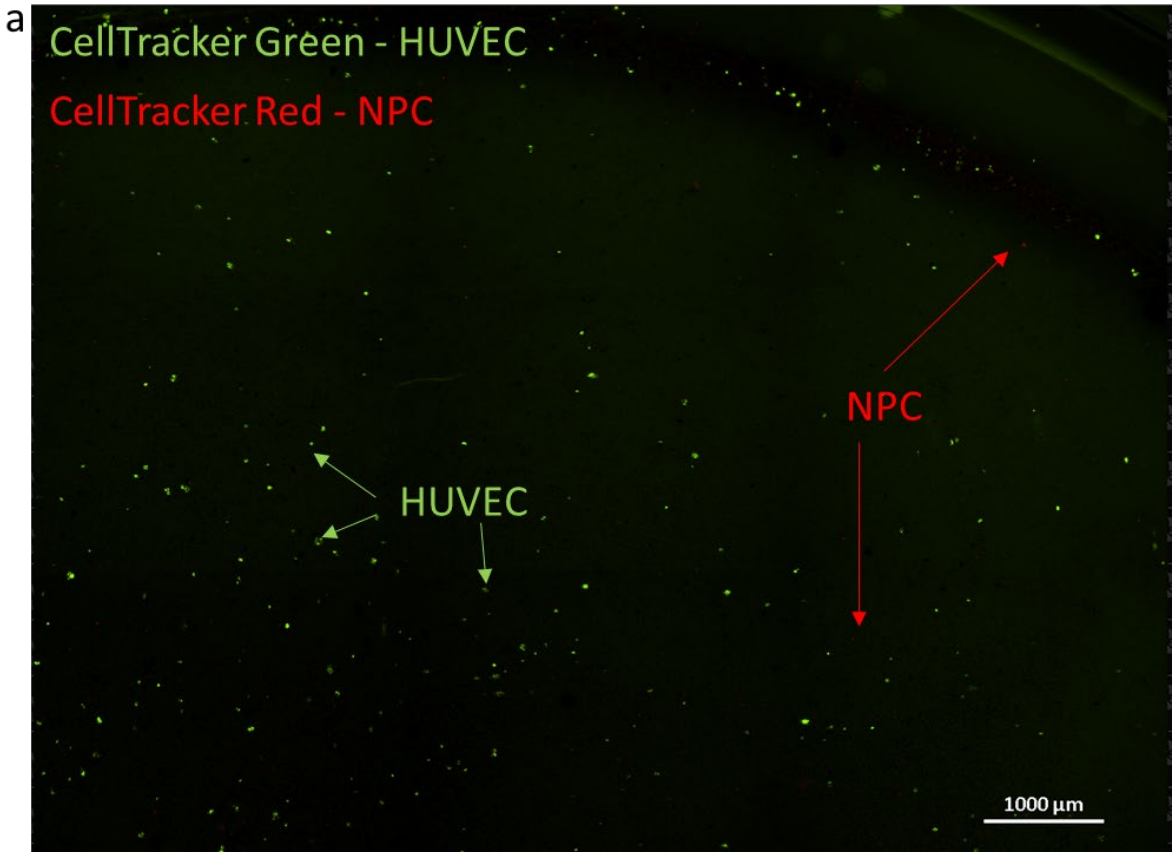

Supplemental Figure S5.10.4. a) HUVEC (green) and NPC (red) after magnetic assisted cell sorting using VR-BP functionalized microcarriers. From a mixed sample of 50% HUVEC and 50% NPC, magnetic VR-BP microspheres bound to and positively selected a population of over 99% HUVEC cells. Scale bar = 1000 um.

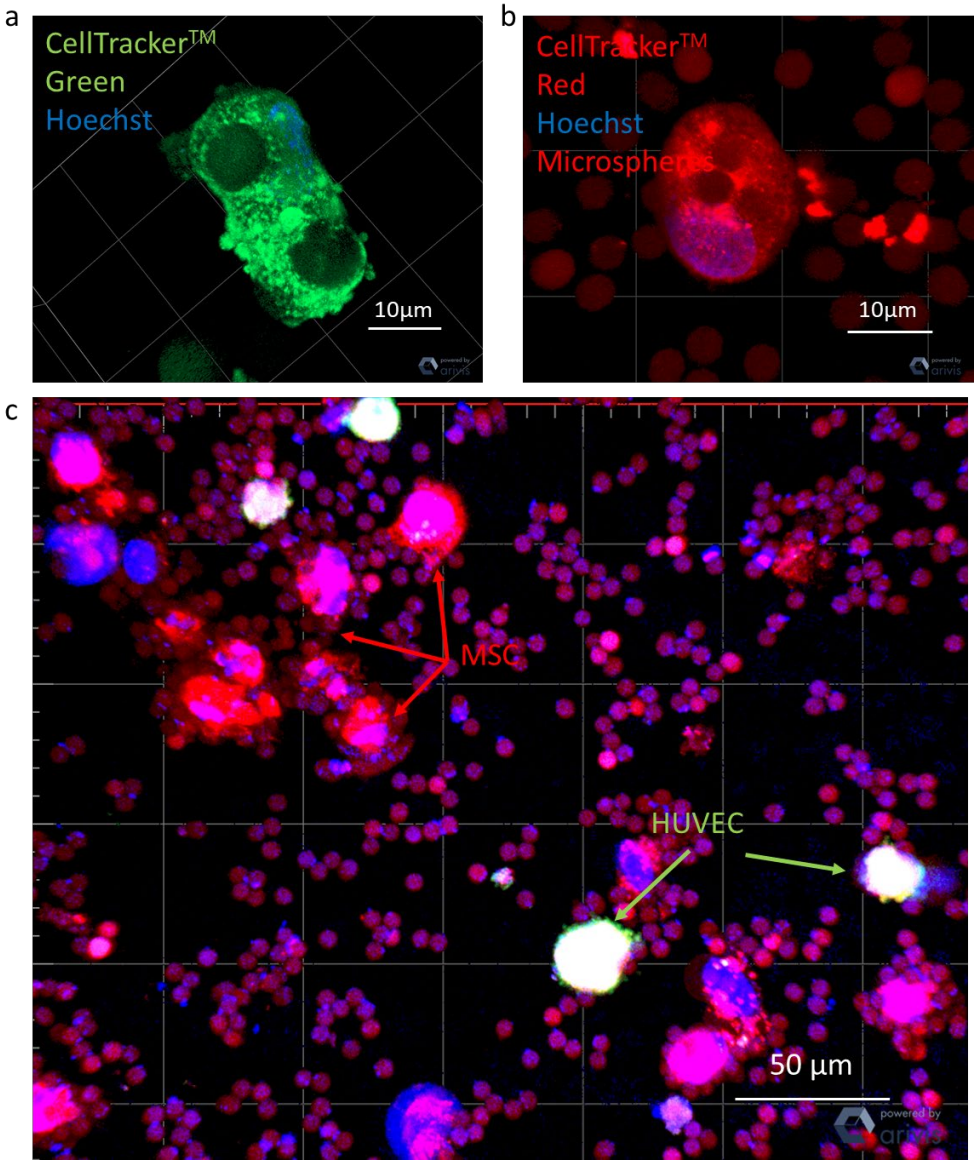

Supplemental Figure S5.10.5. Confocal fluorescent micrographs showing a) HUVEC and b) hMSC internalize VR-BP functionalized PVG coated microbeads of up to 10 µm. Internalization of beads can be seen by the displacement of the CellTracker™ intracellular dye. c) Attempts to sort heterogeneous mixtures of HUVEC (green) and hMSC (red) using VRBP functionalized magnetic microspheres are unsuccessful due to microsphere uptake by hMSC. Red = CellTracker™ Red, microsphere autofluorescence. Green = CellTracker™ Green. Scale bar = a,b) 10 µm; c) 50 µm.